U.S. DEPARTMENT OF COMMERCE
National Technical Information Service

PB-262 202

Midwest Interstate Sulfur Transformation & Transport Project: Aerial Measurements of Urban & Power Plant Plumes, Summer 74

Meteorology Research, Inc, Altadena, Calif

Prepared for

Environmental Sciences Research Lab, Research Triangle Park, N C

Nov 76

021074

EPA-600/3-76-110
November 1976

PB 262 202

Ecological Research Series

UNITED STATES ENVIRONMENTAL PROTECTION AGENCY

REPRODUCED BY
NATIONAL TECHNICAL
INFORMATION SERVICE
U. S. DEPARTMENT OF COMMERCE
SPRINGFIELD, VA. 22161

RESEARCH REPORTING SERIES

Research reports of the Office of Research and Development, U.S. Environmental Protection Agency, have been grouped into five series. These five broad categories were established to facilitate further development and application of environmental technology. Elimination of traditional grouping was consciously planned to foster technology transfer and a maximum interface in related fields. The five series are:

1. Environmental Health Effects Research
2. Environmental Protection Technology
3. Ecological Research
4. Environmental Monitoring
5. Socioeconomic Environmental Studies

This report has been assigned to the ENVIRONMENTAL MONITORING series. This series describes research conducted to develop new or improved methods and instrumentation for the identification and quantification of environmental pollutants at the lowest conceivably significant concentrations. It also includes studies to determine the ambient concentrations of pollutants in the environment and/or the variance of pollutants as a function of time or meteorological factors.

This document is available to the public through the National Technical Information Service, Springfield, Virginia 22161.

TECHNICAL REPORT DATA

(Please read Instructions on the reverse before completing)

1. REPORT NO. EPA-600/3-76-110	2.	3. RECIPIENT'S ACCESSION NO.

4. TITLE AND SUBTITLE MIDWEST INTERSTATE SULFUR TRANSFORMATION AND TRANSPORT PROJECT: Aerial Measurements of Urban and Power Plant Plumes, Summer 1974	5. REPORT DATE November 1976 6. PERFORMING ORGANIZATION CODE
7. AUTHOR(S) W.H. White, J.A. Anderson, W.R. Knuth, D.L. Blumenthal, J.C. Hsiung, and R.B. Husar.	8. PERFORMING ORGANIZATION REPORT NO.
9. PERFORMING ORGANIZATION NAME AND ADDRESS Meteorology Research, Inc. 464 West Woodbury Road Box 637 Altadena, CA 91001	10. PROGRAM ELEMENT NO. 1AA603 11. CONTRACT/GRANT NO. 68-02-1919
12. SPONSORING AGENCY NAME AND ADDRESS Environmental Sciences Research Laboratory Office of Research and Development U.S. Environmental Protection Agency Research Triangle Park, North Carolina 27711	13. TYPE OF REPORT AND PERIOD COVERED FINAL 7/74-6/76 14. SPONSORING AGENCY CODE EPA-ORD

15. SUPPLEMENTARY NOTES

16. ABSTRACT

A portion of the research activities of the Midwest Interstate Sulfur Transformation and Transport Project (Project MISTT) during the summer of 1974 is documented. Using a light plane equipped with instruments for measuring air pollutants and meteorological parameters, investigators mapped the three-dimensional distribution of aerosols and pollutant gases originating in the St. Louis area. Each day's flight plan was designed to characterize a large pollutant plume at discrete distances downwind from its source. The plume from the coal-fired power plant at Labadie, Missouri was followed out to 45 km. Secondary aerosol production within the plume was documented. The estimated average conversion rate for sulfur dioxide to sulfate was about three percent/hour at the distances sampled. The overall removal rate of SO_2 was too small to detect, and no net production of ozone was observed. Large pollutant plumes were also identified downwind of central St. Louis and the Wood River refineries. These urban-industrial plumes were followed out to 60-70 km, where they were characterized by elevated concentrations of ozone and light-scattering aerosols.

17. KEY WORDS AND DOCUMENT ANALYSIS

a. DESCRIPTORS		b. IDENTIFIERS/OPEN ENDED TERMS	c. COSATI Field/Group
*Air pollution	*Plumes		13B
*Sulfur dioxide	*Chemical Reactions		07B
*Sulfate	Transport properties		07D
*Aerosols			10B
Ozone			21B
*Electric power plants			07D

18. DISTRIBUTION STATEMENT RELEASE TO PUBLIC	19. SECURITY CLASS *(This Report)* UNCLASSIFIED	21. NO. OF PAGES 136
	20. SECURITY CLASS *(This page)* UNCLASSIFIED	22. PRICE

EPA Form 2220-1 (9-73)

EPA-600/3-76-110
November 1976

MIDWEST INTERSTATE SULFUR TRANSFORMATION AND TRANSPORT PROJECT:
Aerial Measurements of Urban and Power Plant Plumes, Summer 1974

by

W.H. White, J.A. Anderson, W.R. Knuth
D.L. Blumenthal and J.C. Hsiung
Meteorology Research, Inc.
Altadena, California 91001

R.B. Husar
Washington University
St. Louis, Missouri 63130

68-02-1919

Project Officer

William E. Wilson
Atmospheric Chemistry and Physics Division
Environmental Sciences Research Laboratory
Research Triangle Park, North Carolina 27711

ENVIRONMENTAL SCIENCES RESEARCH LABORATORY
OFFICE OF RESEARCH AND DEVELOPMENT
U.S. ENVIRONMENTAL PROTECTION AGENCY
RESEARCH TRIANGLE PARK, NORTH CAROLINA 27711

DISCLAIMER

This report has been reviewed by the Environmental Sciences Research Laboratory, U.S. Environmental Protection Agency, and approved for publication. Approval does not signify that the contents necessarily reflect the views and policies of the U.S. Environmental Protection Agency, nor does mention of trade names or commercial products constitute endorsement or recommendation for use.

ABSTRACT

A portion of the research activities of the Midwest Interstate Sulfur Transformation and Transport Project (Project MISTT) during the summer of 1974 is documented. Using a light plane equipped with instruments for measuring air pollutants and meteorological parameters, investigators mapped the three-dimensional distribution of aerosols and pollutant gases originating in the St. Louis area. Each day's flight plan was designed to characterize a large pollutant plume at discrete distances downwind from its source. The plume from the coal-fired power plant at Labadie, Missouri was followed out to 45 km. Secondary aerosol production within the plume was documented. The estimated average conversion rate for sulfur dioxide to sulfate was about three percent/hour at the distances sampled. The overall removal rate of SO_2 was too small to detect, and no net production of ozone was observed. Large pollutant plumes were also identified downwind of central St. Louis and the Wood River refineries. These urban-industrial plumes were followed out to 60-70 km, where they were characterized by elevated concentrations of ozone and light-scattering aerosols.

CONTENTS

Abstract iii

List of Figures vi

List of Tables ix

Acknowledgement x

Sections

I Introduction 1

II Experimental Procedure 8

III Meteorology 31

IV Sulfur Chemistry 40

V Oxidant Chemistry 63

VI References 85

Appendices 89

Preceding page blank

FIGURES

No.		Page
1	Outline of SO_2 Plume Downwind of Labadie Power Plant on 14 August 1974	4
2	Horizontal Profiles of the SO_2 Concentration and Light Scattering Coefficient (b_{scat}) Downwind of Greater St. Louis Under Three Different Wind Regimes	5
3	Cessna 206 Sampling Aircraft	9
4	Installation of Electrical Aerosol Analyzer, Royco Electronics, Multichannel Analyzer, and Multifilter Sampling Manifold in MRI Aircraft	12
5	Installation of Grab Bag Sampling System in MRI Aircraft	13
6	Wind Pod Housing Optics for Royco Optical Particle Counter	14
7	Installation of Sulfate Filter Holders in MRI Aircraft	15
8	Installation of Gas Monitors in MRI Aircraft	16
9	Corrected Transient Response of Theta Systems SO_2 Monitor (Markowski, 1975).	18
10	Probes for MRI Airborne Instrument Package	19
11	Installation of Data Loggers in MRI Aircraft	21
12	Sample Intake Manifolds on Left-hand Side of Aircraft	23
13	Instrument Layout in MRI Aircraft	24
14	Sample Flow in MRI Aircraft	25
15	Instrument Schematic for First Data Logger	26
16	Instrument Schematic for Second Data Logger	27
17	Flight Plan for Spiral Soundings	29

FIGURES (continued)

No.		Page
18	Flight Plan for Horizontal Traverses	30
19	St. Louis Weather During Sampling Period	32
20	Weather Map for 0700 CDT on 1 August 1974	33
21	Weather Map for 0700 CDT on 5 August 1974	35
22	Weather Map for 0700 CDT on 12 August 1974	37
23	Weather Map for 0700 CDT on 15 August 1974	39
24	Winds Aloft on 14 August 1974, From Pilot Balloon Measurements at Marthasville, Missouri	41
25	Location of Aircraft Sampling Routes and Pilot Balloon Release Points 14 August 1974	43
26	Horizontal Plume Traverse 10 km Downwind of Labadie Stacks on 14 August 1974	44
27	Horizontal Plume Traverse 21 km Downwind of Labadie Stacks on 14 August 1974	45
28	Horizontal Plume Traverse 45 km Downwind of Labadie Stacks on 14 August 1974	46
29	Composite Side View of Labadie Plume on 14 August 1974	48
30	Vertical Profile from Spiral Descent at Labadie on 14 August 1974, 1045-1121 CDT	49
31	Scatter Plot of Particulate Sulfur Concentrations (S_p) vs. Plume b_{scat} and Background b_{scat} for Labadie Samples	52
32	Scatter Plot of Particulate Sulfur Concentration (S_p) vs. Plume b_{scat} and Background b_{scat} for Wood River Samples	53
33	Two Aerosol/Emissions Ratios in the Labadie Plume on 14 August 1974	56

FIGURES (continued)

No.		Page
34	Horizontal Plume Traverse 21 km Downwind of Labadie Stacks on 14 August 1974	59
35	Horizontal Profiles of Ozone and Oxidant Concentrations Downwind of Greater St. Louis Under Three Different Wind Regimes	64
36	Vertical Profiles of Ozone Concentration and Temperature on 30 July 1974	65
37	Cross Section of Ozone Plume Downwind of Greater St. Louis on the Afternoon of 30 July 1974	66
38	Horizontal Plume Traverse 10 km Downwind of Labadie Stacks on 14 August 1974	69
39	Horizontal Plume Traverse 21 km Downwind of Labadie Stacks on 14 August 1974	70
40	Horizontal Plume Traverse 45 km Downwind of Labadie Stacks on 14 August 1974	71
41	Early-morning Horizontal Profiles of Ozone Concentration, Oxidant (O_3 + NO_2) Concentration, and Light-scattering Coefficient (b_{scat}) Downwind of Greater St. Louis on 3 August 1974	72
42	Horizontal Profiles of Oxidant Concentration and Light-scattering Coefficient (b_{scat}) Downwind of Greater St. Louis Under Three Different Wind Regimes	75
43	Horizontal Plume Traverse 21 km Downwind of Labadie Stacks on 14 August 1974	80
44	Horizontal Plume Traverse 45 km Downwind of Labadie Stacks on 14 August 1974	81

TABLES

No.		Page
1	Summary of 1974 MISTT Aircraft Sampling Program	3
2	Instrumentation of MRI Aircraft for 1974 MISTT Field Program	10
3	Aircraft Sampling Schedule, 14 August 1974	42
4	Particulate Sulfur in the Labadie and Wood River Plumes	51
5	Sampling Environment of Sulfate Filters	58
6	Parameters Used in Model Calculations	83

ACKNOWLEDGEMENTS

An experimental program of this size could not have been completed without the coordinated efforts of many individuals. Key responsibilities in the collection and processing of data were shared by S. Gregg, S. Muller, and K. Lamb of MRI, J. Husar, K. Horton, and N. Gillani of Washington University, and B. Cantrell and K. Whitby of the University of Minnesota. Active support was given by many others. Valuable comments on the interpretation of the data were received from J. Ogren (MRI), W. Wilson (U. S. Environmental Protection Agency), H. Walker (Monsanto Polymers and Petrochemicals Co.), and P. McMurry (California Institute of Technology). Typing and illustrations for this report were supervised by T. Herrick and C. Williams.

SECTION I

INTRODUCTION

PROJECT MISTT AIRCRAFT SAMPLING PROGRAM

During July and August of 1973, 1974, and 1975, the U.S. Environmental Protection Agency (EPA) funded a series of coordinated field studies in the St. Louis area as part of Project MISTT (Midwest Interstate Sulfur Transformation and Transport). Meteorology Research, Inc. (MRI) provided aircraft monitoring support for these studies, using an instrumented light plane to map the three-dimensional distribution of aerosols and pollutant gases in large plumes. This report presents a description of the 1974 aircraft sampling program, together with an analysis of the results. The data from the program are presented in summary form here; with the exception of particle size distributions, which will be reported separately by the Particle Technology Laboratory of the University of Minnesota, a complete listing of the 1974 aircraft data is available in White, et al (1975). The results of the 1973 aircraft sampling program were reported by Anderson and Blumenthal (1974).

A fixed-wing aircraft offered certain advantages as a sampling platform, beyond its obvious three-dimensional mobility. The speed of the MRI Cessna 206 enabled it to sample large areas in a short time interval, making it possible to determine the large-scale geometry of pollutant plumes. Flying a few hundred meters above the ground, monitoring instruments were not "blinded" by small local sources as they sometimes are on the ground. These features are well illustrated by Figures 1 and 2, which show how clearly large plumes can be identified in the data taken by the aircraft. Finally, as will be discussed later, knowledge of the vertical distribution of pollutants was necessary for the calculation of pollutant budgets.

The MRI Cessna 206 flown in the 1974 MISTT field program was equipped for the continuous monitoring of gas concentrations (SO_2, O_3, NO, NO_x, CO), aerosol indices (light-scattering coefficient, condensation nuclei count), and meteorological variables (temperature, relative humidity, turbulent dissipation). Data from these instruments were recorded at 0.4-second intervals on magnetic tape cartridges. An on-board electrical mobility analyzer/optical particle counter/multichannel analyzer system determined the particle size distributions of grab samples, and a multiplefilter sampling system collected aerosol for later sulfate analysis at Washington University. A detailed description of the aircraft, instrumentation, and experimental procedure is given in Section II.

Intensive airborne sampling was conducted on 10 days of 1974, extending from 30 July to 15 August (Table 1). The meteorology of the sampling period is summarized in Section III. Each day's flight plan, outlined in Appendix A, was designed to characterize a large pollutant plume at discrete distances downwind from its source. Selected for study were the plumes from three major sources: the coal-fired power plant at Labadie, Mo., an elevated point source; the refinery complex at Wood River, Ill., a concentrated low-level area source; the central St. Louis urban-industrial area including East St. Louis and Granite City, a diffuse low-level area source. The plumes from all three sources are identifiable in Figures 1 and 2, and are analyzed in Sections IV and V.

The pollutant flow downwind of the Labadie power plant was mapped by the MRI aircraft on four days during the 1974 MISTT field program. Shifting winds during the initial attempt on 31 July restricted sampling to the immediate vicinity of the plant. On the morning of 1 August and early evening of 5 August, the plume was characterized at three downwind distances, from 1 km to 16-18 km. Under nearly steady-state wind conditions during the middle of the day on 14 August, the plume was characterized at 10, 21, 32, and 45 km downwind of the plant (Figure 1).

The St. Louis and Wood River plumes were usually mapped together (Figure 2), and it is convenient to refer to the combined plumes as "the urban-industrial plume." This plume was mapped by the MRI aircraft on six days during the 1974 MISTT field program. On most of these days the plume was characterized in one set of passes immediately downwind of the metropolitan area and again in a second set of passes 30-60 km farther out. On 12 August it was characterized at three downwind distances.

RESULTS AND CONCLUSIONS OF 1974 PROGRAM

The Labadie Plume

Much of the analysis in this report is focused on the Labadie plume, which possesses the advantages of relatively well-defined geometry and chemistry, together with a minimal interaction with the ground. Peak sulfur dioxide concentrations measured within the plume varied from over 10 ppm at 1 km from the plant to about 0.06 ppm at 45 km from the plant. Peak sulfate concentrations at 10 km from the

Table 1. SUMMARY OF 1974 MISTT AIRCRAFT SAMPLING PROGRAM

Date	Time (CDT)	Plume
30 July	0900-1615	Urban-Industrial
31 July	0645-0900	Power Plant
1 August	0800-1115	Urban Industrial
3 August	0815-1615	Urban-Industrial
5 August	1730-2015	Power Plant
10 August	1500-1815	Urban-Industrial
11 August	0900-1300	Urban-Industrial
12 August	1100-1500	Urban-Industrial
14 August	1045-1515	Power Plant
15 August	0945-1230	Urban-Industrial

Urban-industrial plume sampling was conducted downwind of greater St. Louis area, including Wood River (Illinois), East St. Louis (Illinois), and Granite City (Illinois); power plant plume sampling was conducted downwind of coal-fired steam generating station at Labadie (Missouri).

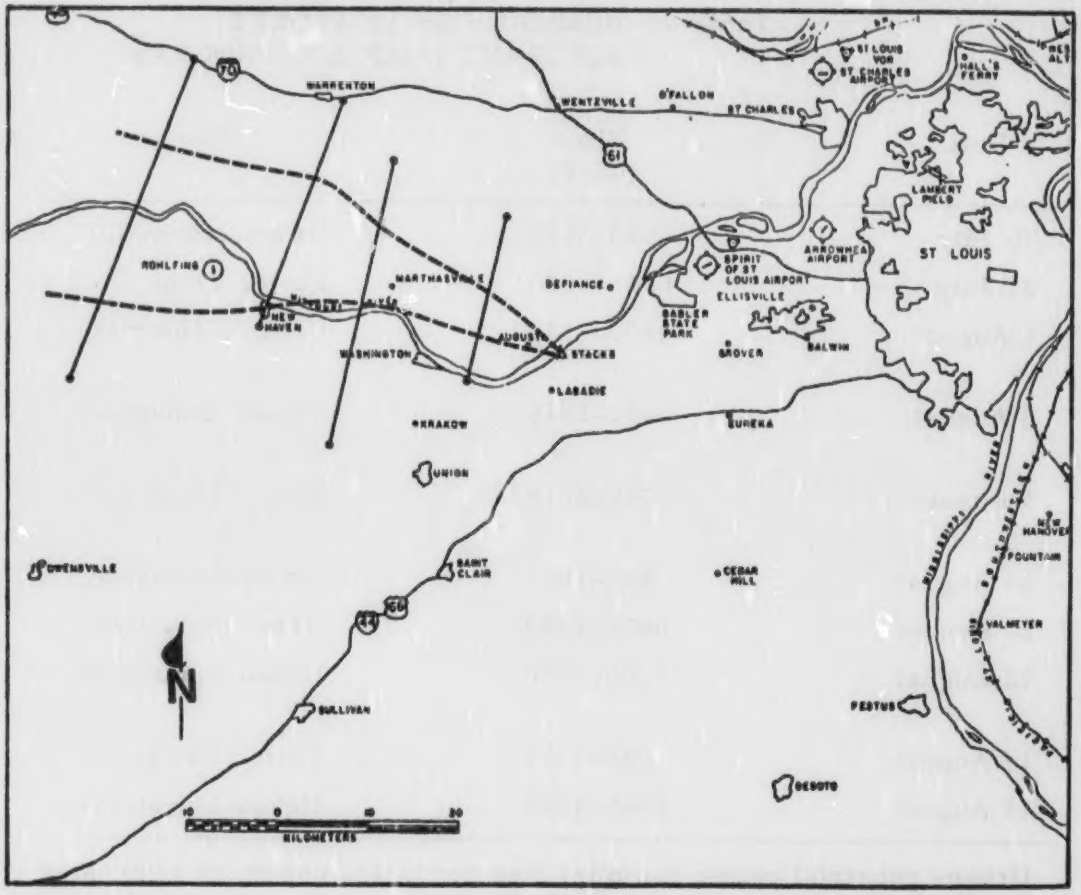
70
WARRENTON
WENTZVILLE
O'FALLON
ST CHARLES
61
ST LOUIS
VOR
ST CHARLES AIRPORT
HALL'S FERRY
LAMBERT FIELD
ARROWHEAD AIRPORT
ST LOUIS
SPIRIT OF ST LOUIS AIRPORT
ELLISVILLE
BABLER STATE PARK
ROHLFING
MARTHASVILLE
DEFIANCE
NEW HAVEN
AUGUSTA
WASHINGTON
STACKS
GROVER
BALWIN
LABADIE
KRAKOW
EUREKA
UNION
SAINT CLAIR
CEDAR HILL
OWENSVILLE
66
44
N
SULLIVAN
NEW HANOVER
FOUNTAIN
VALMEYER
MISSISSIPPI RIVER
FESTUS
DESOTO
10
0
10
20
KILOMETERS

Figure 1. Outline of SO_2 plume downwind of Labadie power plant on 14 August 1974. Solid lines show sampling paths, dashed curves indicate region in which SO_2 concentrations above 0.01 ppm were measured between 455 and 610 m (1500 and 2000 ft) msl. Sampling began near the plant at 1045 CDT, ended 45 km downwind at 1515 CDT.

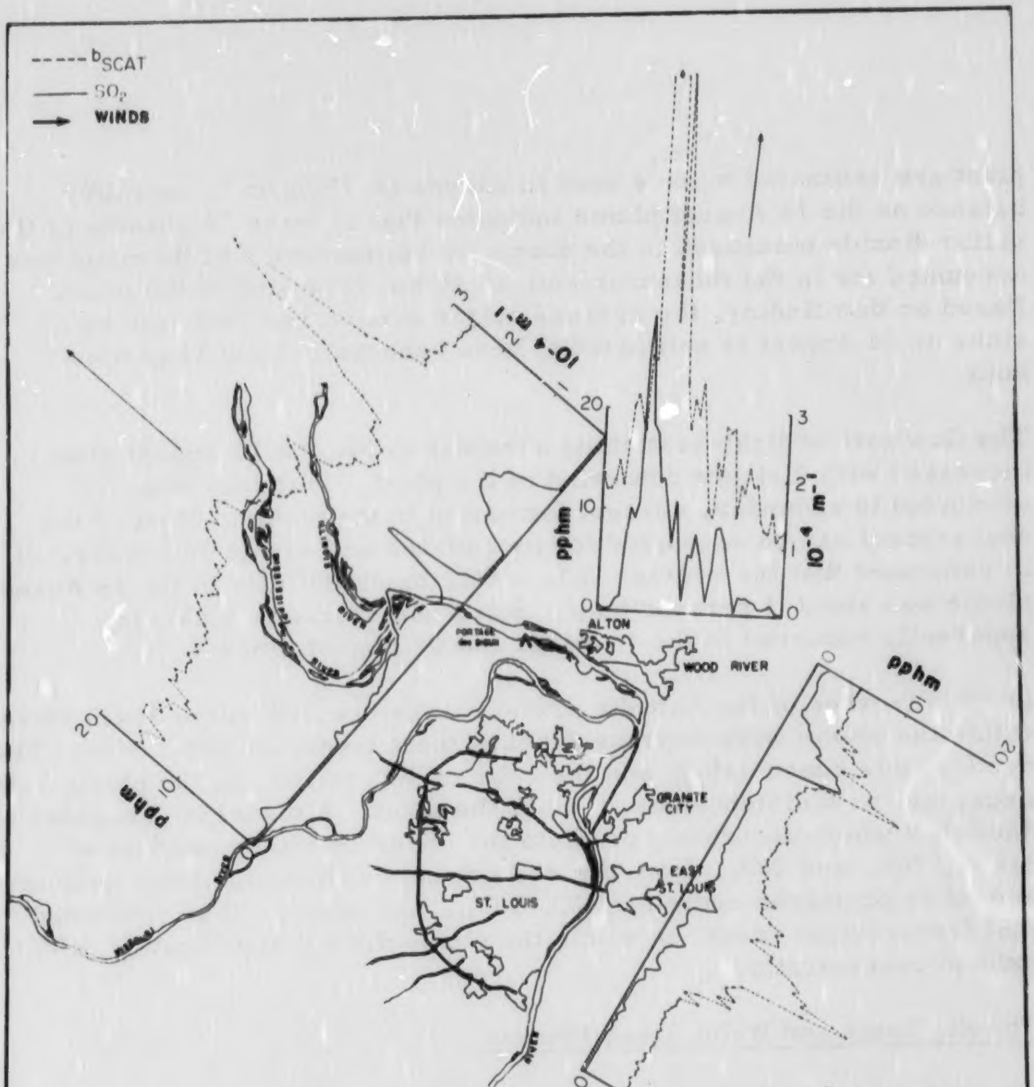
b_SCAT
SO₂
WINDS
pphm
10⁻⁴ m⁻¹
0
10
20
1
2
3
ALTON
WOOD RIVER
GRANITE CITY
EAST ST. LOUIS
ST. LOUIS
0
20
40
KILOMETERS

Figure 2. Horizontal profiles of the SO_2 concentration and light scattering coefficient (b_{scat}) downwind of Greater St. Louis under three different wind regimes. Profiles were recorded during traverses of profile baselines at the following altitudes and times: (counter-clockwise from lower right) 455 m (1500 ft) msl, 0933-0952 CDT, 30 July 1974; 610 m (2000 ft) msl, 1145-1152 CDT, 12 August 1974; 455 m (1500 ft) msl, 1027-1048 CDT, 15 August 1974. Arrows show average winds measured in mixing layer during sampling period; their lengths equal distance covered in one hour at average wind speed. Large aerosol plumes can be identified downwind of Wood River and Central St. Louis.

plant are estimated to have been in excess of 75 $\mu g/m^3$. A sulfur balance on the 14 August plume indicates that at least 75 percent of the sulfur dioxide measured in the plume 10 km downwind of the plant was accounted for in the measurements at 45 km downwind of the plant. Based on this finding, the average sulfur dioxide removal rate by all sinks on 14 August is estimated to have been well below 11 percent/hour.

The flow rate of light-scattering aerosols within the 14 August plume increased with distance downwind of the plant. This increase is attributed to secondary aerosol formation in the plume. Most of the new aerosol can be accounted for by sulfates and associated water. It is estimated that the average SO_2 - $SO_4^=$ oxidation rate in the 14 August plume was about 3 percent/hour. Some homogeneous nucleation apparently occurred in the 1 August and 14 August plumes.

In all traverses of the Labadie plume, ozone concentrations encountered within the plume were depressed below their levels on either side. The depth of this ozone deficit and the ratio of NO to NO_x in the plume both decreased with distance downwind of the plant. A model is presented in Section V which accurately predicts the observed plume profiles of ozone, NO, and NO_x, from the background conditions, plume geometry, and basic photolytic cycle for NO, NO_2, and ozone. It is concluded that free-radical reactions within the plume did not significantly affect oxidant concentrations.

The St. Louis and Wood River Plumes

An important result of the aircraft sampling program was the identification and documentation of a large, well-defined pollutant plume downwind of greater St. Louis. The geometry of the urban-industrial plume strongly depended on the prevailing wind direction. Under westerly or easterly conditions, parallel plumes from Wood River and St. Louis could be distinguished in the traverses immediately downwind of the metropolitan area. The combined initial width of the two plumes was about 50 km. On 12 August the two plumes were apparently superimposed by southerly flow, although this cannot be established with certainty because of the variability and disorganization of the measured winds. The single narrow plume mapped north of Wood River on this day contained the highest light-scattering coefficients (over 10×10^{-4} m^{-1}) and ozone concentrations (up to 0.20 ppm) measured by the aircraft during the 1974 program.

The photochemistry of the St. Louis/Wood River plume was markedly different from that of the Labadie plume, as net production of oxidant was observed in both the St. Louis and Wood River plumes less than 15 km downwind of hydrocarbon source areas. Indeed, ozone concentrations above background levels were the most conspicuous indicator of the downwind St. Louis/Wood River plume, and it is calculated that roughly 100 tons/hour of ozone was generated in this plume on the afternoon of 30 July. This is five times the estimated hourly rate of hydrocarbon emissions in the St. Louis/Wood River urban-industrial area (averaged over the year), and indicates that the ozone yield of hydrocarbons in the atmosphere may be significantly greater than is measured in smog chambers. High oxidant concentrations in the St. Louis/Wood River plume were generally associated with high light-scattering coefficients, suggesting that much of the light-scattering aerosol was produced photochemically.

SECTION II

EXPERIMENTAL PROCEDURE

AIRCRAFT

Meteorology Research, Inc. (MRI) employed an instrumented Cessna 206 as its sampling platform during the 1974 MISTT field program. This aircraft is shown in Figure 3. It is equipped with Robertson STOL modification to permit slower sampling speeds, which were particularly advantageous in the Labadie power plant plume. An added belly pod increased the space available for instrumentation.

INSTRUMENTATION

Instrumentation of the aircraft took place early in 1974. The basic criteria used for instrument selection were low weight and bulk and low power requirements, in addition to the required sensitivity and a fast time response. The specific instruments used are listed in Table 2, together with their ranges and time responses. The instruments can be divided into four groups: aerosol monitors, gas monitors, meteorological sensors, and position sensors.

Aerosol Monitors

The MRI aircraft carried an integrating nephelometer, a condensation nuclei counter, an electrical mobility analyzer, an optical particle counter and a multifilter sulfate sampling manifold. The integrating nephelometer and condensation nuclei monitor are continuous instruments, well suited to the airborne sampling environment because of their ruggedness and fast time response. The mobility analyzer and optical counter were operated in an intermittent mode, analyzing bag samples obtained at specific points during each sampling pass. The multifilter sulfate sampling system collected integrated aerosol samples for later sulfate analysis at Washington University.

The MRI integrating nephelometer measures the total light scattering coefficient of ambient air by detecting the light scattered from an illuminated air sample, as described by Ahlquist and Charlson (1968). The light scattering coefficient is roughly proportional to the mass concentration of aerosol particles in the $0.2\ \mu m - 2.0\ \mu m$ diameter range.

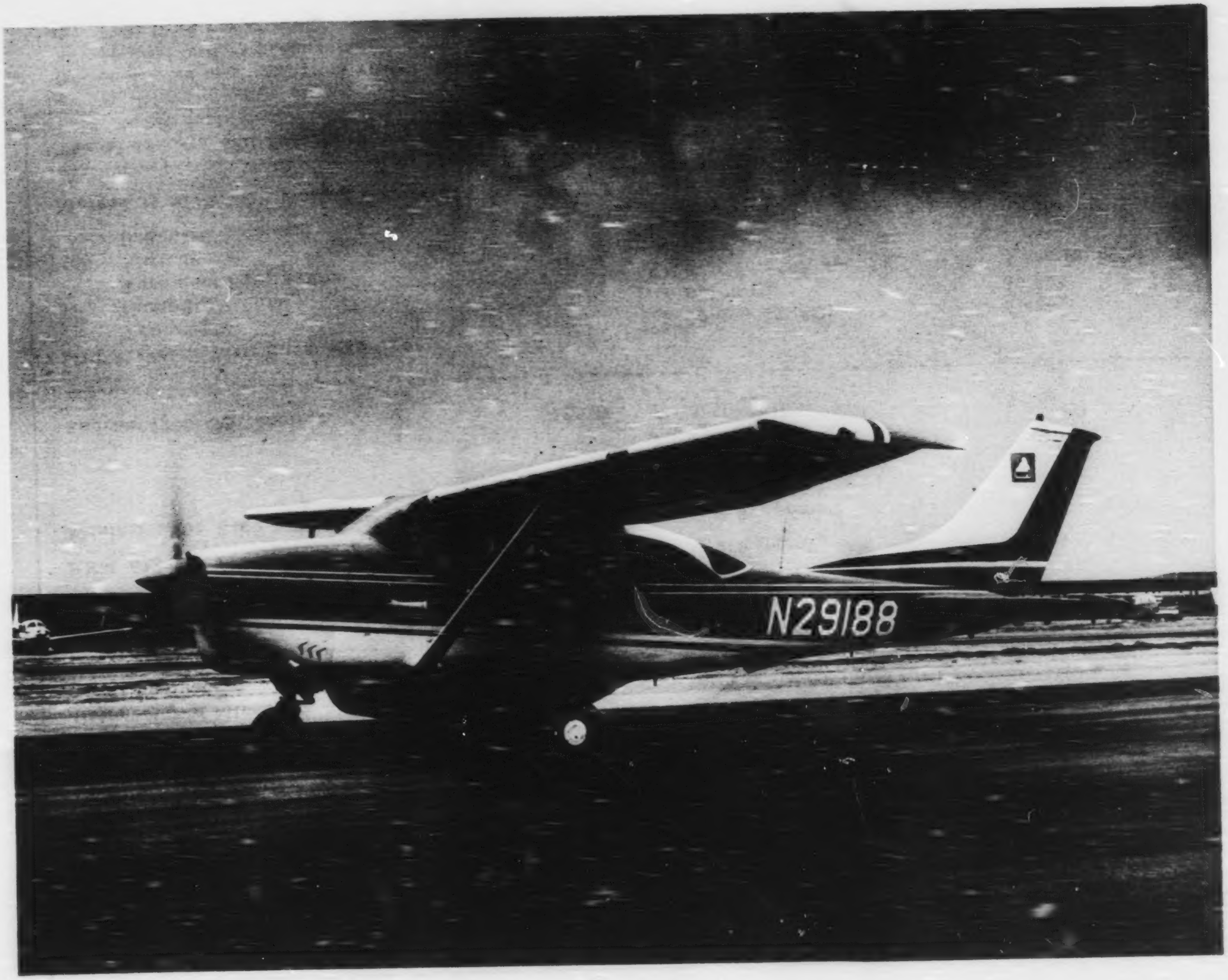

Figure 3. Cessna 206 sampling aircraft. Photograph shows added belly pod, exhaust venturis, and sample inlets.

Table 2. INSTRUMENTATION OF MRI AIRCRAFT FOR 1974 MISTT FIELD PROGRAM

Instrument	Power Required	Ranges Used	Response Time (to 90%)
MRI 1550B Integrating Nephelometer	70 W	0-10 (10^{-4} m^{-1})	1 sec
Environment One Condensation Nuclei Monitor (Rich 100)	70 W	0-100* (10^3 cm^{-3}) 0-300 (10^3 cm^{-3})	5 sec
Thermo Systems 3030 Electrical Aerosol Size Analyzer	≈125W		≈ 2 min per analysis
Royco 218 Optical Particle Counter	≈50 W		
University of Minnesota Multichannel Analyzer	≈50 W		
Theta Sensor LS-400 SO_2 Monitor	7 W	0-1* (ppm) 0-10 (ppm)	15 sec[a]
REM 612 Ozone Monitor	60 W	0-0.5 (ppm)	5 sec
Monitor Labs 8440 NO/NO_x Monitor	400 W	0-0.5* (ppm) 0-1 (ppm) 0-2 (ppm) 0-5 (ppm)	5 sec
Andros 7000 CO Monitor	125 W	0-50(ppm)	5 sec[b]
MRI Airborne Instrument Package:			
Temperature		-5 to + 45 (°C)	5 sec
Humidity		0-100 (%)	30 sec
Turbulent Dissipation		0-10 ($cm^{2/3}$ sec^{-1})	3 sec (to 60%)
Altitude		0-10,000 (ft)	1 sec
Indicated Airspeed		50-150 (mph)	1 sec
Metrodata M/8 VOR Analog Converter	10 W		1 sec
Two Metrodata 620 Data Loggers, 20 channels each	35 W (each)		48 channels/sec (each)

* Normal operating range.

(a) Improved to an effective response time of 3 sec through transient response corrections applied in data processing.

(b) Fast time response by special order.

The Environment One condensation nuclei monitor described by Rich (1970) is sensitive to particles less than 0.1 micron in diameter, and thus complements the nephelometer. The instrument humidifies an air sample and expands it in a cloud chamber, causing condensation on the particles in this size range. The resulting cloud attenuates a light beam which is focused on a light-sensitive element.

The Thermo Systems, Inc. (TSI), electrical aerosol analyzer and the Royco optical particle counter, shown in Figure 4, together measure the particle size distribution of the ambient aerosol. The electrical aerosol analyzer sizes the smaller particles by their electrical mobility, and the optical counter sizes the larger particles by their scattering cross section. These two instruments, together with their accompanying multichannel analyzer, were installed and maintained by the University of Minnesota personnel associated with the project. Details of their operation have been given by Sem (1975) and Liu et al. (1973).

The mobility analyzer was operated in conjunction with a grab bag sampling system, shown in Figure 5. The normal mode of operation consisted of rapidly filling the bag (less than 3 sec) and then starting the analysis of its contents. This analysis took nearly two minutes. The bag would then be completely emptied, flushed (filled and emptied), and the system readied for the next sampling. Normally, only one sample was obtained during a particular traverse due to the cycle time required by the system.

The optics and sampling probe for the optical particle counter were mounted in a protective pod (Figure 6) attached to the wing of the airplane. Vacuum and electrical lines were strung through the wing to the interior of the aircraft.

The components of the multifilter sulfate sampling system are shown in Figures 4 (control manifold) and 7 (filter holders). Operation of the system was controlled from the filter manifold by the use of manual valves and a method of determining the flow. A single filter was normally exposed during all of the plume traverses at a given distance from the source, as indicated in Appendix A. The exposed filter was later analyzed for sulfate at Washington University by a sensitive flash vaporization/flame photometric technique described by Husar, et al (1975).

Gas Monitors

The MRI aircraft carried monitors for sulfur dioxide, NO and NO_x, ozone, and carbon monoxide. These instruments are shown in Figure 8.

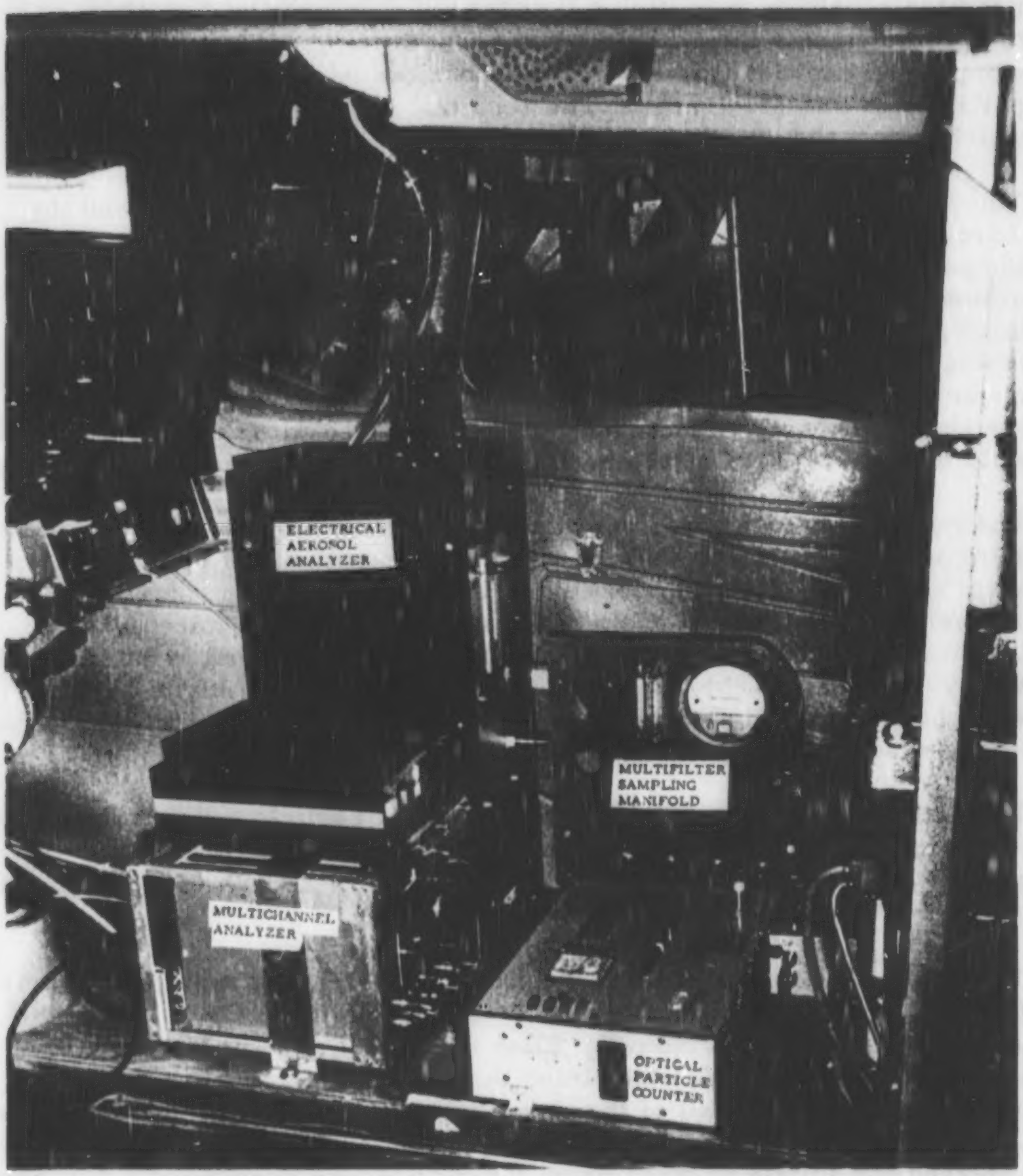
ELECTRICAL AEROSOL ANALYZER
MULTIFILTER SAMPLING MANIFOLD
MULTICHANNEL ANALYZER
OPTICAL PARTICLE COUNTER

Figure 4. Installation of electrical aerosol analyzer, Royco electronics, multichannel analyzer, and multifilter sampling manifold in MRI aircraft.

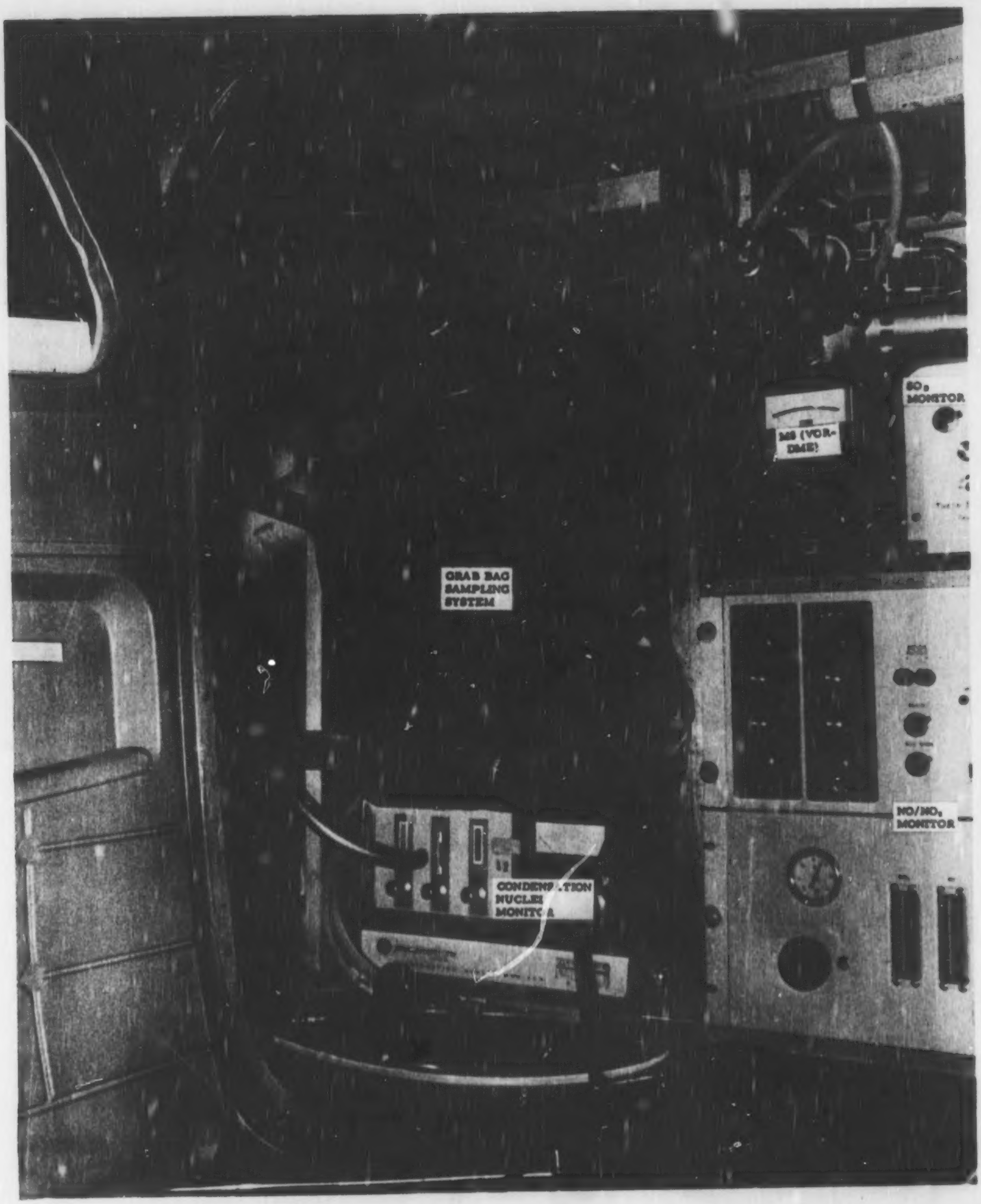
SO₂ MONITOR
MS (VOR-DME)
GRAB BAG SAMPLING SYSTEM
NO/NOₓ MONITOR
CONDENSATION NUCLEI MONITOR

Figure 5. Installation of grab bag sampling system in MRI aircraft. Bag supplied sample to electrical aerosol analyzer.

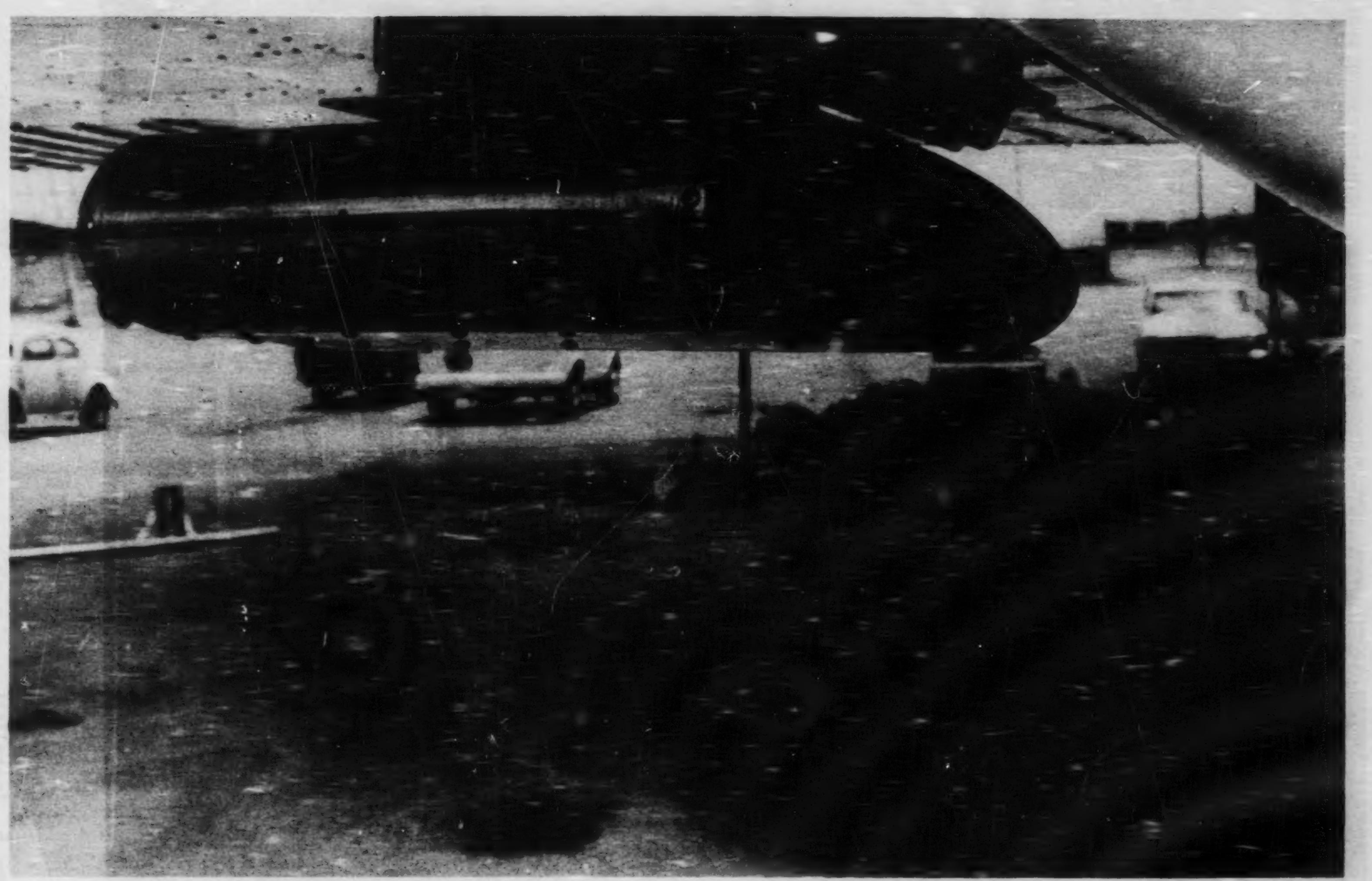

Figure 6. Wing pod housing optics for Royco optical particle counter. Sampling probe (not shown) was inserted in center orifice.

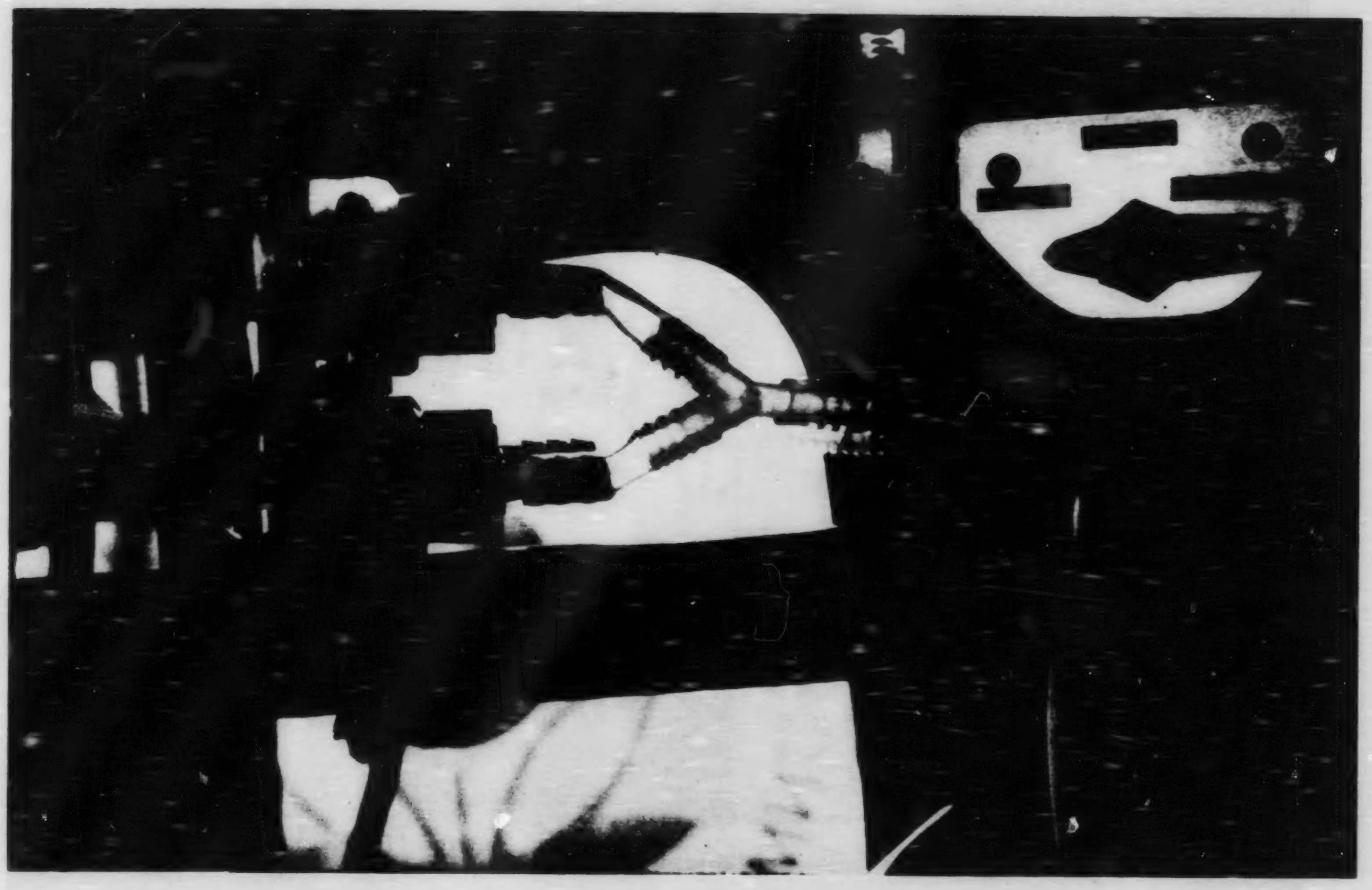

Figure 7. Installation of sulfate filter holders in MRI aircraft.

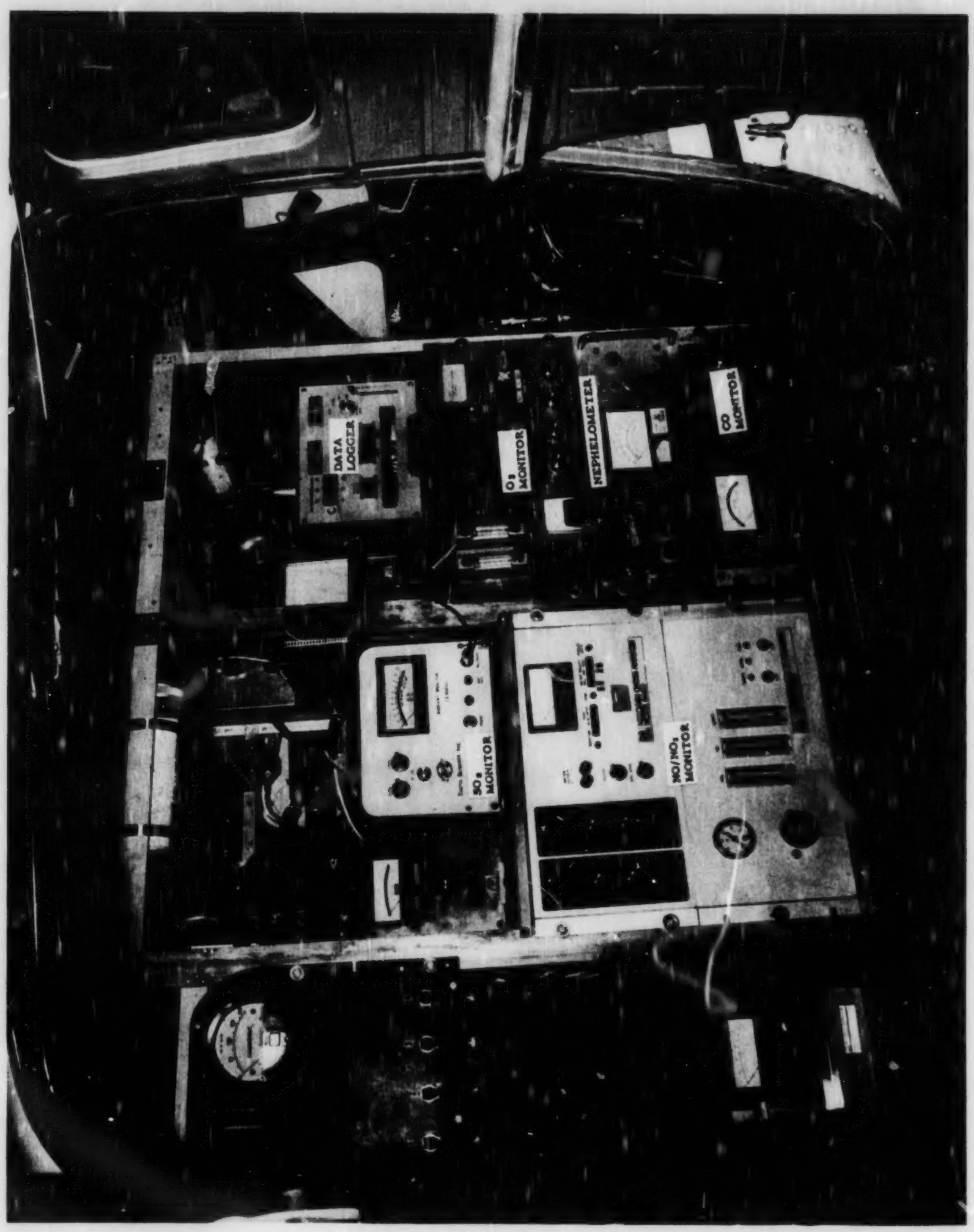
DATA LOGGER
O_2 MONITOR
NEPHELOMETER
CO MONITOR
SO_2 MONITOR
NO/NO_2 MONITOR

Figure 8. Installation of gas monitors in MRI aircraft.

The Theta Sensor SO_2 monitor utilizes an electrochemical cell to measure the concentration of SO_2. This instrument was the slowest responding of the continuous monitors, with a response time to 90 percent of 15 seconds. Through the incorporation of a transient response correction subroutine into the data reduction software, as described by Markowski (1975), the effective response time of this instrument was cut to only 3 seconds (Figure 9). The small size and limited power demands of the instrument are its principal advantages.

The REM ozone monitor is a chemiluminescent device that measures the amount of light produced by the reaction of ozone and ethylene. A small lecture bottle mounted behind the pilot's seat was the source of the necessary ethylene.

The Monitor Labs NO/NO_x monitor has dual reaction chambers for the simultaneous chemiluminescent detection of NO and NO_x (NO_x = NO + NO_2). The concentration of NO is determined from the light produced by its reactions with internally generated ozone. The NO_x concentration is measured by first passing the sample through a catalytic converter which reduces NO_2 to NO.

The Andros 7000 CO Monitor employs the dual isotope fluorescent source nondispersive infrared absorption technique described by Link, et al (1971). The principal advantage of the technique is the elimination of interference by water vapor and carbon dioxide.

Meteorological Sensors

Ambient temperature, relative humidity, and turbulent dissipation were measured in the aircraft as part of the MRI Airborne Instrument Package (Figure 10). The ambient temperature outside the aircraft is measured by a vortex temperature sensor using a thermister for the sensing element. The relative humidity sensor uses a strain gage to measure the stress on a cellulose fiber, the accuracy of the measurement being about ±5 percent RH. Turbulence is measured by an MRI Universal Indicated Turbulence System described by MacCready, et al (1965). The sensor is a standard pitot-static probe connected to a Validyne P-24, 0.7 psid differential pressure transducer. The instrument measures pressure fluctuations in the 2 to 40 Hz range and the signal is processed to give an output proportional to the energy dissipation rate to the 1/3 power. The scale of 0 to 10 $cm^{2/3}$ sec^{-1} spans a range from calm air to what is considered severe turbulence for a light plane. The output of the instrument is independent of the speed of the aircraft for air speeds above 50 mph.

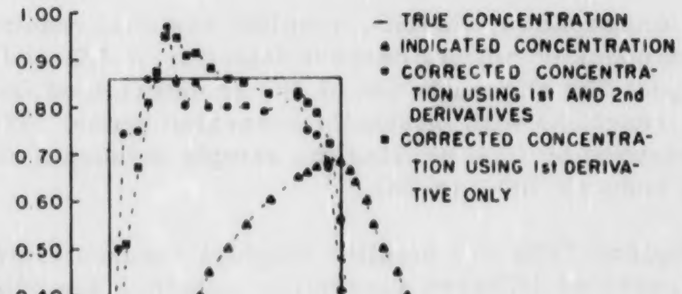

10 second input pulse

Figure 9. Corrected transient response of Theta Systems SO_2 monitor (Markowski, 1975). Corrections were incorporated in data reduction software to speed effective time response of instrument.

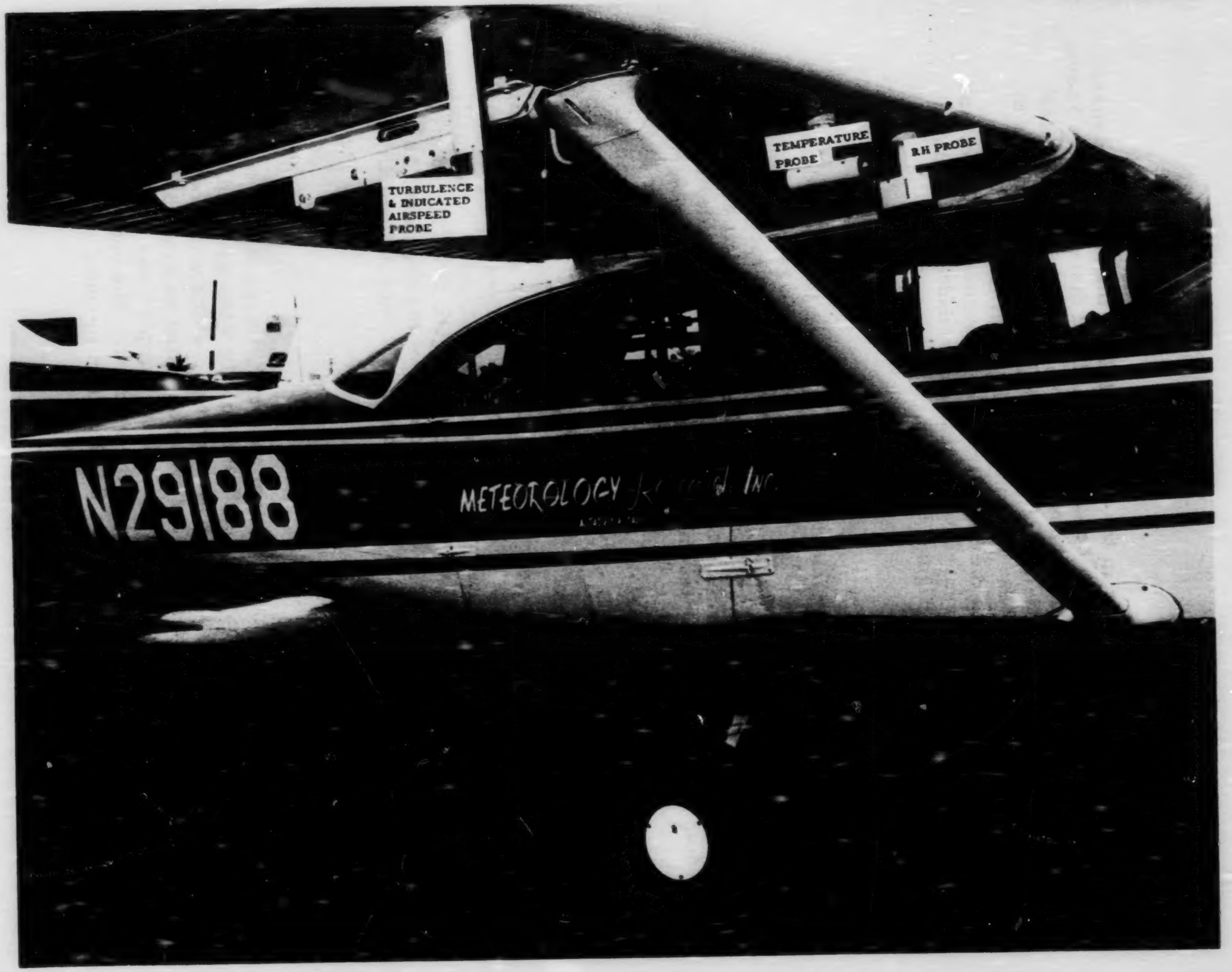
TURBULENCE & INDICATED AIRSPEED PROBE
TEMPERATURE PROBE
RH PROBE
N29188
METEOROLOGY Research Inc

Figure 10. Probes for MRI airborne instrument package.

Position Sensors

The position instrumentation in the aircraft utilized the standard aircraft VOR and DME systems, which detect the radial and distance from a known ground omnidirectional radio transmitter. The aircraft VOR and DME were interfaced to a Metrodata M/8 package to convert their signals to an analog output. Altitude was measured by a Validyne P-24 15 psi absolute pressure sensor in the MRI Airborne Instrument Package, and indicated airspeed was measured by a pressure transducer associated with the turbulence probe (Figure 10).

Data Recording System

The output of the above instruments was recorded on two Metrodata 620 digital data loggers (Figure 11). The first data logger recorded twenty channels of data, including the position information, all meteorological parameters, all gas measurements, and the light scattering coefficient and condensation nuclei count. The second data logger was dedicated to recording the particle size distribution measurements of the electrical aerosol analyzer/optical particle counter/multichannel analyzer system. The outputs of the nephelometer, condensation nuclei monitor, and SO_2 NO, NO_x, and CO monitors were recorded on this second data logger as well.

Both data loggers recorded at a rate of 48 channels per second, and internal digital clocks were simultaneously set for the two units. The clocks provided time in hours, minutes, and seconds to each unit. A manually operated Mode/Event switch (ten different modes with ON/OFF positions) was used to mark events during the flight on one of the channels, and another channel was labeled with the tape code as a backup identification system.

Support System

All instruments except the multichannel analyzer, temperature, turbulence, indicated airspeed, altitude, and relative humidity were powered by a 1 kw-110 v inverter run off the aircraft power system, which was modified to a 24 volt system. The above exceptions were operated on available aircraft DC power. The vacuum source for the sulfate sampler was provided by two venturi mounted on the left wing of the aircraft. The vacuum source for the bag system was provided by a third venturi mounted on the left engine cowling.

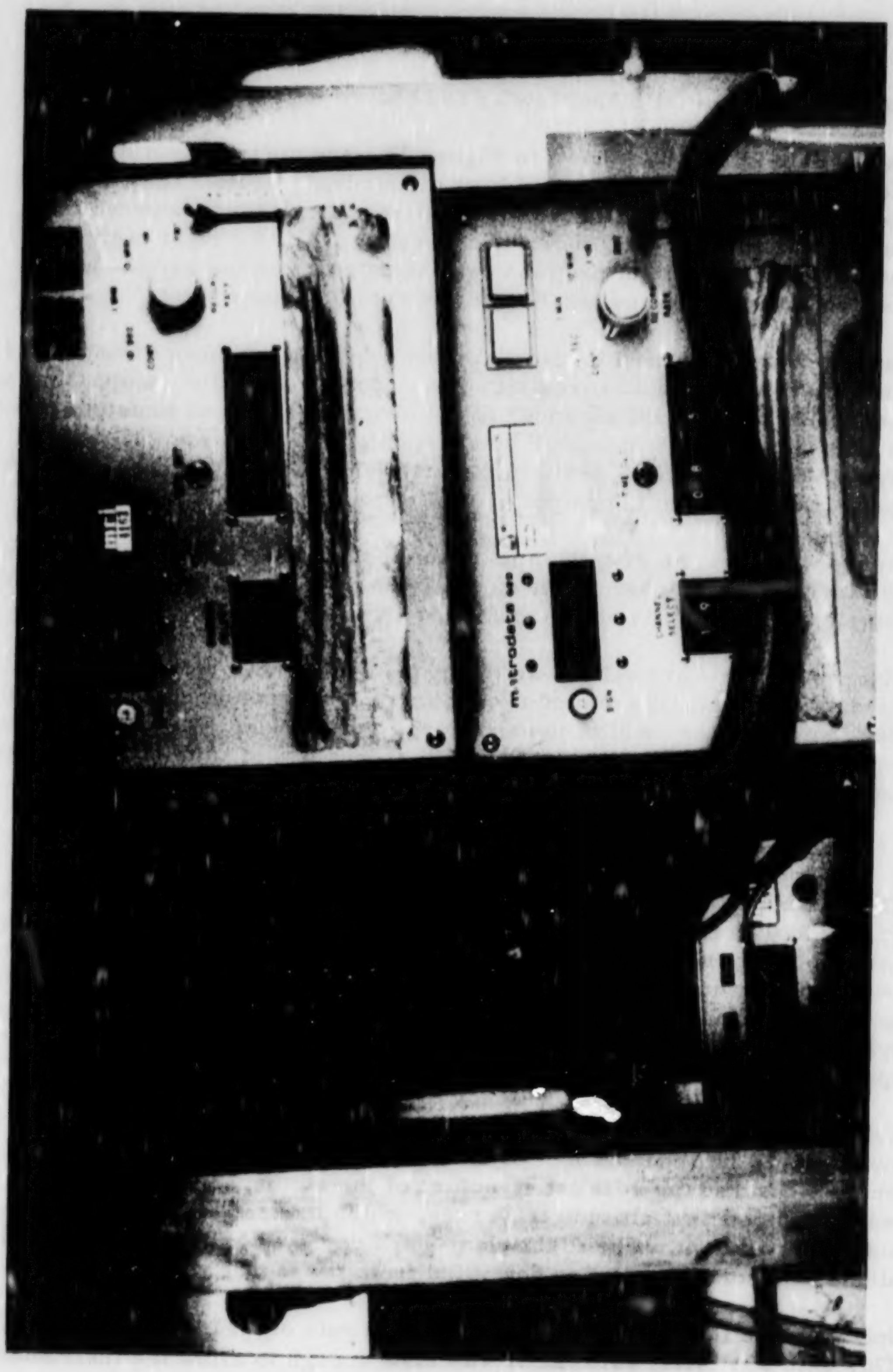

Figure 11. Installation of data loggers in MRI aircraft.

CONFIGURATION OF SAMPLING SYSTEM

The sample inlet tubes shown in Figure 12 were mounted in a dummy window panel on the left-hand side of the aircraft. Flight tests by MRI and normally recorded data both indicate no interference between the sample inlets and the engine exhaust located under the right engine cowling. The effects of propwash and slipstream on the sample have been reported by Adams and Koppe (1969) to be unimportant.

Ram pressure was used to move air through the inlet tubes during flight. Since there were few flow restrictions, the velocity in the sample tube was reasonably close to the airspeed of the aircraft. The gas monitors were connected to the inlet manifold by short lengths of 1/4 inch OD Teflon tubing. Static sampling ports in the manifold prevented changes in flight speed from affecting the output of the instruments.

Figure 13 shows the arrangement of the instruments in the aircraft cabin. The inverter, not shown in the figure, was installed in the belly pod. The sample flow system is shown in Figure 14.

Figures 15 and 16 are schematic diagrams of the instrument wiring used for the data loggers. The output of each instrument was directed through the junction box to the input of the appropriate data logger. All instruments were plugged into the junction box with banana plugs, thus facilitating any necessary wiring changes.

FLIGHT AND SAMPLING PROCEDURES

The first flight of each sampling day was preceded by a 1-1/2 hour warm-up period with the instruments connected to 110 v ground power. When several flights were made during the day, the instruments were also run on ground power between flights. A standard preflight procedure was used to check out the instruments, the data acquisition system, and the sampling system; the gas and aerosol monitors were zeroed and, where possible, spanned electronically.

The sampling patterns flown during the 1974 MISTT field program are summarized in Appendix A. Each flight consisted of spiral soundings, which measured the vertical structure of the atmosphere above a given point, and constant altitude traverses, which mapped the horizontal distribution of pollutant. The flight plans were designed to characterize a given plume at discrete distances downwind from its source.

Spirals were flown at an ascent or descent rate of 500 feet per minute. This rate was fairly critical; it was slow enough to allow the instruments to

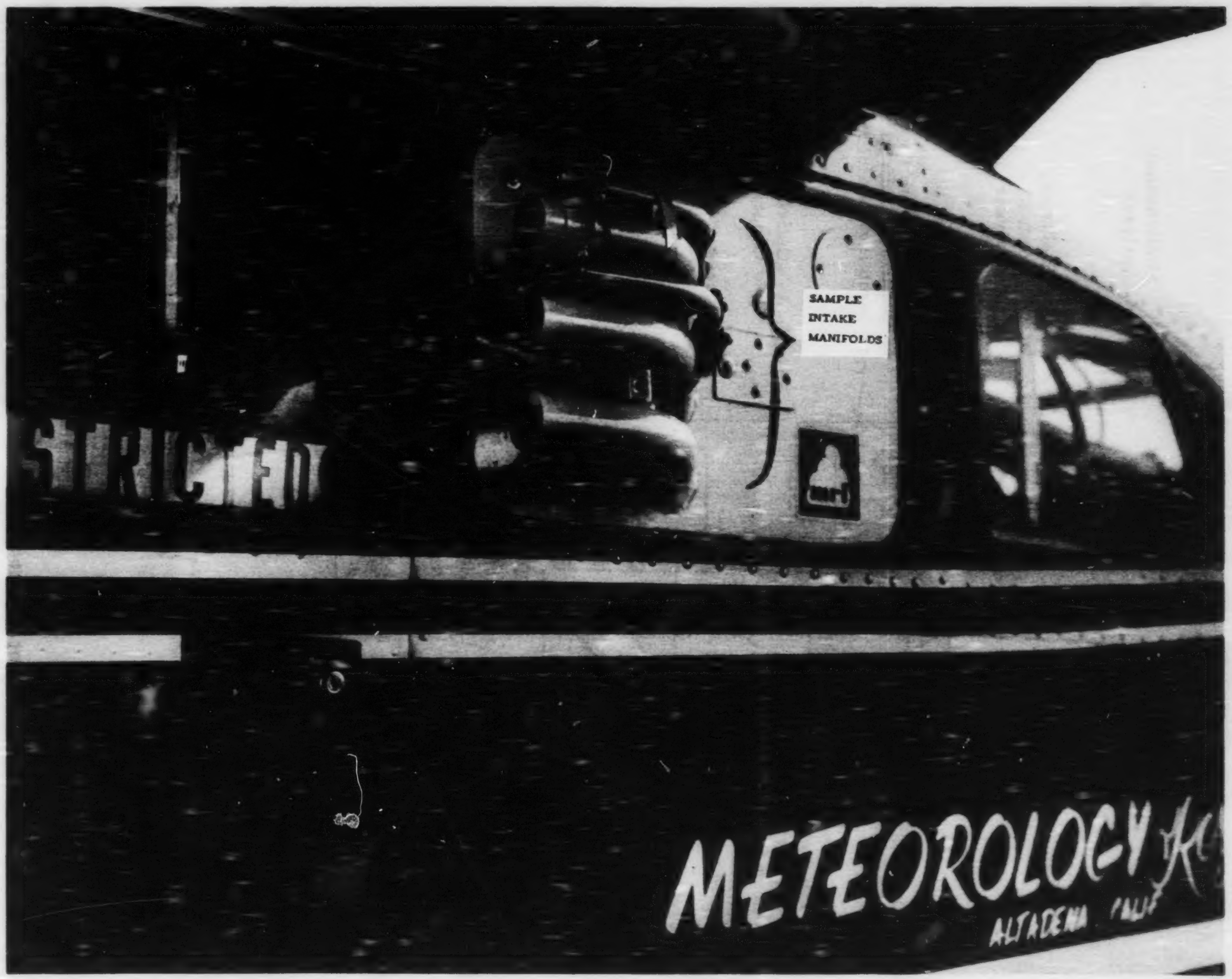
SAMPLE
INTAKE
MANIFOLDS
STRICTED
METEOROLOGY
ALTADENA CALIF

Figure 12. Sample intake manifolds on left-hand side of aircraft.

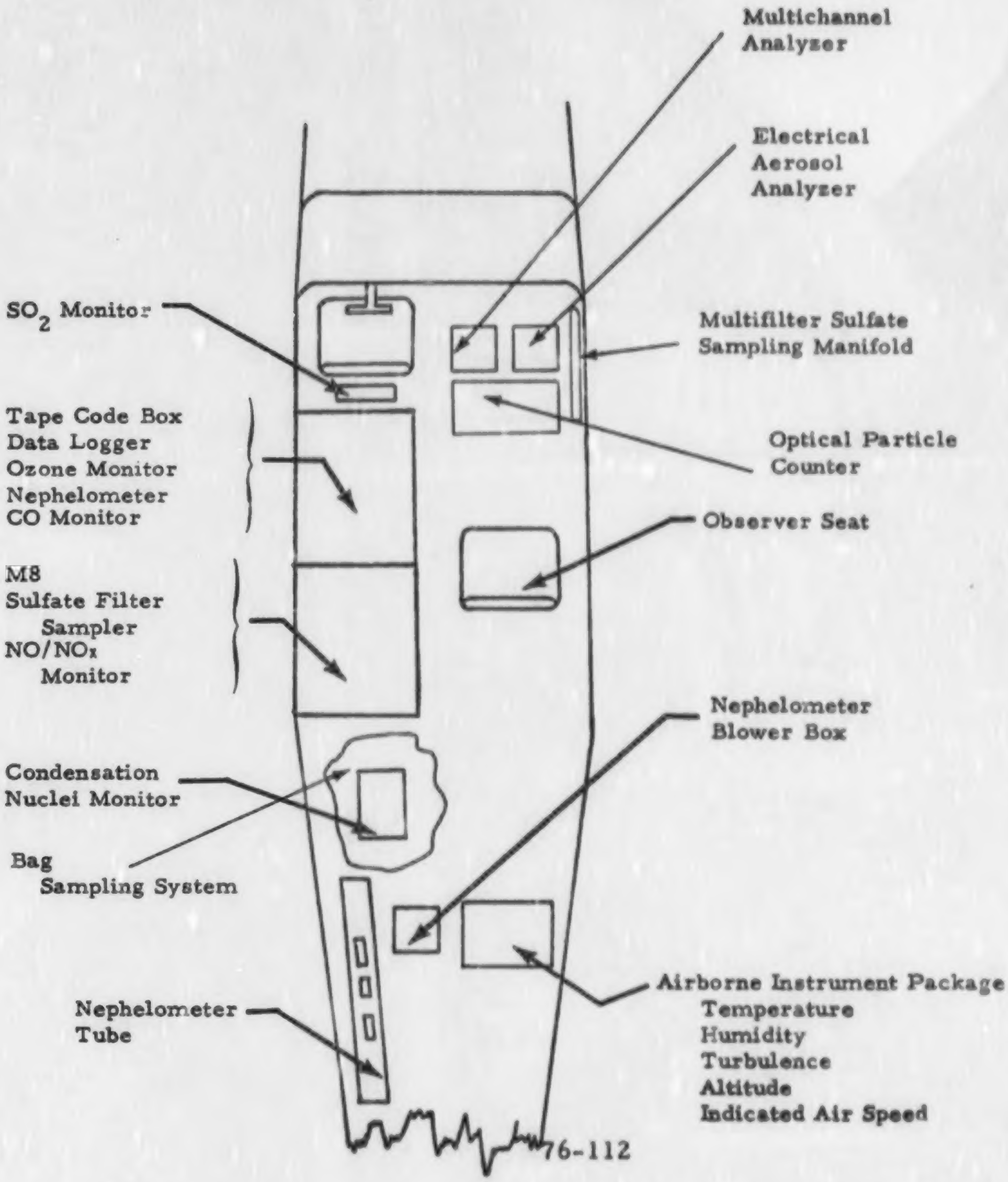
Multichannel Analyzer
Electrical Aerosol Analyzer
SO_2 Monitor
Multifilter Sulfate Sampling Manifold
Tape Code Box
Data Logger
Ozone Monitor
Nephelometer
CO Monitor
Optical Particle Counter
Observer Seat
M8
Sulfate Filter Sampler
NO/NOx Monitor
Nephelometer Blower Box
Condensation Nuclei Monitor
Bag Sampling System
Nephelometer Tube
Airborne Instrument Package
Temperature
Humidity
Turbulence
Altitude
Indicated Air Speed
76-112

Figure 13. Instrument layout in MRI aircraft.

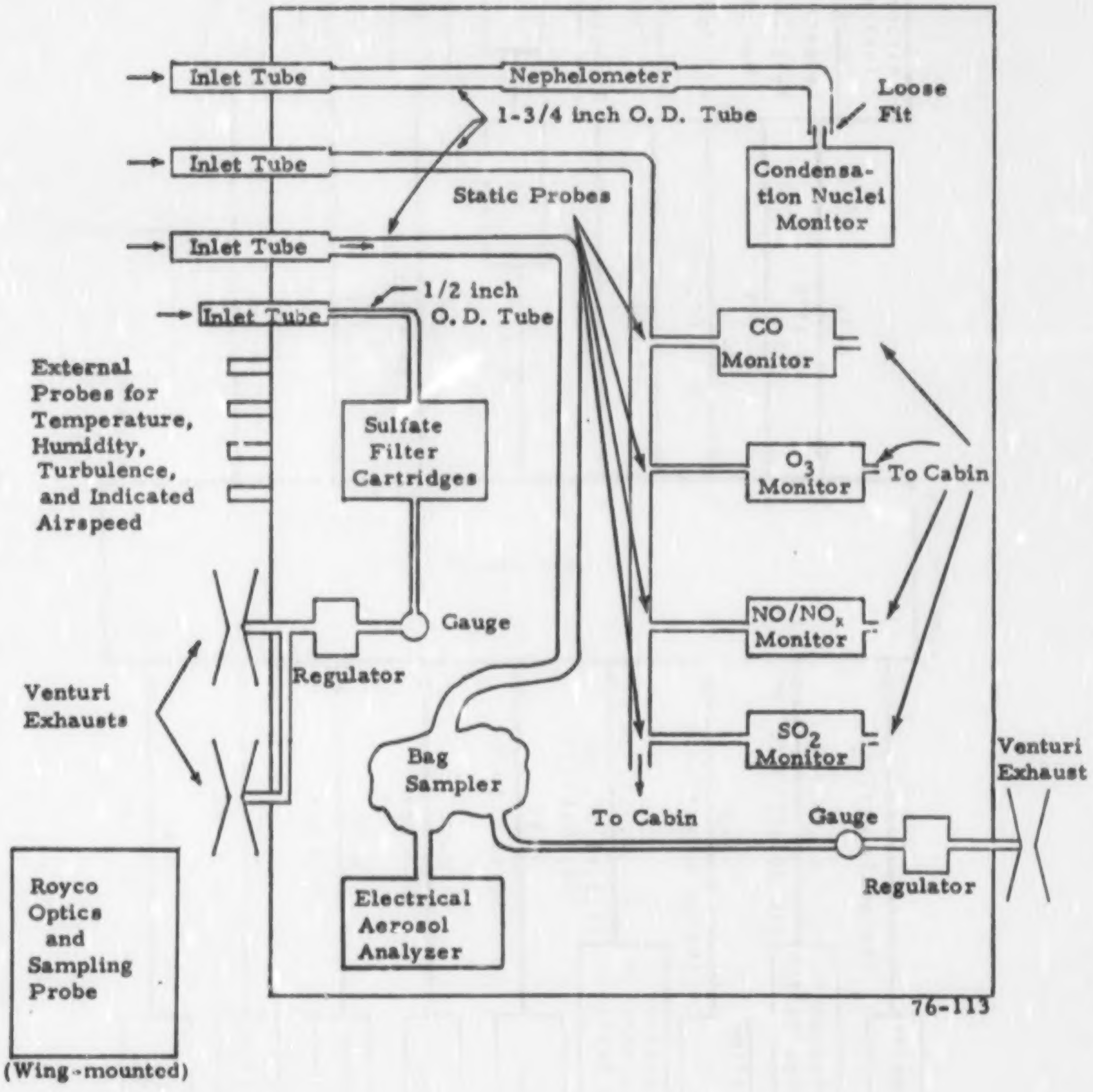
Inlet Tube
Nephelometer
Loose Fit
1-3/4 inch O. D. Tube
Inlet Tube
Condensation Nuclei Monitor
Static Probes
Inlet Tube
1/2 inch O. D. Tube
Inlet Tube
CO Monitor
External Probes for Temperature, Humidity, Turbulence, and Indicated Airspeed
Sulfate Filter Cartridges
O3 Monitor
To Cabin
NO/NOx Monitor
Gauge
Regulator
Venturi Exhausts
SO2 Monitor
Venturi Exhaust
Bag Sampler
To Cabin
Gauge
Regulator
Royco Optics and Sampling Probe
(Wing-mounted)
Electrical Aerosol Analyzer
76-113

Figure 14. Sample flow in MRI aircraft.

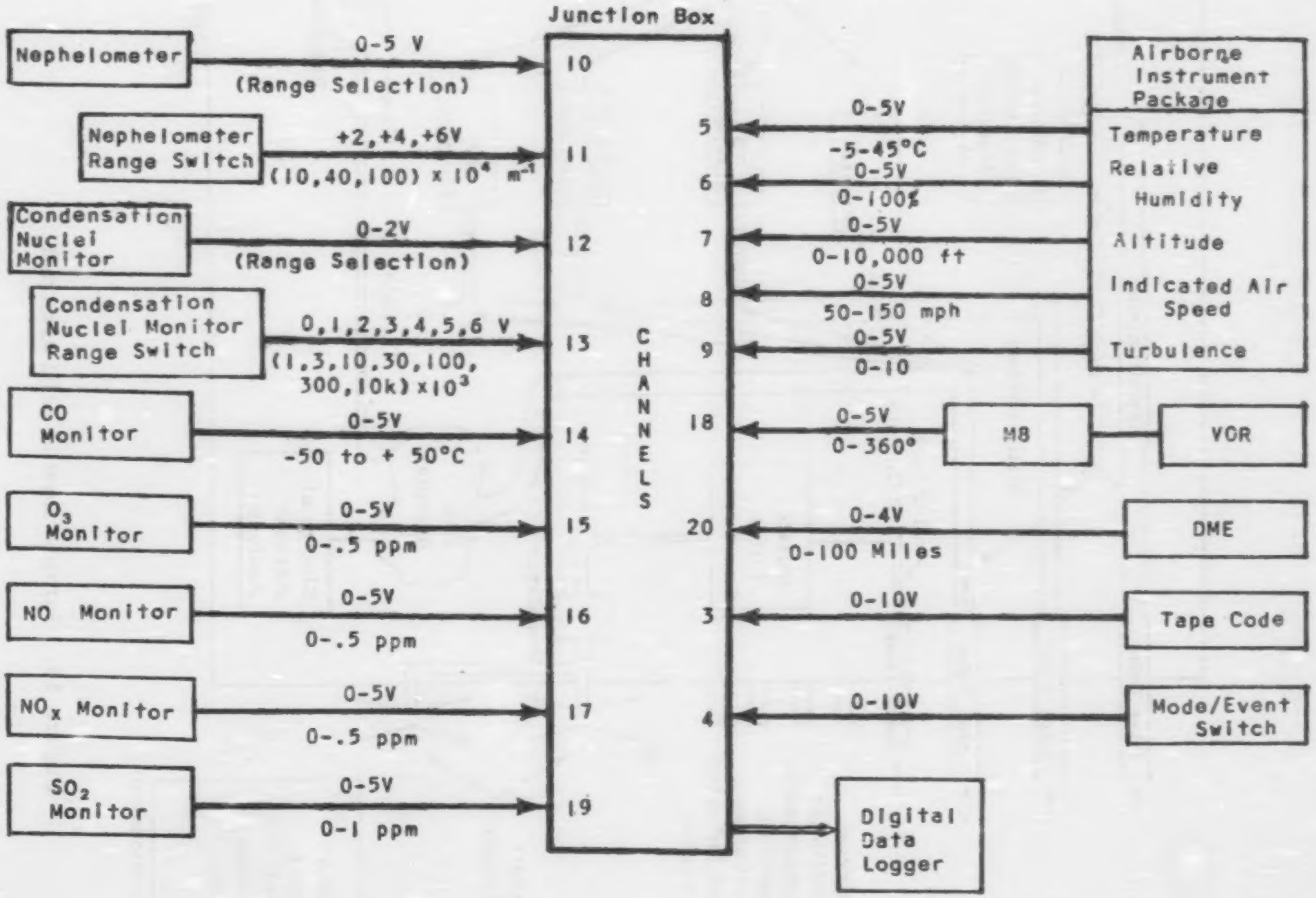
Junction Box
Nephelometer
0-5 V
(Range Selection)
10
Nephelometer Range Switch
+2,+4,+6V
(10,40,100) x 10⁴ m⁻¹
11
Condensation Nuclei Monitor
0-2V
(Range Selection)
12
Condensation Nuclei Monitor Range Switch
0,1,2,3,4,5,6 V
(1,3,10,30,100, 300,10k) x10³
13
CO Monitor
0-5V
-50 to + 50°C
14
O₃ Monitor
0-5V
0-.5 ppm
15
NO Monitor
0-5V
0-.5 ppm
16
NOₓ Monitor
0-5V
0-.5 ppm
17
SO₂ Monitor
0-5V
0-1 ppm
19
CHANNELS
Airborne Instrument Package
Temperature
0-5V
-5-45°C
5
Relative Humidity
0-5V
0-100%
6
Altitude
0-5V
0-10,000 ft
7
Indicated Air Speed
0-5V
50-150 mph
8
Turbulence
0-5V
0-10
9
VOR
M8
0-5V
0-360°
18
DME
0-4V
0-100 Miles
20
Tape Code
0-10V
3
Mode/Event Switch
0-10V
4
Digital Data Logger

Figure 15. Instrument schematic for first data logger.

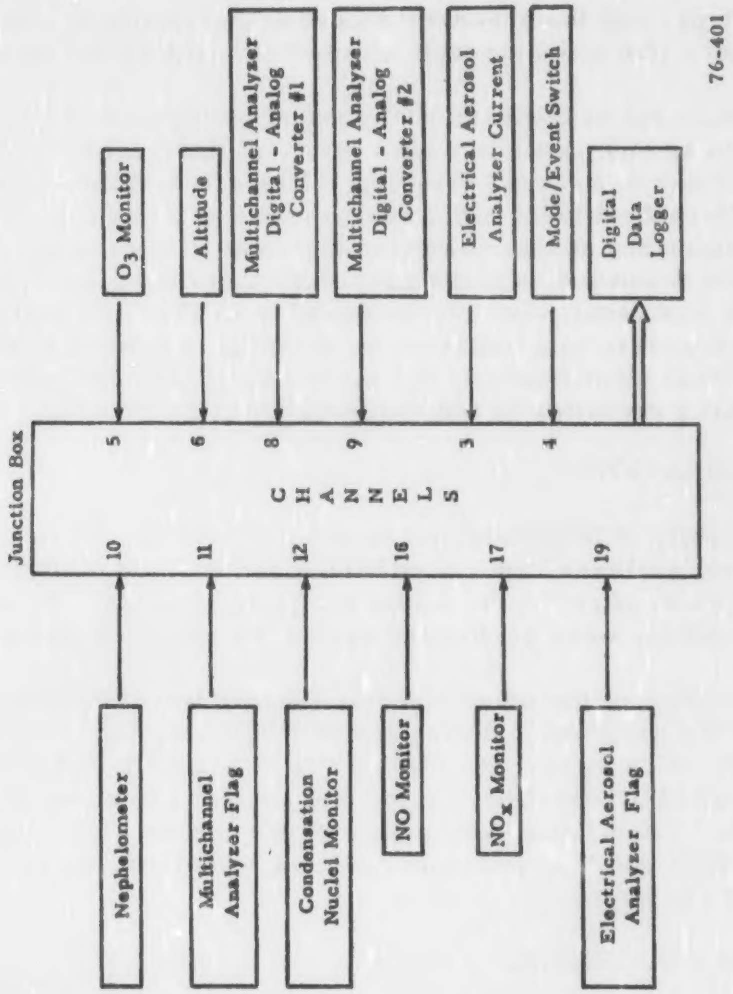
Nephelometer
Multichannel Analyzer Flag
Condensation Nuclei Monitor
NO Monitor
NO_x Monitor
Electrical Aerosol Analyzer Flag
Junction Box
10
11
12
16
17
19
CHANNELS
5
6
8
9
3
4
O_3 Monitor
Altitude
Multichannel Analyzer Digital - Analog Converter #1
Multichannel Analyzer Digital - Analog Converter #2
Electrical Aerosol Analyzer Current
Mode/Event Switch
Digital Data Logger
76-401

Figure 16. Instrument schematic for second data logger.

respond, but slower ascent/descent rates had to be avoided because of the possibility of sampling aircraft exhaust from the previous turn of the spiral. The radius of a spiral was typically 1/2 km. The bottom of the spiral was usually as low as safety permitted, and the top was determined by meteorological conditions. The event switch was used to mark the spiral on the data tape, and the observer recorded the beginning and ending times and altitudes (from the aircraft altimeter) of the spiral (see Figure 17).

For each set of horizontal traverses, recognizable ground landmarks were chosen as end points in such a way that the traverse path was nearly perpendicular to the wind direction. The aircraft then made several flights at different altitudes along the traverse path until the plume had been well characterized at that downwind distance. New end points were then chosen further downwind, and the procedure repeated (see Figure 18). The airspeed was usually as slow as possible to allow for instruement response. Each traverse was indicated on the magnetic tape by the event switch; for additional identification, the times and altitudes of each traverse were manually recorded by the observer on flight records.

CALIBRATION

University of Minnesota personnel performed calibrations of the electrical aerosol analyzer, optical particle counter, and multichannel analyzer before and after the St. Louis sampling program. In addition, two in-field calibrations were performed during the sampling period.

Calibration of the other aircraft sensors were performed both before and after the program. During the study period, the gas monitors were calibrated twice by Mr. R. Rhodes (QAS/QAEML) of the EPA as a part of the "RAPS Cross-Comparison Program for Gaseous Pollutant Measurements." Additional field audits of the gas monitors were performed by both EPA and MRI personnel using a commercially available (Monitor Labs 8500) calibrator.

DATA PROCESSING

All data from the aircraft were processed by Washington University as described by Gillani (1975).

PILOT BALLOON OBSERVATIONS

Observations of wind aloft were made hourly at up to three different locations during each intensive sampling period. Pilot balloons with standard ascent rates were tracked to 1140 m agl by theodolite, and the winds at 110 m altitude intervals calculated by triangulation. Data collection and reduction was performed by MRI personnel under a separate contract.

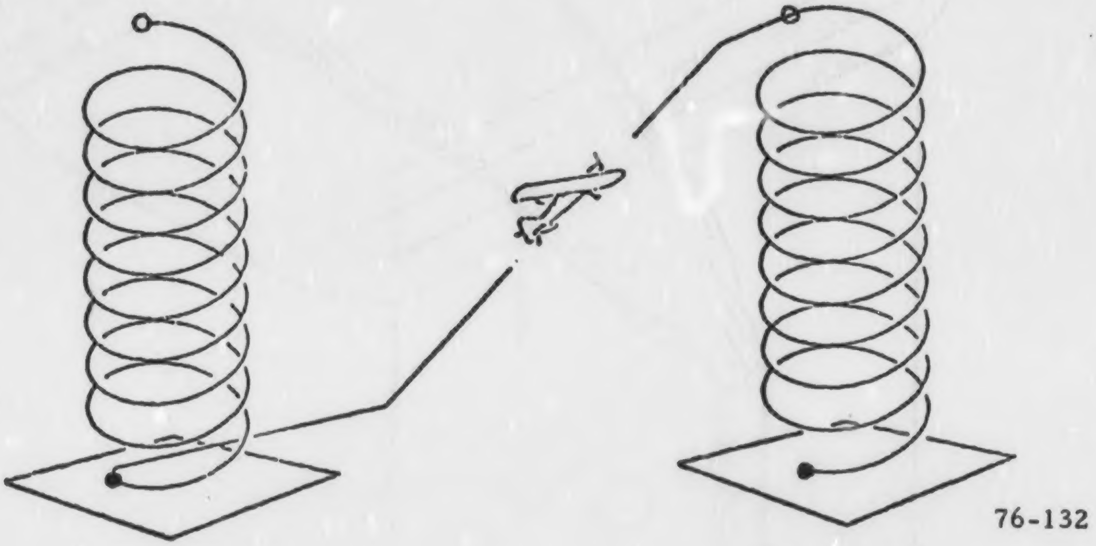

○ Event on, time, altitude, & location noted.

● Event off, time, and altitude noted.

Figure 17. Flight plan for spira[illegible]ndings.

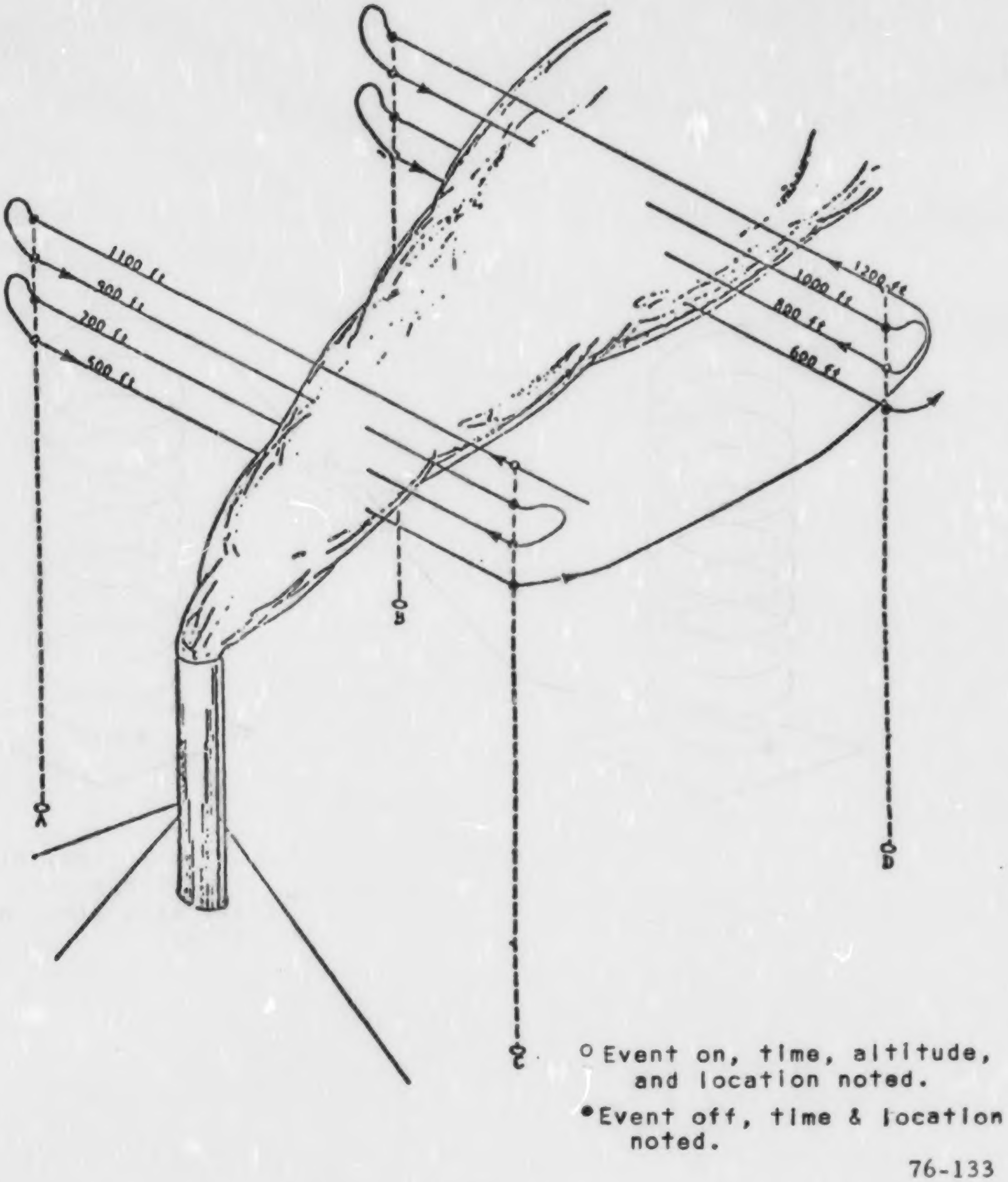
1100 ft
900 ft
700 ft
500 ft
1200 ft
1000 ft
800 ft
600 ft
A
B
C
D
○ Event on, time, altitude, and location noted.
● Event off, time & location noted.
76-133

Figure 18. Flight plan for horizontal traverses. Points A, B, C, and D are ground reference points selected during flight.

SECTION III

METEOROLOGY

INTRODUCTION

During the period from 30 July 1974 through 15 August 1974, two types of synoptic weather regimes affected the St. Louis sampling area. The more prevalent regime was one characterized by moderate to weak anticyclonic surface circulation and weak or disorganized flow patterns aloft. These anticyclonic periods alternated with transition regimes of general cyclonic surface circulation, more clearly defined upper air patterns, and unsettled local weather. The chronology of the two types of regimes is outlined in Figure 19. The following paragraphs describe the synoptic patterns in each period and relate them to the local weather in the sampling area.

30 JULY 1974 - 1 AUGUST 1974 (ANTICYCLONIC)

After the passage of a midlatitude cyclone across the central Mississippi Valley on 28 July, a large dry continental polar air mass moved into the Great Plains Region during 29 and 30 July. By the morning of 31 July, the air mass had spread out and modified into a large flat warm high pressure area occupying the entire eastern half of the country (Figure 20). At the same time, a low center to the north had moved into eastern Canada, leaving very weak westerly flow aloft south of 40° N latitude. As a result, the St. Louis sampling area experienced rather stagnant weather conditions through 1 August, with large and scattered low clouds.

High temperature readings at Lambert Field in St. Louis increased from +30° C to +33° C during this period, while dew points advanced from +13° C to 16° C. The increase in temperature and moisture corresponded directly with the onset of light south-to-southeasterly anticyclonic flow around the surface high pressure center in the eastern part of the country. Aloft, a pronounced subsidence inversion capped the surface mixing layer at around 2130 m (7000 ft) msl during most of the period, inhibiting convective activity and dispersion above the lowest layer of the atmosphere. On 1 August, however, the establishment of neutral to unstable temperature lapse rates throughout the lower 6400 m (20,000 ft) of the atmosphere signaled the beginning of a cyclonic transitional period. By midafternoon on 1 August, a broken ceiling of towering cumulus clouds dominated the St. Louis area.

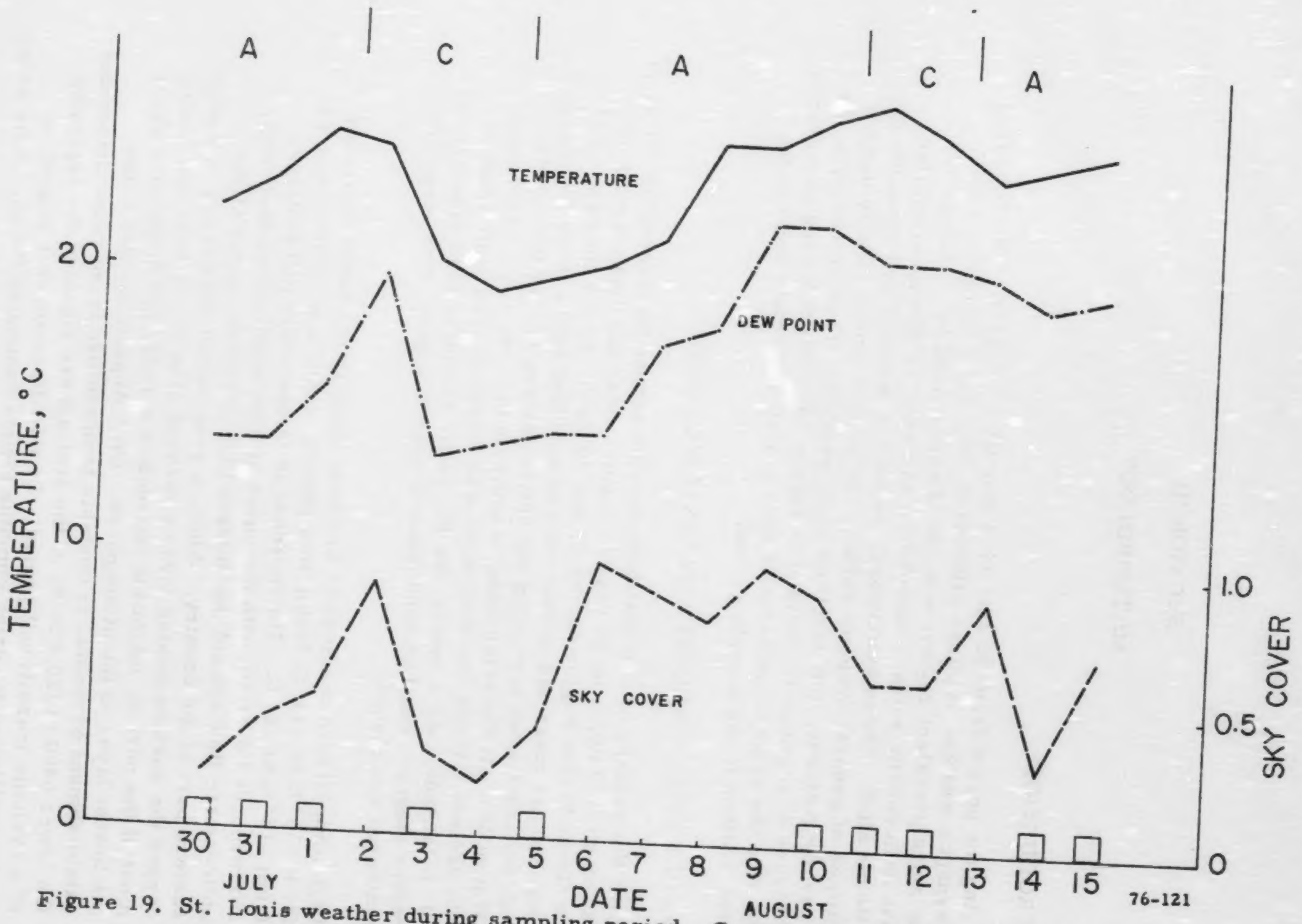

Figure 19. St. Louis weather during sampling period. Curves show daily temperature (24-hour average), dew point (24-hour average), and sky cover (sunrise to sunset average) at Lambert Field, St. Louis (U.S. Department of Commerce, 1974). Type of synoptic regime (C - cyclonic, A - anticyclonic) affecting sampling area is shown at upper edge of graph. Temperature and dew point tended to increase during passage of anticyclones. Sampling days are indicated at bottom of graph.

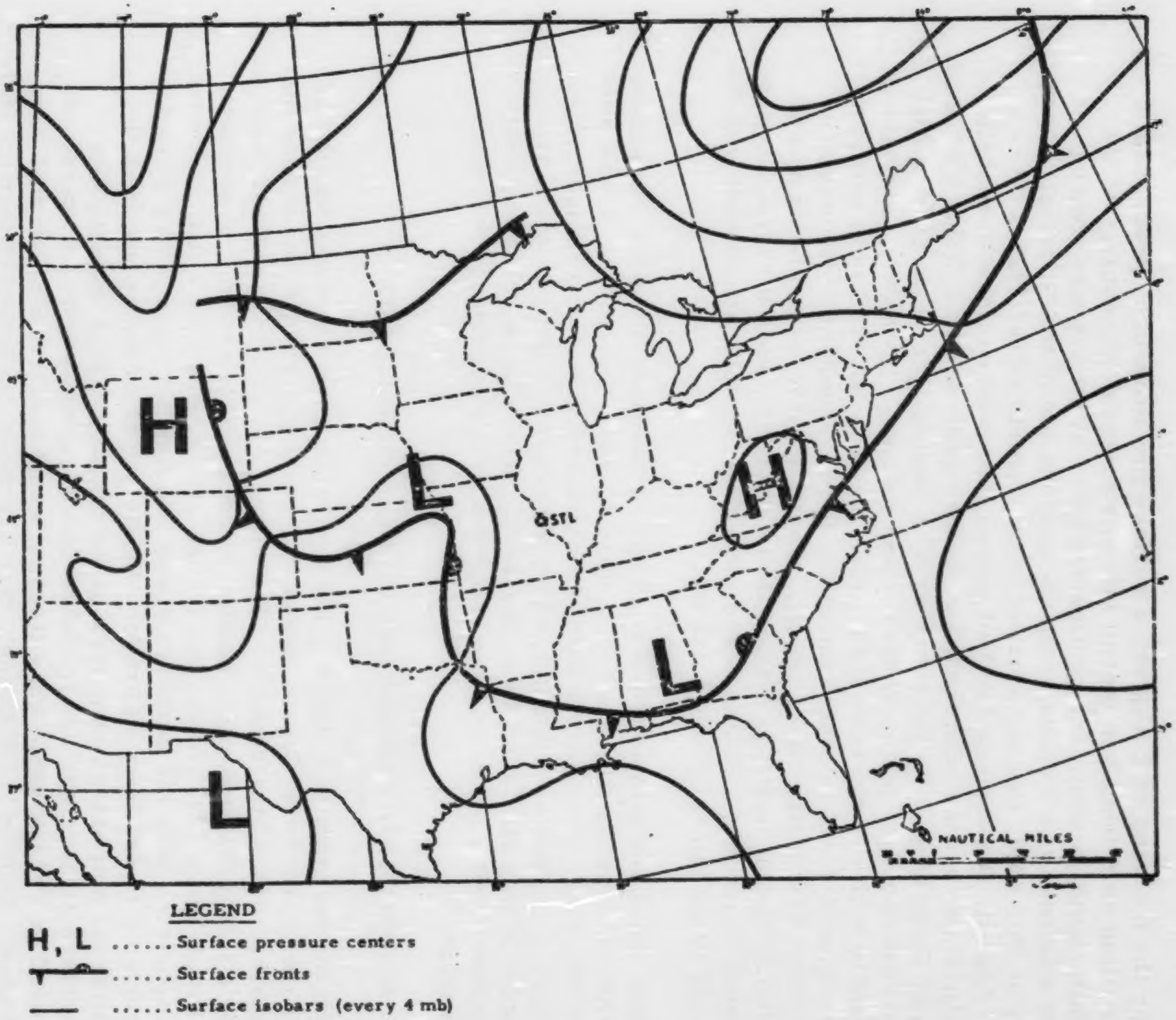
H
L
H
H
L
L
STL
NAUTICAL MILES
LEGEND
H, L ......Surface pressure centers
......Surface fronts
......Surface isobars (every 4 mb)

Figure 20. Weather map for 0700 CDT on 1 August 1974. St. Louis sampling area had been experiencing rather stagnant weather conditions within the large flat high pressure area occupying the eastern half of the country.

2 AUGUST 1974 - 4 AUGUST 1974 (CYCLONIC AND POSTCYCLONIC)

By the morning of 2 August, a surface low pressure system with a trailing cold front had moved into northcentral Missouri. At the same time, a cool, dry continental polar air mass was moving out of southwestern Canada along the eastern lee of the Rockies. By the time this cool, dry air arrived in the central Great Plains late on 3 August, the surface low had moved into northeastern Wisconsin, while the trailing cold front had pushed eastward into Ohio, Kentucky, and Tennessee. By the morning of 4 August, the center of the high pressure ridge was in Nebraska and Kansas. However, the onset of stable anticyclonic flow did not take place in the St. Louis sampling area until 5 August, because of the slow movement of the surface low in Wisconsin. As a result, conditions favorable to mixing and pollutant dispersion persisted in the sampling area through 4 August, even though the cloudiness and inclement weather associated with the cold front had ended on 3 August.

Dew point and temperature readings at Lambert Field reached their highs during the afternoon of 2 August, when the cold front was still to the west. The lowest absolute moisture values and temperatures were recorded on 4 August, when the cool, dry anticyclone was approaching St. Louis from the west. Winds were southwesterly before frontal passage, then northwesterly to northerly through 4 August.

5 AUGUST 1974 - 10 AUGUST 1974 (ANTICYCLONIC)

On the morning of 5 August, the dry continental air mass which had moved down from Canada began to modify and spread out across the eastern half of the country. The center of this air mass was marked by a high pressure ridge located in northern Missouri and southern Iowa (Figure 21). Aloft, the trough of low pressure which had been associated with the surface cyclonic system of 2 and 3 August had moved into northern Labrador, leaving light westerly winds in the midwest and eastern sections of the country. By 6 August, the surface anticyclone had modified into a moist, warm air mass, centered in Pennsylvania but extending westward to the Western Plains states. During 7 - 9 August, this air mass continued to warm, while additional moisture circulated into the central and eastern states from the Gulf of Mexico. The center of the high pressure ridge during that time drifted slowly from central Pennsylvania to Cape Hatteras, finally dissipating over western South Carolina on 9 August.

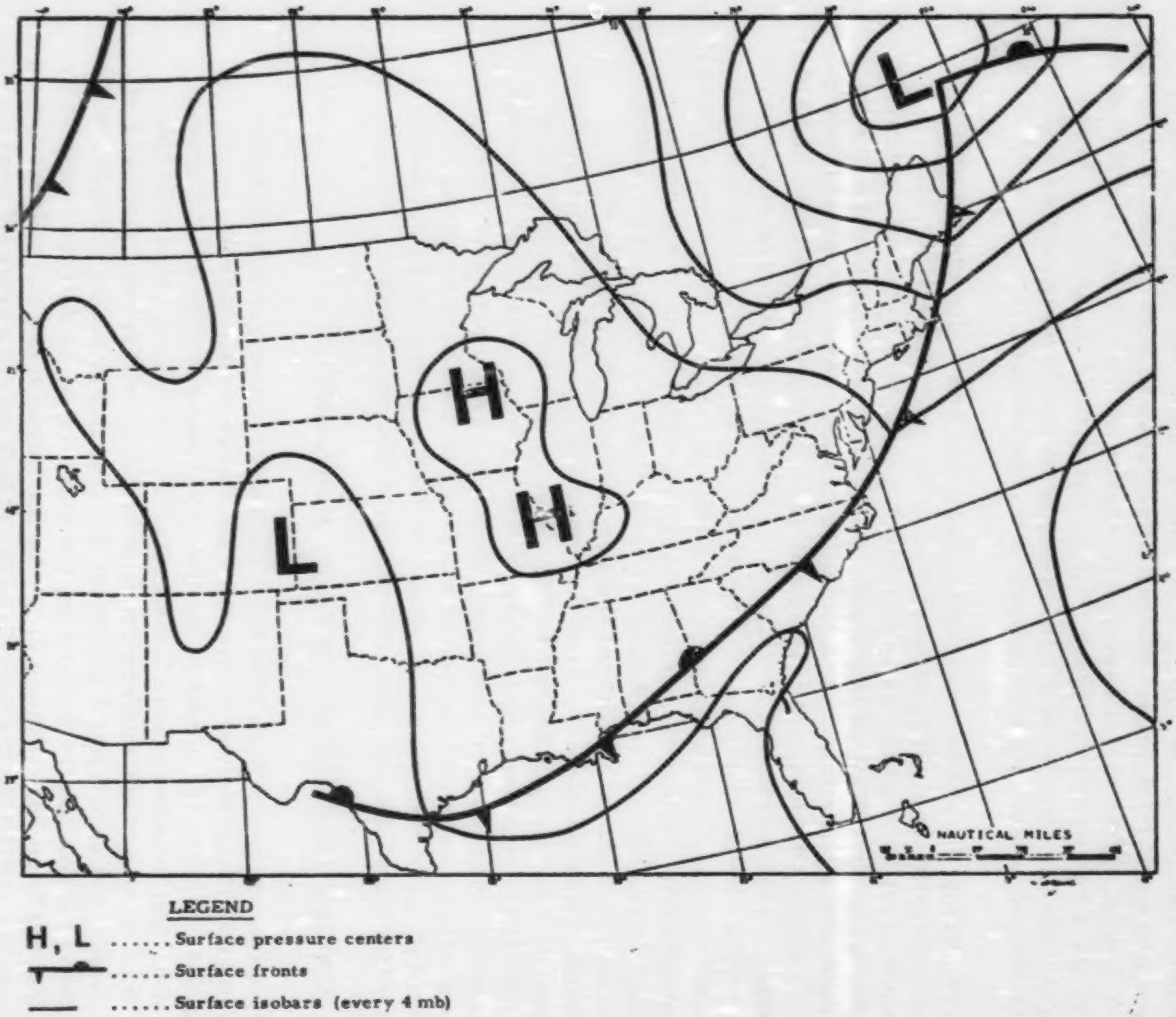
H
H
L
L
NAUTICAL MILES
LEGEND
H, L ...... Surface pressure centers
...... Surface fronts
...... Surface isobars (every 4 mb)

Figure 21. Weather map for 0700 CDT on 5 August 1974. St. Louis sampling area experienced increasing temperature and humidity over next few days as anticyclonic circulation brought in Gulf air.

At that time, a new maritime polar air mass drifted southward from Quebec, extending into the entire eastern half of the United States by the morning of 10 August. Despite the change in high pressure centers, on 9 August light, moist easterly to southeasterly air flow persisted over the Mississippi and Ohio Valleys throughout the period. In the upper atmosphere, weak ridging prevented the development of well-established system path trajectories on the surface.

Skies during the entire five day period were generally cloudy with early morning fog and hazy midday conditions. Some light rain occurred on 10 August due to the development of a cyclonic system to the west, but most of the clouds which persisted during the period lacked enough vertical development to produce rain. Typical temperature soundings during the period showed a neutral or slightly unstable mixing layer below 2438 m (8000 ft) msl capped by a more stable layer above that level. Only on 10 August did the lapse rate show unstable characteristics above the elevated stable layer. Surface temperatures showed daily increases through 8 August, with the daily maximum rising from +26° C on 5 August to +31° C on 8 August. Increasing cloudiness reduced maximum temperatures slightly on 9 and 10 August. Dew points also rose throughout the period, increasing from a low of +14° C on 5 August to +22° C on 9 August. Since the low level winds recorded after 5 August were consistently east to southeasterly, there can be no doubt that the St. Louis sampling area was receiving an extended exposure to advected maritime tropical air circulating around the weak but persistent anticyclone to the east. It wasn't until 10 August that this pattern began to change.

11 AUGUST 1974 - 12 AUGUST 1974 (CYCLONIC)

The broad ridge of high pressure aloft over the eastern half of the continent finally moved to the Atlantic Coast on the morning of 11 August. Behind it, a rather shallow long wave trough aloft began to sink southeastward into the Central Plains. This triggered the formation of a weak surface low and trailing cold front. Because of the weak and short-lived nature of the trough aloft, the surface cyclone became rather poorly defined by the morning of 12 August, especially in its southern half (Figure 22). As the surface low moved northward out of the United States into Canada, it left only a series of weak, quasi-stationary fronts in the middle of the country. As flow aloft south of 45° N latitude continued to dissipate, a rather flat, stagnant synoptic weather pattern began to reestablish itself late on 12 August.

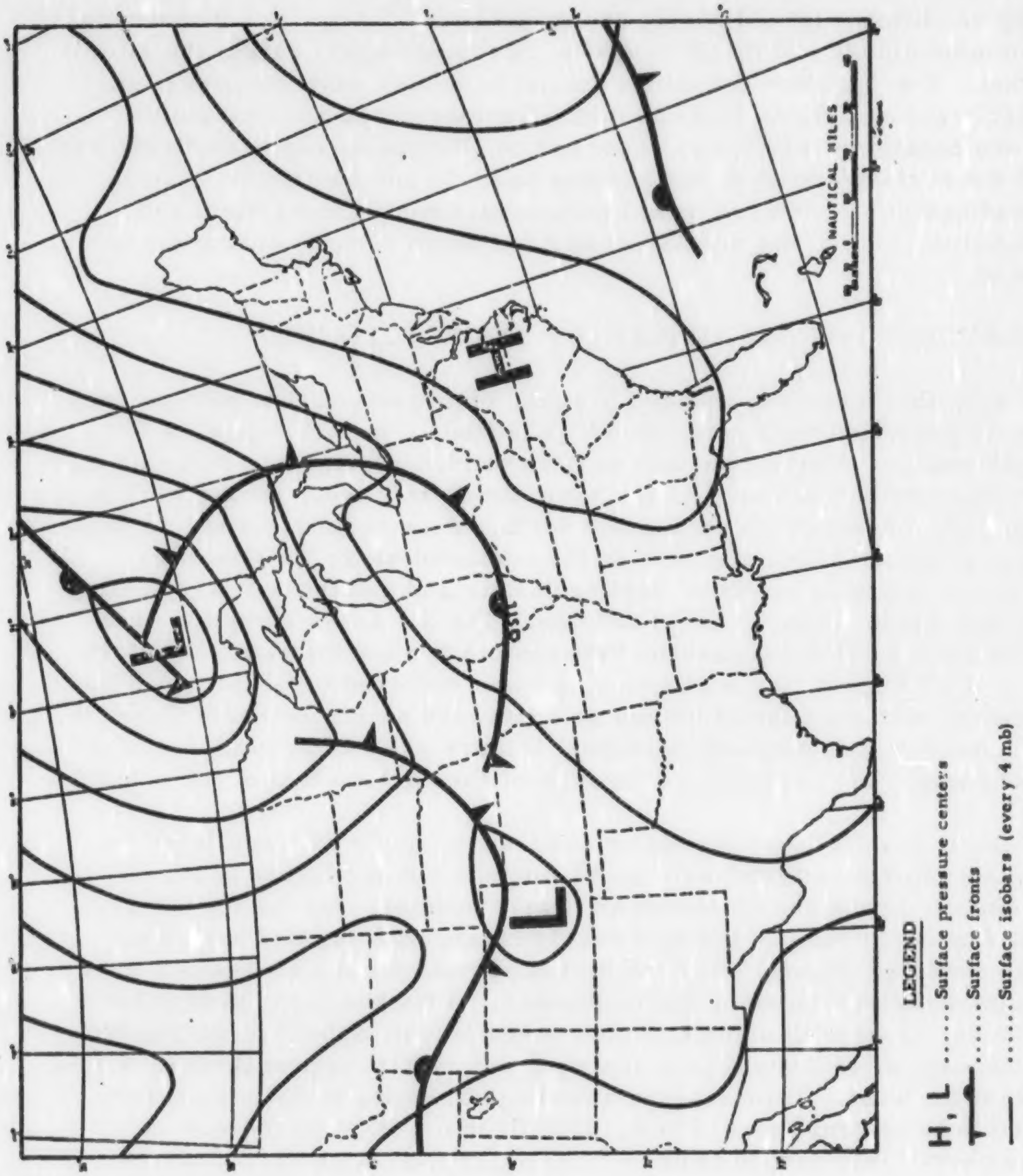
LEGEND
H, L ....Surface pressure centers
.......Surface fronts
.......Surface isobars (every 4 mb)
NAUTICAL MILES
H
L
L

Figure 22. Weather map for 0700 CDT on 12 August 1974. St. Louis sampling area experienced scattered thunderstorm activity from 10 August to 13 August.

Skies were broken to overcast during most of 11 August, with some scattered thunderstorms in the St. Louis sampling area. Improved sky conditions existed during the morning of 12 August, but towering cumulus clouds and thundershowers developed again during the afternoon. Temperature soundings during both days were relatively unstable above 2740 m (9000 ft) msl. Temperatures and dew points were consistent with those recorded on 10 August, but wind directions at the surface and aloft had become south to southwesterly. Local readings of all meteorological parameters were inconsistent and variable close to the persistent thunderstorm activity during the two days.

13 AUGUST 1974 - 15 AUGUST 1974 (ANTICYCLONIC)

During this three-day period, a weak, disorganized flow pattern once again prevailed aloft south of 40° N latitude. In that region, a flat, featureless, synoptic surface pattern produced stagnant, motionless, warm, humid weather. At the same time, relatively strong west to east air movement existed to the north. As a result, a weak surface high pressure ridge slid across the continent along the Canadian border, bringing modified continental air and anticyclonic circulation to the region north of 40° N latitude. The St. Louis sampling area was situated at the transition between the two air masses. By morning of 15 August, the northern ridge was centered in Quebec with the anticyclonic circulation extending southward as far as North Carolina, Tennessee, and southern Missouri (Figure 23). Flow aloft continued very weak and disorganized throughout the eastern half of the country.

Skies in the St. Louis sampling area were cloudy with scattered thunderstorm activity early on 13 August, but conditions began to improve during the afternoon and early evening. By the morning of 14 August, skies had become nearly clear, with fog and haze near the surface. Sunny, hazy conditions prevailed until 15 August, with night and early morning fog continuing. A broken layer of high level clouds, along with some cumulus development, appeared during the afternoon of 15 August as a new cyclonic system approached St. Louis from the west. Temperature soundings throughout the period were stable to neutral above 910 m (3000 ft) msl. High temperatures at Lambert Field ranged from +27° C on 13 August to +31° C on 14 and 15 August. Dew point readings near +20° C persisted throughout the three days. Wind directions remained east to southeasterly due to the anticyclonic circulation around the high to the east.

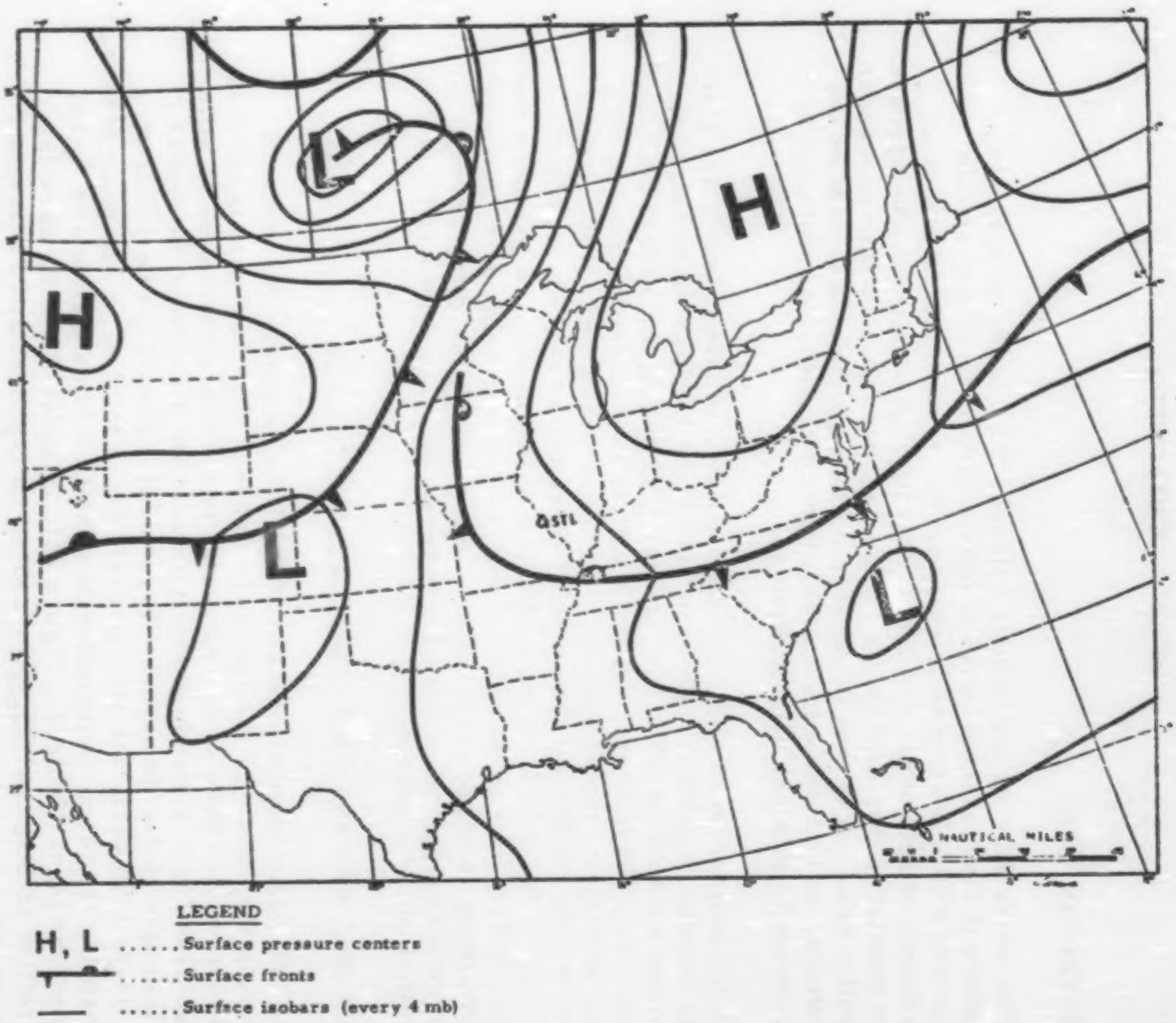
H
L
H
L
L
H
STL
NAUTICAL MILES
LEGEND
H, L ......Surface pressure centers
......Surface fronts
......Surface isobars (every 4 mb)

Figure 23. Weather map for 0700 CDT on 15 August 1974. St. Louis sampling area was situated near transition between two air masses.

SECTION IV

SULFUR CHEMISTRY

INTRODUCTION

The combustion of fossil fuels releases SO_2 to the atmosphere, where it then oxidizes to form sulfate aerosols. These sulfate aerosols have been implicated as causative agents for many of the adverse effects of air pollution. Further, particulate sulfur appears to persist in the troposphere for much longer periods than gas-phase sulfur does. It is thus of great importance to be able to predict the effects, on ambient sulfate aerosol concentrations, of projected increases in national SO_2 emissions.

In the neighborhood of St. Louis, a coal-fired steam generating plant at Labadie (Mo.) and a group of refineries at Wood River (Ill.) are major sources of SO_2. On several days during the 1974 MISTT field program, the MRI aircraft made detailed measurements of the SO_2 concentration, particulate sulfur concentration, and aerosol light-scattering coefficient downwind of these two source areas. In this chapter, the data from these flights are discussed. Particular attention will be paid to the rates at which SO_2 was oxidized to $SO_4^=$ and otherwise removed from the atmosphere, as these rates are critical in determining the relationship between SO_2 emissions and ambient sulfate concentrations.

AN SO_2 BALANCE FOR THE LABADIE PLUME

An unusually complete record of the Labadie plume was obtained during the middle of the day on 14 August 1974. Meteorological conditions at this time were well suited to the characterization of pollutant flow, with a steady easterly flow of air throughout the lowest kilometer of the atmosphere (Figure 24). During the period from 1100 to 1500 CDT, the MRI aircraft flew a total of 19 sampling passes, mapping the plume in considerable detail out to a distance of 45 km from the plant (Table 3 , Figure 25). Figures 26 - 28 show the profiles of SO_2 and b_{scat} measured on representative horizontal traverses of the plume.

The rate at which SO_2 was lost from the plume through all mechanisms can be estimated by comparing the mass flow rates of SO_2 at increasing distances downwind of the plant. These flow rates, which are not affected by cross-plume and vertical dispersion, are

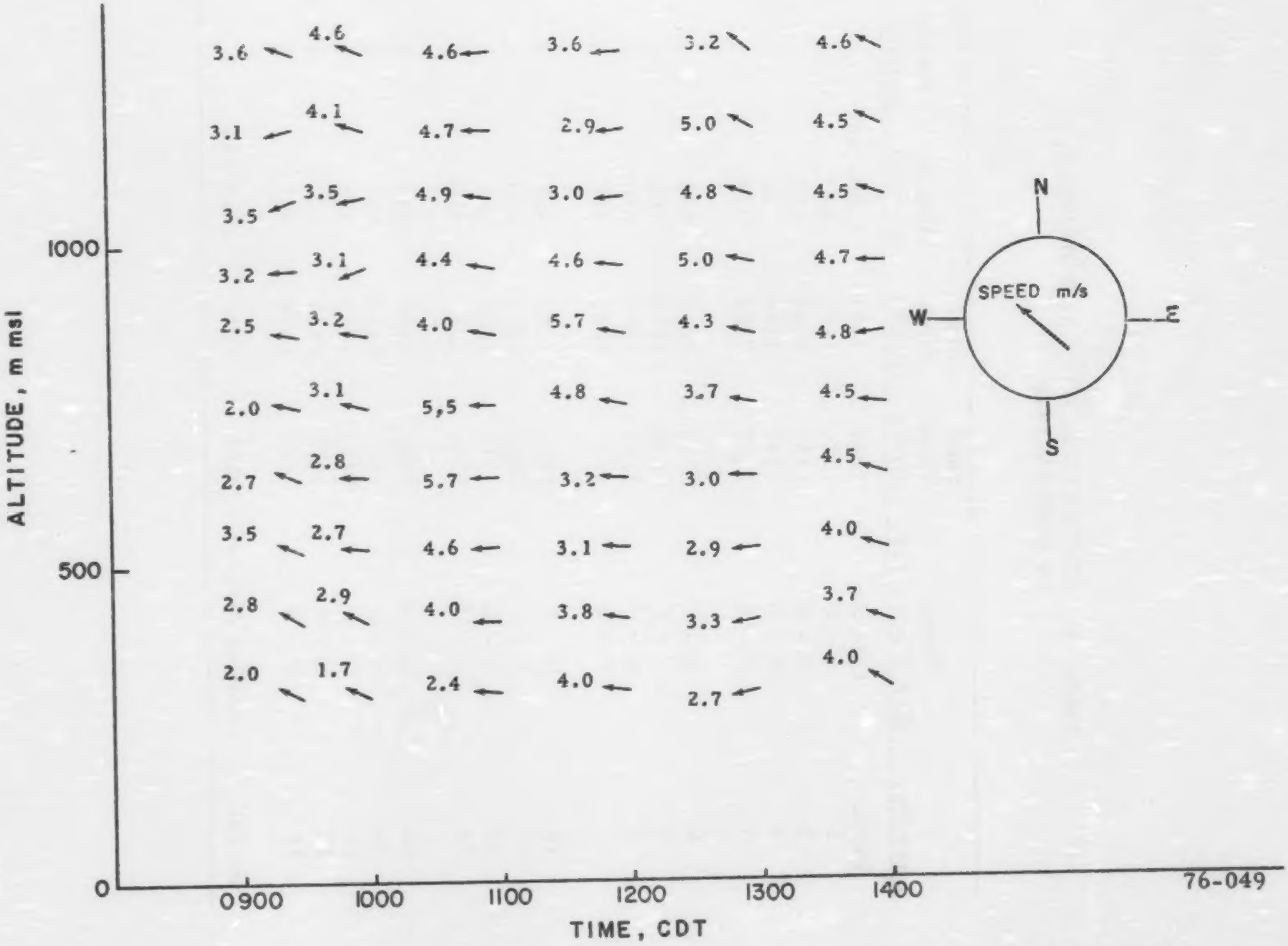

Figure 24. Winds aloft on 14 August 1974, from pilot balloon measurements at Marthasville, Missouri (see Figure 25 for location). 76-049

Table 3. AIRCRAFT SAMPLING SCHEDULE, 14 AUGUST 1974

Pass No.	Route (See Figure 25)	Start Time (CDT)	Stop Time (CDT)	Altitude (m msl)	Filter Number
Spiral	Labadie	1045	1121	3505-153	
2	A - B	1129	1135	457	1
3	B - A	1137	1144	610	1
4	A - B	1147	1154	762	1
5	B - A	1157	1204	914	1
6	E - F	1210	1215	914	2
7	F - E	1218	1223	762	2
8	E - F	1225	1231	610	2
9	F - G	1233	1243	457	2
10	H - J	1251	1259	457	3
11	J - H	1302	1310	610	3
12	K - L	1316	1323	762	3
13	L - K	1326	1332	914	3
14	M - N	1351	1405	1220	4
15	N - O	1407	1414	914	4
16	O - N	1416	1423	762	4
17	N - P	1425	1436	610	4
18	P - N	1438	1451	457	4
Spiral	Rohlfing Airport	1501	1518	1829-153	

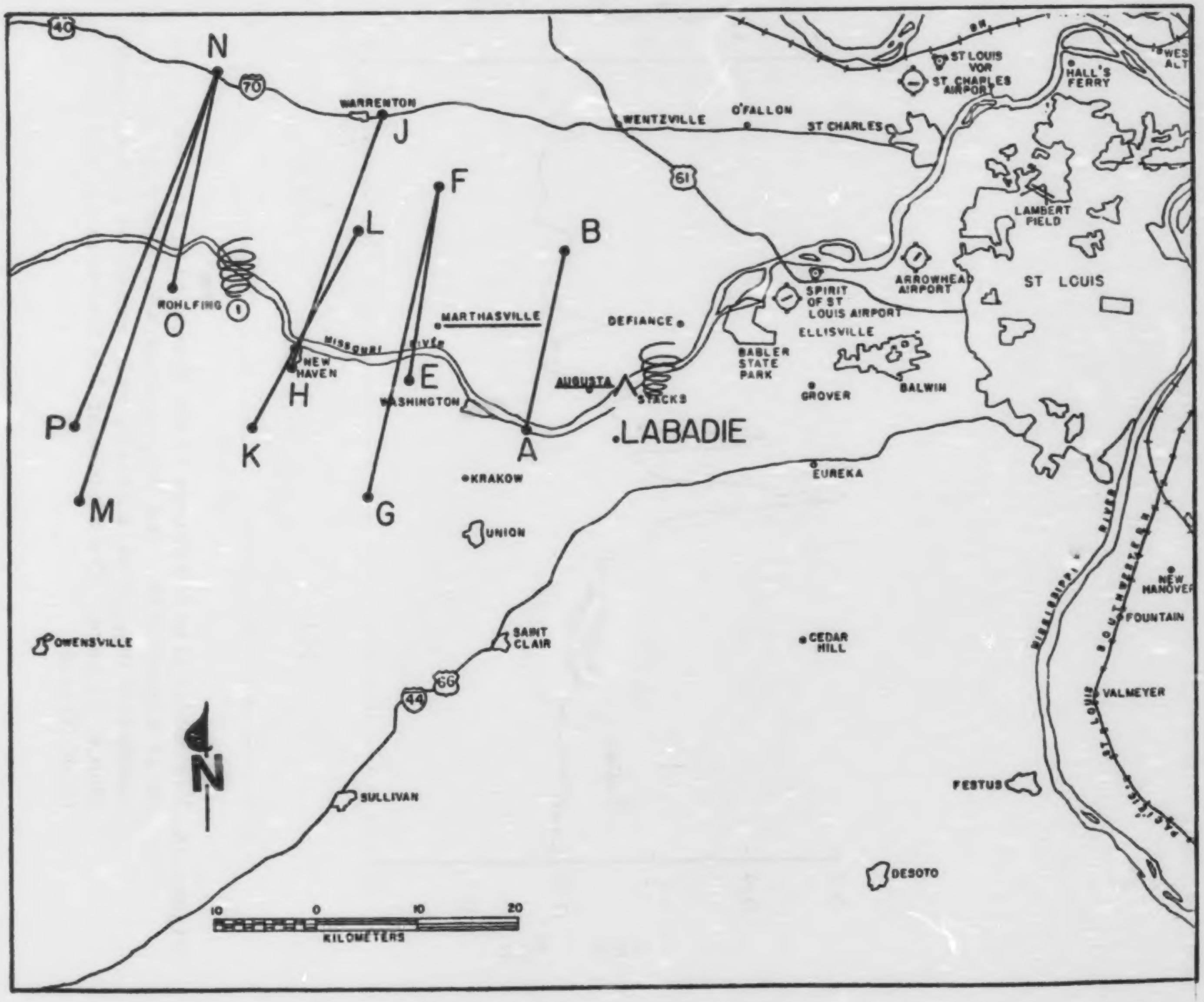
N
O
P
M
J
L
H
K
F
E
G
B
A
LABADIE
STACKS
AUGUSTA
MARTHASVILLE
DEFIANCE
ROHLFING
NEW HAVEN
WASHINGTON
MISSOURI RIVER
WARRENTON
WENTZVILLE
O'FALLON
ST CHARLES
ST LOUIS VOR
ST. CHARLES AIRPORT
HALL'S FERRY
LAMBERT FIELD
ST LOUIS
ARROWHEAD AIRPORT
SPIRIT OF ST LOUIS AIRPORT
ELLISVILLE
BABLER STATE PARK
GROVER
BALWIN
EUREKA
KRAKOW
UNION
SAINT CLAIR
SULLIVAN
OWENSVILLE
CEDAR HILL
FESTUS
DESOTO
NEW HANOVER
FOUNTAIN
VALMEYER
MISSISSIPPI RIVER
40
70
61
66
44
N
10
0
10
20
KILOMETERS

Figure 25. Location of aircraft sampling routes and pilot balloon release points (underlined) 14 August 1974.

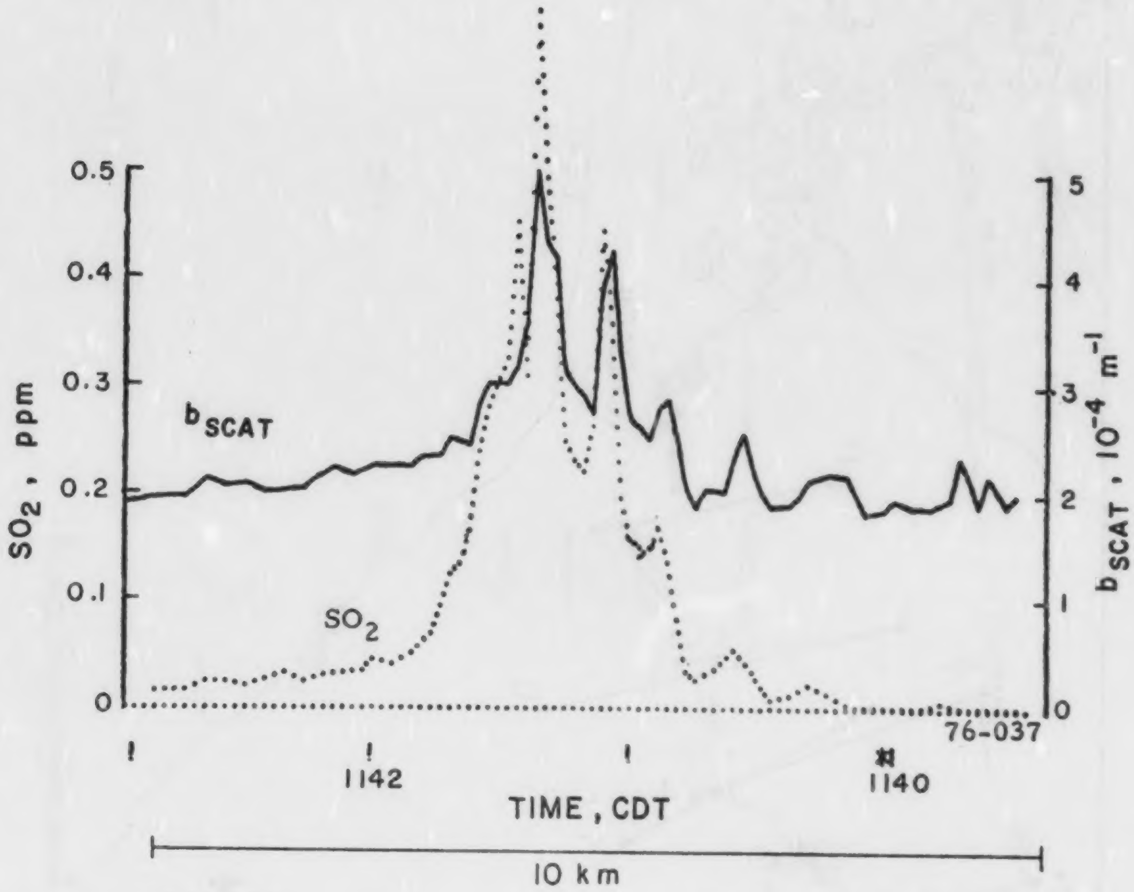

Figure 26. Horizontal plume traverse 10 km downwind of Labadie stacks on 14 August 1974. The SO_2 concentration and light-scattering coefficient (b_{scat}) were usually well correlated in the Labadie plume, as here. The altitude of this traverse was 610 m (2000 ft) msl.

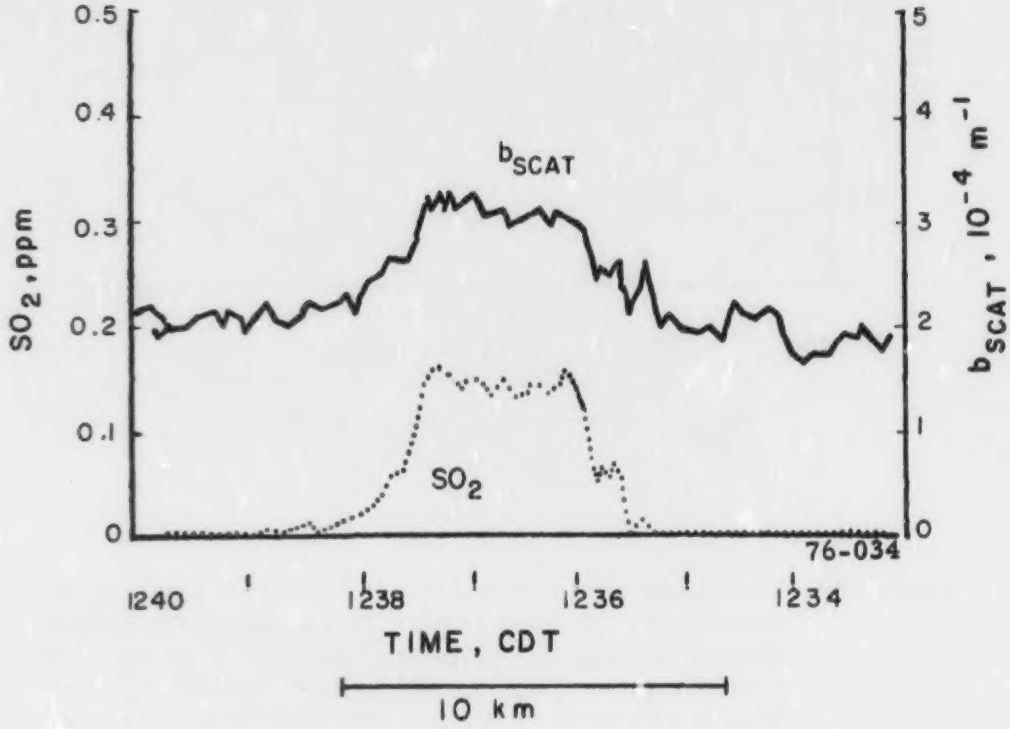

Figure 27. Horizontal plume traverse 21 km downwind of Labadie stacks on 14 August 1974. The elevated light-scattering coefficients outside the SO_2 plume represent the contributions of background aerosols. This traverse was made at 455 m (1500 ft) msl.

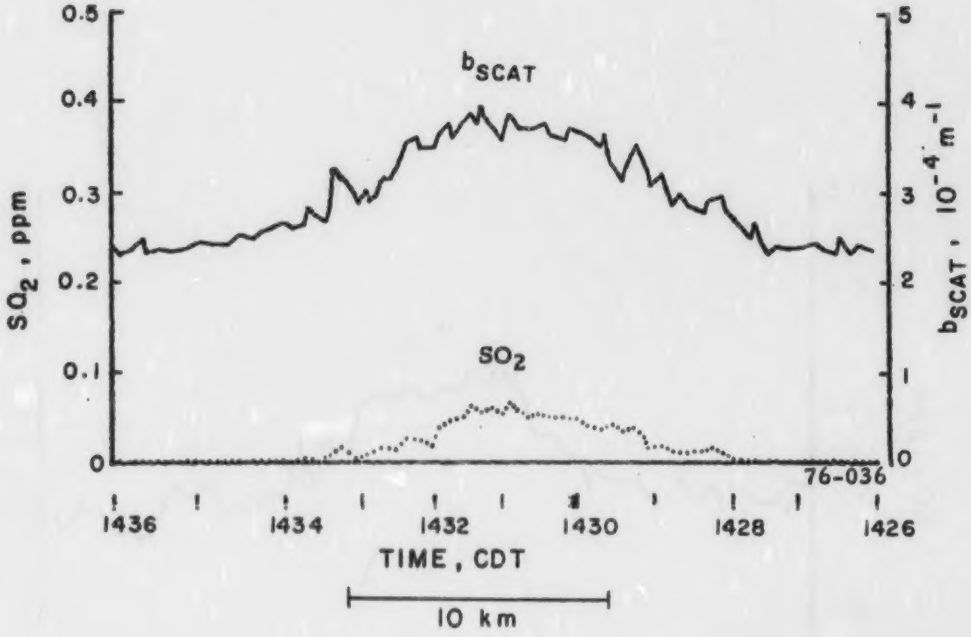

Figure 28. Horizontal plume traverse 45 km downwind of Labadie stacks on 14 August 1974. Compared to traverses nearer the stacks, plume is broader, peak SO_2 concentrations are lower, and ratio of excess b_{scat} to SO_2 in plume is greater. The altitude of this traverse was 610 m (2000 ft) msl.

calculated from the following integral:

$$F(x) = u_x(x) \iint c(x, y, z)\, dy\, dz,$$

where

F = the mass flow rate of SO_2

x = distance downwind of the plant,

y, z = cross-plume and vertical coordinates, extending beyond plume boundaries,

u_x = wind speed, and

c = the concentration of SO_2.

Figure 29 displays the inner integrals

$$\int c(x, y, z)\, dy$$

calculated from the individual plume traverses. These values, together with an average wind speed of 4 m/sec, yield the following flow rates for SO_2 when substituted in the above formula:

Distance from plant (km)	10	21	32	45
Flow rate of SO_2 within 455 m - 915 m layer (kg/sec)	2.0	1.9	1.7	1.5

These flow rates take into account only the SO_2 within the horizontal layer between 455 m (1500 ft) and 915 m (3000 ft) msl, where most plume traverses were made. Over the 35 km distance spanned by the plume measurements, the flow rate of SO_2 within the layer declined by 25 percent, or about 11 percent/hour.

The above estimate for the rate of SO_2 loss from the sampling layer of course represents not only the SO_2 removed from the atmosphere by deposition and oxidation but also the SO_2 which simply diffused out of the layer into the air above and below. The changing vertical gradients in Figure 29 make it clear that a substantial fraction of the decrease in SO_2 flow was in fact due to diffusion out of the layer. The vertical profiles of temperature and turbulent dissipation support this conclusion, indicating vigorous mixing through the lowest kilometer of the atmosphere (Figure 30). The value of 11 percent/hour

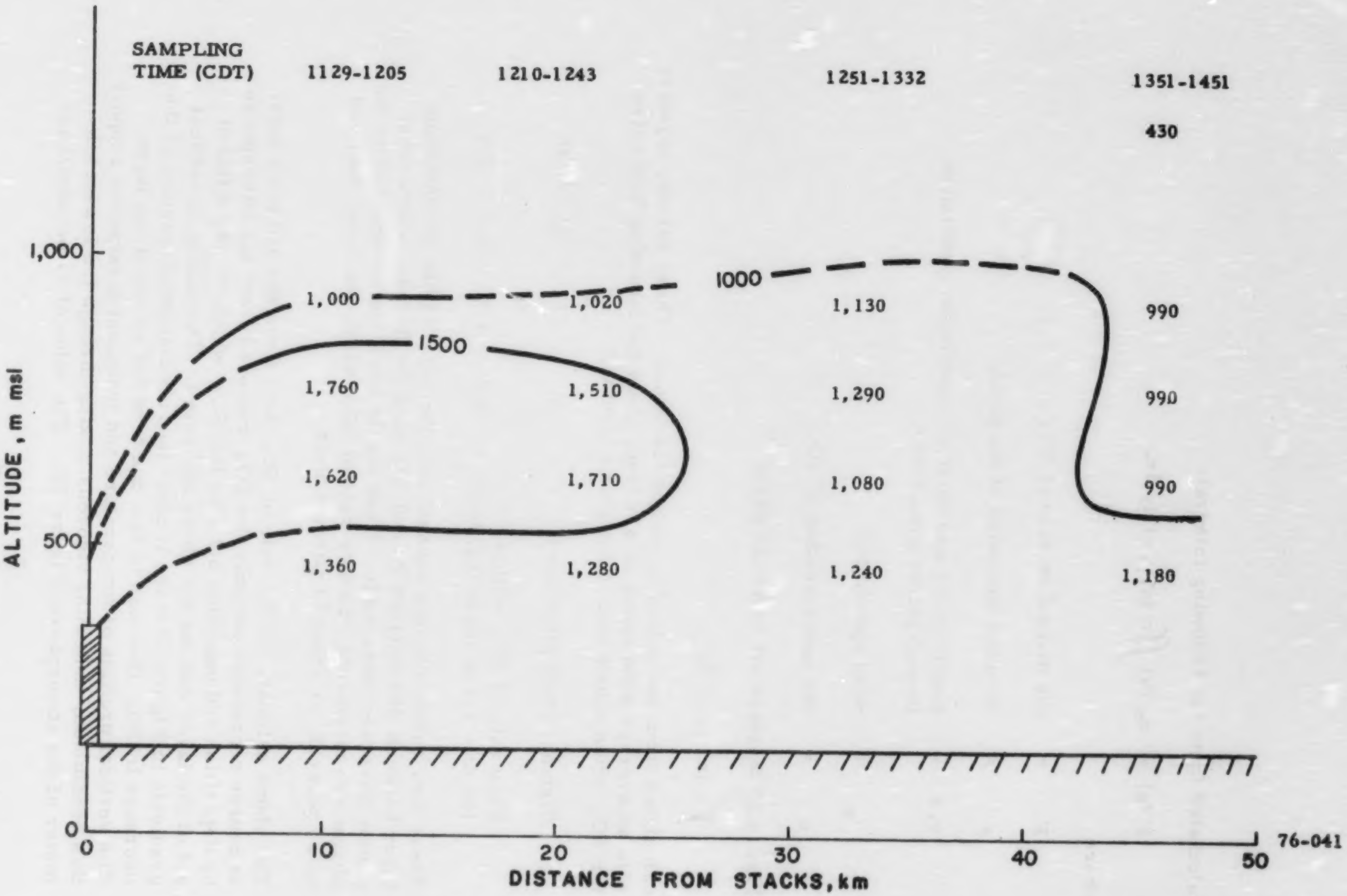

Figure 29. Composite side view of Labadie plume on 14 August 1974. Numbers give crosswind integral, $\int [SO_2]\, dy$, of SO_2 concentration measured on each traverse. Relatively slow decline in SO_2 integrals with increasing distance from the stacks indicates that broadening of the plume caused most of the decrease in peak SO_2 concentrations seen in Figures 26, 27, and 28.

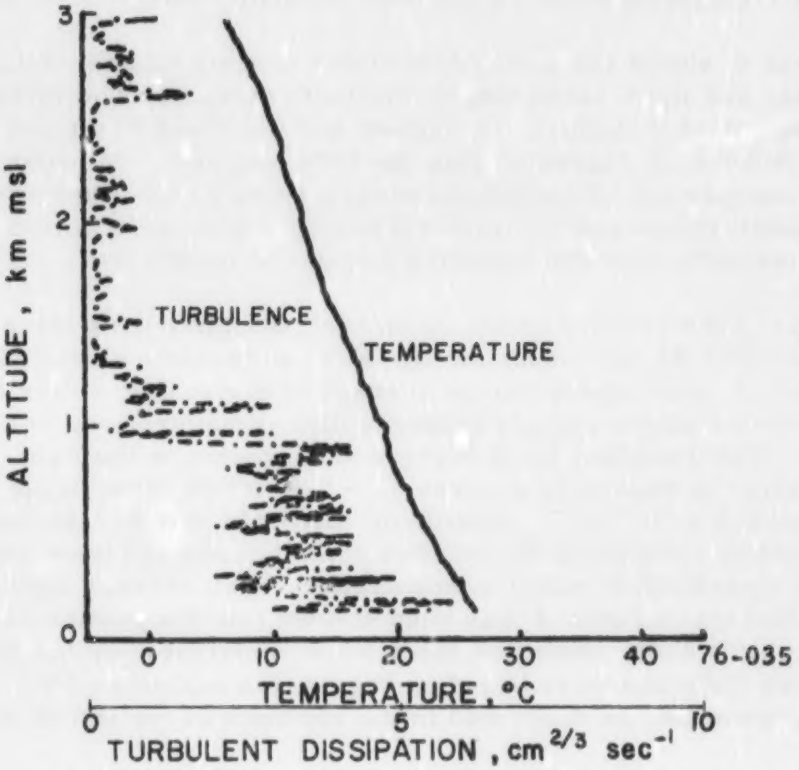

Figure 30. Vertical profile from spiral descent at Labadie on 14 August 1974, 1045-1121 CDT. Good mixing is indicated in the lowest kilometer of the atmosphere.

must therefore be understood as a very conservative (i.e., high) upper bound for the rate at which SO_2 was lost from the plume. This bound is consistent with the results of English workers on deposition velocity (Owens and Powell, 1974, Shepherd, 1974). Their estimates of about 1 cm/sec for the dry deposition velocity of SO_2 correspond to a removal rate of 3-4 percent/hour for a plume well mixed through the lowest kilometer of the atmosphere. Together with an SO_2 - $SO_4^=$ conversion rate of 3 percent/hour, this would give a combined SO_2 loss rate of about 6 percent/hour.

PARTICULATE SULFUR IN THE LABADIE AND WOOD RIVER PLUMES

Table 4 shows the particulate sulfur concentrations, SO_2 concentrations, and light-scattering coefficients measured downwind of the Labadie power plant (5 August, 14 August) and the Wood River industrial area (12 August, 15 August) during the 1974 program. In order to facilitate the comparison of continuous measurements with filter samples, the SO_2 concentrations and the light-scattering coefficients have been averaged numerically over the sampling periods of the filters.

Much of the aerosol collected on each sampling pass came from sources other than the one under study. Each particulate sulfur concentration in Table 4 thus represents an average of particulate sulfur concentrations within the plume and particulate sulfur concentrations in the background air. The contribution of background aerosols to the light-scattering coefficient is evident in Figures 26 - 28, which show b_{scat} levels of $1.8 - 2.5 \times 10^{-4}\ m^{-1}$ outside the SO_2 plume from the Labadie plant. To aid in estimating the relative contributions of plume and background to the particulate sulfur concentration, each average light-scattering coefficient in Table 4 has been divided into the portion contributed by the plume under study and the portion contributed by the background. These divisions were based on regression analysis of the b_{scat} and SO_2 profiles, as described in the appendix at the end of this section.

Figures 31 and 32 show the particulate sulfur concentration plotted against background b_{scat} and plume b_{scat}. It is clear from these figures that the particulate sulfur concentration is more sensitive to changes in plume b_{scat} than it is to changes in background b_{scat}. If it is assumed that b_{scat} is proportional to the submicron aerosol mass concentration, an interpretation which is supported by the uniformity of measured particle size distributions (Whitby et al., 1976), then it can be inferred that the plume aerosols contain higher fractions of sulfur than the background aerosols do.

Table 4. PARTICULATE SULFUR IN THE LABADIE AND WOOD RIVER PLUMES

Filter	Description	(a) Background b_{scat} (10^{-4} m^{-1})	(a) Plume b_{scat} (10^{-4}m^{-1})	(a) S_p (μg/m^3)	(a,b) Plume S_p (μg/m^3)	(a) SO_2 (ppm)	(c) Plume S_pS_T
8/05 1		1.54	0	2.52	0	0	-
2	Labadie (1 km)	1.45	0.43	6.09	3.30	0.171	0.015
3	Labadie (4 km)	2.06	0.14	5.53	1.18	0.060	0.015
4	Labadie (18 km)	1.83	0.14	4.33	1.01	0.031	0.024
8/12 1	Wood River (12 km)	1.60	1.41	7.45	5.81	0.055	0.075
2	Wood River (25 km)	1.64	1.58	8.63	6.85	0.050	0.094
3	Wood River (50 km)	1.15	0.68	3.68	2.59	0.023	0.079
8/14 1	Labadie (10 km)	2.01	0.27	6.20	2.17	0.042	0.038
2	Labadie (21 km)	1.96	0.35	5.53	2.30	0.040	0.042
3	Labadie (32 km)	2.13	0.33	5.48	2.10	0.026	0.059
4	Labadie (45 km)	2.52	0.39	6.10	2.33	0.014	0.114
8/15 1	Wood River (10 km)	2.64	0.51	5.73	2.50	0.044	0.042
2	Wood River (28 km)	2.50	0.86	4.96	2.87	0.036	0.058

(a) Average over filter sample period.

(b) Estimated: plume $S_p = \left(\frac{4 \text{ plume } b_{scat}}{\text{background } b_{scat} + 4 \text{ plume } b_{scat}} \right) S_p$.

(c) Plume S_p/S_T = plume S_p/(plume $S_p + S_g$); $S_g = SO_2$ as sulfur, averaged over filter sample period.

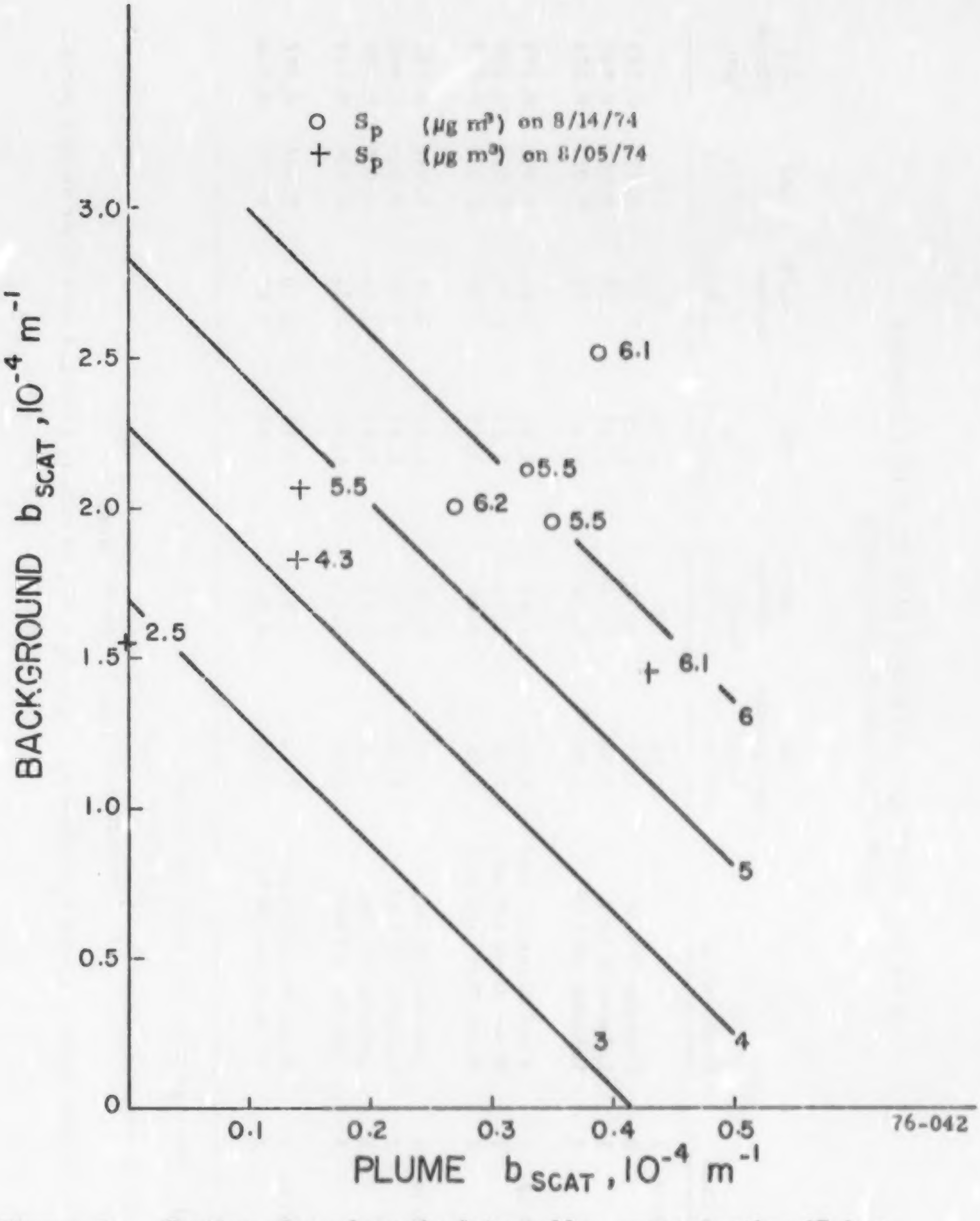

Figure 31. Scatter plot of particulate sulfur concentration (S_p) vs. plume b_{scat} and background b_{scat} (note different scales) for Labadie samples. Sloping lines indicate best-fit linear relationship: S_p = 7.18 plume b_{scat} + 1.77 background b_{scat}

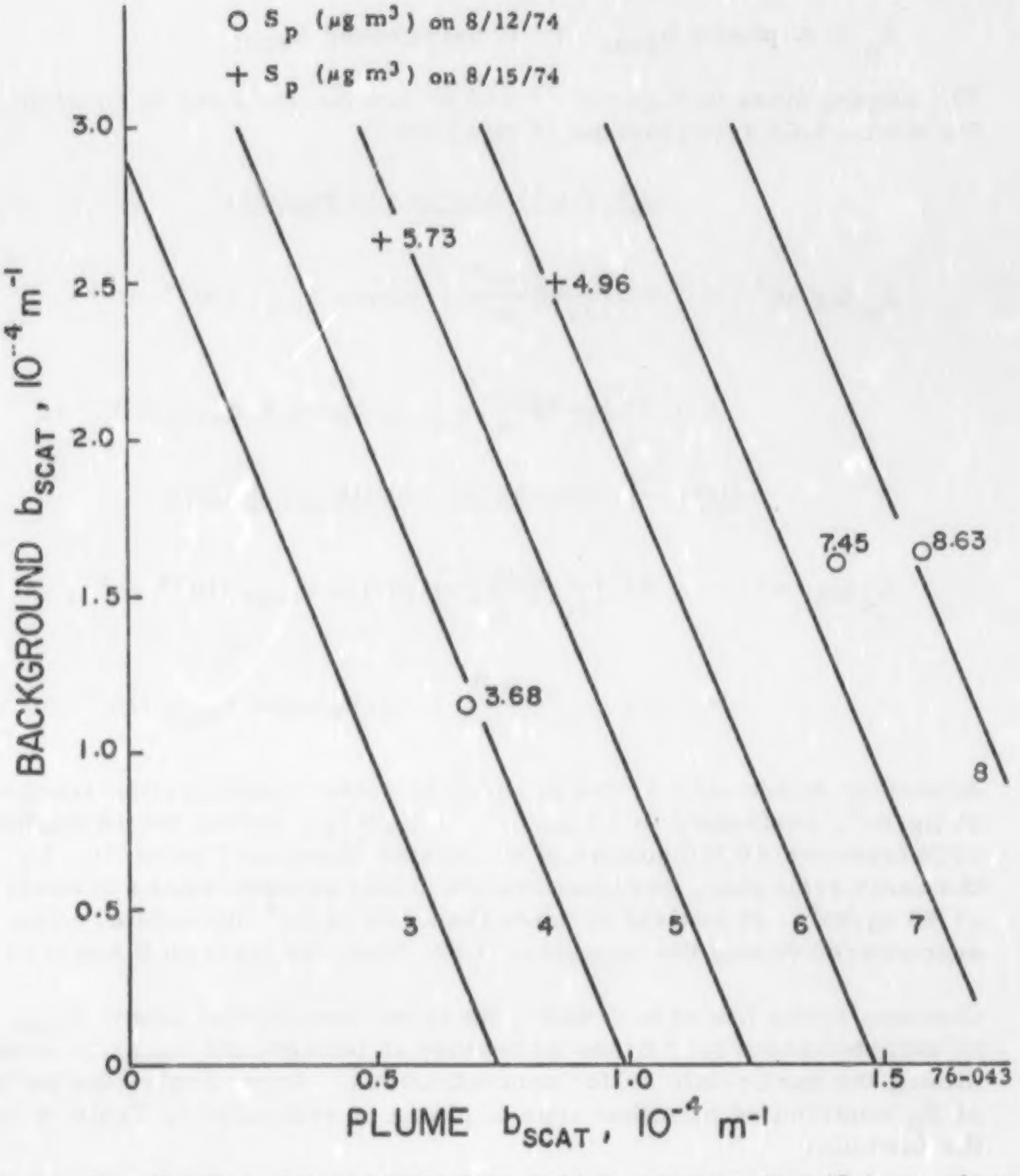

Figure 32. Scatter plot of particulate sulfur concentration (S_p) vs. plume b_{scat} and background b_{scat} (note different scales) for Wood River samples. Sloping lines indicate best-fit linear relationship: $S_p = 4.04$ plume b_{scat} + 1.04 background b_{scat}

If the sulfur fraction of the plume aerosol and the sulfur fraction of the background aerosol are each fairly constant, then the particulate sulfur concentration is described by the following approximate relationship:

$$S_p = A \text{ plume } b_{scat} + B \text{ background } b_{scat} .$$

The sloping lines in Figures 31 and 32 are the contours of constant S_p for the best-fit relationships of this form:

Labadie (5 August, 14 August)

$$S_p\ (\mu g/m^3) = 7.18 \left(\frac{\mu g/m^3}{10^{-4}\ m^{-1}}\right) \text{ plume } b_{scat}\ (10^{-4}\ m^{-1})$$

$$+\ 1.77 \left(\frac{\mu g/m^3}{10^{-4}\ m^{-1}}\right) \text{ background } b_{scat}\ (10^{-4}\ m^{-1}) \qquad (1)$$

Urban-Industrial (12 August, 15 August)

$$S_p\ (\mu g/m^3) = 4.04 \left(\frac{\mu g/m^3}{10^{-4}\ m^{-1}}\right) \text{ plume } b_{scat}\ (10^{-4}\ m^{-1})$$

$$+\ 1.04 \left(\frac{\mu g/m^3}{10^{-4}\ m^{-1}}\right) \text{ background } b_{scat}\ (10^{-4}\ m^{-1}) \qquad (2)$$

According to formula 1, the particulate sulfur concentration reached 26 $\mu g/m^3$, equivalent to 80 $\mu g/m^3$ of H_2SO_4, during the 14 August 1974 traverse 10 km downwind of Labadie shown in Figure 26. By the same reckoning, peak particulate sulfur concentrations in excess of 50 $\mu g/m^3$, equivalent to more than 150 $\mu g/m^3$ of sulfate, were encountered during the traverses 1 km from the plant on 5 August 1974.

Common to the fits of both data sets is the feature that plume b_{scat} is weighted about four times as heavily as background b_{scat} in determining the particulate sulfur concentrations. Accordingly, the portion of S_p contributed by either type of plume is estimated in Table 4 by the formula:

$$\text{plume } S_p = \left(\frac{4 \text{ plume } b_{scat}}{4 \text{ plume } b_{scat} + \text{background } b_{scat}}\right) S_p .$$

In the last column of Table 4, this is expressed as a fraction of S_T, the total (gas and particulate) sulfur concentration in the plume. The calculated fraction of plume sulfur in the particulate phase ranges from 1.5 percent in the Labadie plume 1 km downwind of the stacks, which is about what would be expected in the absence of significant atmospheric conversion, to 11.4 percent in the Labadie plume 45 km downwind of the stacks.

SULFUR CONVERSION IN THE LABADIE PLUME

In the Labadie plume of 14 August 1974, the fraction of plume sulfur in the particulate phase grew with distance downwind of the stacks (Table 4, Figure 33. Over the 35 km interval spanned by sampling, the increase in plume S_p/S_T was over 200 percent. According to the estimates made from the sulfur balance earlier in this section, less than one-sixth of this increase can be attributed to loss of sulfur from the plume. The remainder of the growth in the particulate sulfur fraction was presumably due to the oxidation of SO_2 to $SO_4^=$. The average pseudo-first-order rate constant required to produce this degree of conversion would be about 3 percent/hour, although it is clear from Figure 33 that the rate is not constant.

A second indicator of the rate of aerosol production in the 14 August 1974 plume was the changing ratio of light-scattering aerosols to SO_2. The ratio plume b_{scat}/SO_2 shown in Figure 33 is calculated from the continuous b_{scat} and SO_2 record by regression analysis as described in the appendix at the end of this section. It is computationally independent of the ratio plume S_p/S_T, which is calculated from filter measurements and the background and average light-scattering coefficient and SO_2 concentration. Figure 33 shows that plume b_{scat}/SO_2 displayed a pattern of downwind growth similar to that of plume S_p/S on 14 August 1974. Since loss of SO_2 from the plume cannot account for more than a small fraction of the change, the increase in plume b_{scat}/SO_2 confirms that light-scattering aerosols were being generated in the plume.

Some insight into the composition of the Labadie plume aerosol can be gained by examining the ratios S_p/b_{scat} and b_{scat}/V, where V ($\mu m^3/cm^3$) is aerosol volume concentration. In the preceding subsection, the ratio S_p/b_{scat} was estimated to be about 7 in the Labadie plume, based on the observed variation of S_p with plume b_{scat} and background b_{scat} (Formula 1). The ratio b_{scat}/V can be calculated theoretically from the average particle size distribution measured in the plume by the University of Minnesota on 14 August 1974 (Whitby et al, 1976); based on Mie theory for spherical particles of refractive index 1.5 (White et al, 1975), this ratio was about 0.043.

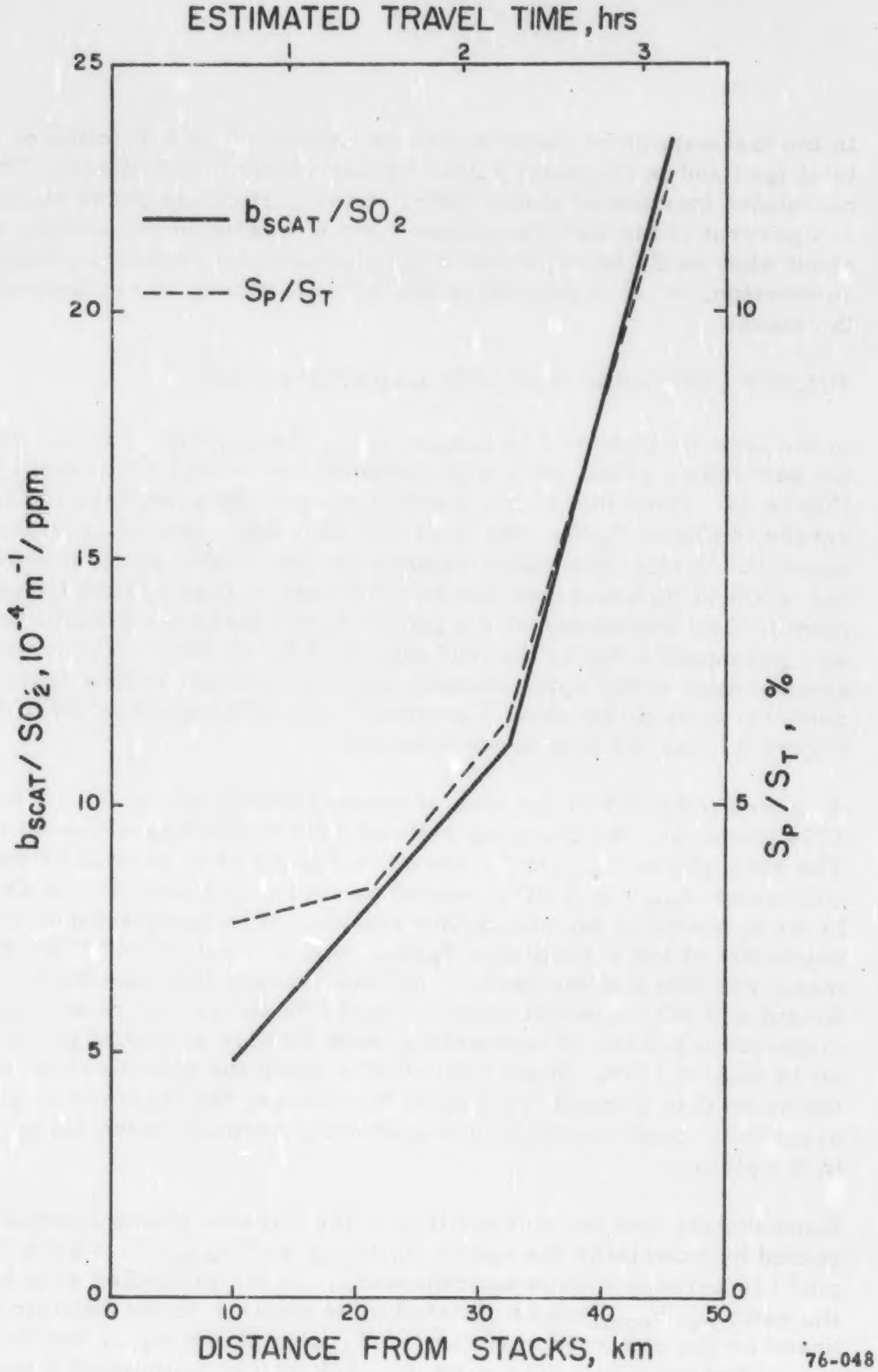

Figure 33. Two aerosol/emissions ratios in the Labadie plume on 14 August 1974. The downwind increase in both ratios reflects growth of aerosol within the plume. Lower scale shows actual distance downwind of stacks, upper scale shows equivalent travel time for average wind of 4 m/sec.

The product of the two ratios, $(S_p/b_{scat})\ (b_{scat}/V) + S_p/V$, is a quantity which can be calculated directly for liquid particles of known composition. The empirical ratio, $S_p/V = 7 \times 0.043 = 0.30$, falls between the theoretical ratios for pure sulfuric acid ($S_p/V = 0.60$) and sulfuric acid in equilibrium with water vapor at the ambient humidity ($S_p/V = 0.24$) (Whitby et al, 1976). This observation indicates that the observed light-scattering coefficient in the Labadie plume can be completely accounted for by sulfate aerosol and associated water.

A clue to the mechanism of aerosol production in the Labadie plume is contained in a CN profile recorded 21 km downwind of the stacks on 14 August 1974 (Figure 34). The sharp peaks in the nuclei count encountered at the edges of the plume on this traverse indicate that homogeneous nucleation probably was occurring there. Well-defined CN peaks of this magnitude were not recorded on other traverses, although sampling in the Labadie plume on 1 August 1974 showed CN counts which increased with distance downwind of the stacks. The occurrence of homogeneous nucleation implies that material of very low vapor pressure, presumably a sulfate compound, was being produced by reactions in the gas phase. These gas phase reactions may or may not have been the dominant mechanism for the conversion of SO_2 to $SO_4^=$ throughout the Labadie plume. Calculations for such a gas phase system, based on the average SO_2 oxidation rate estimated above, the average aerosol size distribution measured in the plume (Whitby et al, 1976), and Fuch's expression for diffusional transport to a sphere (Husar, 1971), indicate that the average pseudo-steady-state concentration of gas phase sulfate compounds in the 14 August 1974 Labadie plume would have been on the order of 6×10^{-6} ppm. This average concentration is roughly one-twentieth of the concentration of H_2SO_4 calculated to be necessary for homogeneous nucleation in a pure H_2SO_4 - H_2O system at 75 percent relative humidity (Mirabel and Katz, 1974). The CN peaks of Figure 34 could be due to locally high concentrations of H_2SO_4, or to the production of a compound of lower vapor pressure, such as $(NH_4)_2SO_4$.

SAMPLING ENVIRONMENT OF SULFATE FILTERS

Table 5 summarizes the temperature and humidity of the air sampled by each of the filters. The dependence of ambient temperature on altitude has been eliminated by converting measured temperature to potential temperature, the temperature a given parcel of air would have when transported adiabatically to the 1000 mb level. For computational purposes the adiabadic lapse rate was taken to be 1° C/

Table 5. SAMPLING ENVIRONMENT OF SULFATE FILTERS

Filter		Description	(a) Potential Temperature (°C)	(a) Dew Point (°C)	Plume S_p/S_T (%)
5 Aug	2	Labadie (1 km)	26	7	1.5
	3	Labadie (4 km)	26	8	1.5
	4	Labadie (18 km)	25	7	2.4
12 Aug	1	Wood River (12 km)	29	18	7.5
	2	Wood River (25 km)	29	19	9.4
	3	Wood River (50 km)	29	19	7.9
14 Aug	1	Labadie (10 km)	27	17	3.8
	2	Labadie (21 km)	28	16	4.2
	3	Labadie (32 km)	28	15	5.9
	4	Labadie (45 km)	29	12	11.4
15 Aug	1	Wood River (10 km)	25	16	4.2
	2	Wood River (28 km)	26	17	5.8

(a) Average over filter sample period.

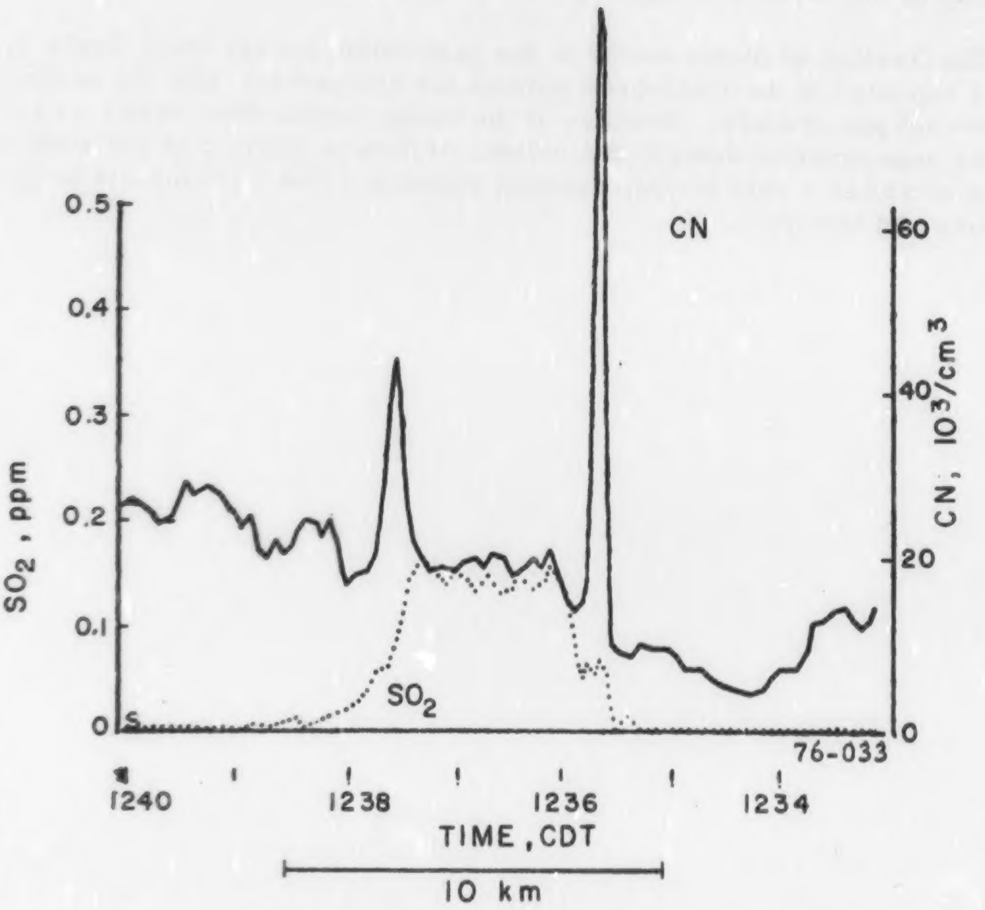

Figure 34. Horizontal plume traverse 21 km downwind of Labadie stacks on 14 August 1974. Condensation nuclei peaks at edge of plume indicate probable homogeneous nucleation. (The same traverse is shown in Figure 27.)

100 m, with sea level at 1013.25 mb. Similarly, the dependence of relative humidity on temperature, and hence on altitude, has been eliminated by converting measured humidity to dew point. This conversion was based on an empirical formula derived from the relationship of the saturation vapor pressure to the temperature.

The fraction of plume sulfur in the particulate phase, from Table 4, is repeated in the right-hand column for comparison with the environmental parameters. Because of the many uncontrolled variables in the experimental design, the volume of data in Table 5 is not adequate to establish a relationship between reaction rates and ambient temperature and humidity.

APPENDIX TO SECTION 4

DETERMINATION OF BACKGROUND b_{scat} AND PLUME b_{scat}/SO_2 BY REGRESSION ANALYSIS

When studying the pollutant plume from a specific source, it is often desirable to separate the measured concentration of a pollutant into the plume concentration, which is the excess contributed by the plume, and the background concentration, which is the concentration which would be present in the absence of the plume. For the Labadie plume, this is conveniently done by regression analysis, using SO_2 as a tracer for the plume.

Figures 26, 27, and 28 show that the light scattering coefficient correlated well with the SO_2 concentration during individual traverses of the 14 August 1974 Labadie plume. This means that on each traverse there was an approximate linear relationship between the two parameters:

$$b_{scat} \cong A\,[SO_2] + B .$$

As part of the data screening process, the coefficients A and B which minimize the mean square error in this relationship were determined for each traverse, using standard computational methods (Bevington, 1969). For the traverses shown in Figures 26 - 28, the results were as follows:

Regression Coefficients for 14 August 1974
Labadie Plume Traverses

Figure Number	Pass Number	A (10^{-4} m^{-1}/ppm)	B (10^{-4} m^{-1})	ρ^2 Percent
26	3	4.9	1.8	85
27	9	7.8	2.0	91
28	17	25.0	2.5	87

The column ρ^2 gives the percent of the variance of b_{scat} which is "explained" by the linear relationship with SO_2.

The constant term B gives the relationship's prediction for the light-scattering coefficient when no SO_2 is present. Since the SO_2 concentration outside the plume was generally below the detection threshold of the instrument, B is interpreted as the average light-scattering coefficient of the background aerosol. This interpretation is supported by comparison of the values for B given above with the b_{scat} levels seen outside the plume in Figures 26 - 28. (The coefficients A and B were calculated for the full traverses, which included more sampling outside the plume than is shown in the figures.)

The physical significance of the coefficient A can be seen by rewriting the regression relationship in the following way: $A = (b_{scat} - B)/[SO_2]$. The slope of the relationship thus represents the ratio between plume b_{scat} and SO_2, averaged across the plume. Computation of the ratio in this way eliminates the variability associated with ratios calculated from a single data point.

SECTION V

OXIDANT CHEMISTRY

INTRODUCTION

The polluted St. Louis atmosphere was generally an oxidizing environment during the 1974 MISTT field program. Ozone concentrations exceeding the 8 pphm Federal Ambient Standard were recorded on most sampling days, and concentrations as high as 20 pphm were measured near the city on 12 August 1974 (Figure 35).

Elevated concentrations were not confined to the metropolitan area, but were regularly carried well downwind in an identifiable plume. On the afternoon of 30 July 1974, for example, ozone concentrations of 13 pphm were found over rural Illinois, 60 km downwind of the Arch (Figures 36 and 37). These high concentrations were restricted to the region directly downwind of Greater St. Louis, and ozone concentrations on either side were uniformly about 6 pphm.

The overall contribution of the metropolitan area to regional ozone levels can be judged by the flow rate of ozone within the downwind plume. This flow rate is calculated from the measured ozone cross section of the plume and the pilot balloon observations of winds aloft:

$$\text{Flow Rate} = u_x \iint ([O_3] - [O_3]_{\text{background}})\, dy\, dz,$$

where u_x is the wind speed and y and z are the crosswind and vertical coordinates. On the afternoon of 30 July 1974, the calculated ozone flow rate in the St. Louis/Wood River plume was about 100 tons/hour. Wind speeds during the day were fairly steady, so this figure can be interpreted as the approximate net rate at which ozone was generated from the emissions of the urban industrial area in the first 60 km (roughly 3 hours travel time) downwind.

The elevated concentrations of ozone and other oxidizing gases present in the sampling area are of interest both for their direct impact on human health (Hackney, 1975) and for their promotion of sulfur oxidation and secondary aerosol formation (Wilson et al, 1972, Roberts, 1975). This section discusses the observations of the $O_3/NO/NO_x$ system made by the MRI aircraft.

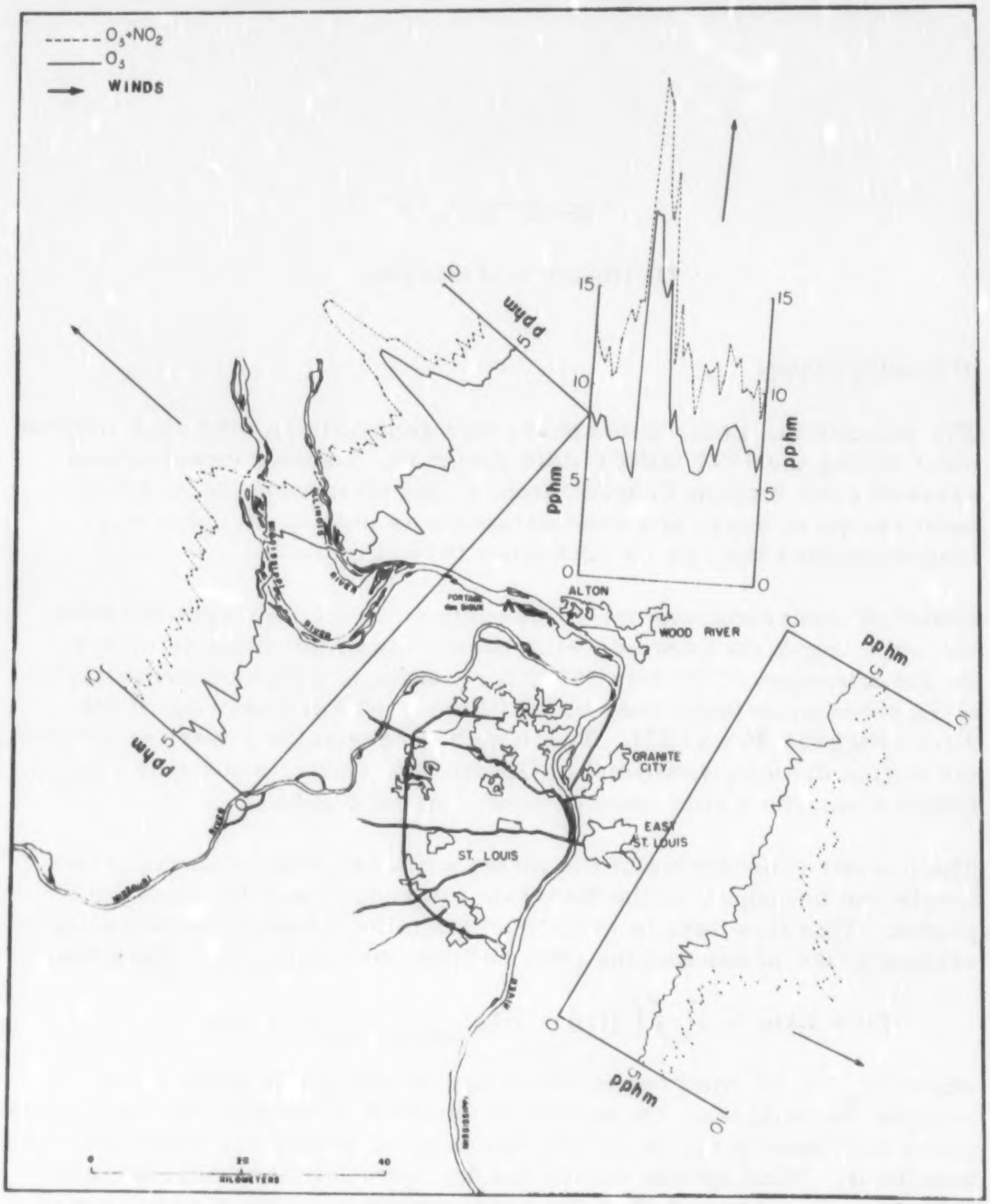
O$_3$+NO$_2$
O$_3$
WINDS
pphm
15
10
5
0
ALTON
WOOD RIVER
GRANITE CITY
EAST ST. LOUIS
ST. LOUIS
PORTAGE des SIOUX
MISSISSIPPI RIVER
ILLINOIS RIVER
MISSOURI RIVER
0
20
40
KILOMETERS

76-135

Figure 35. Horizontal profiles of ozone and oxidant concentrations downwind of Greater St. Louis under three different wind regimes. Profiles were recorded during traverses of profile baselines at the following altitudes and times: (counter-clockwise from lower right) 455 m (1500 ft) msl, 0933-0952 CDT, 30 July 1974; 610 m (2000 ft) msl, 1145-1152 CDT, 12 August 1974; 455 m (1500 ft) msl, 1027-1048 CDT, 15 August 1974. Arrows show average winds measured in mixing layer during sampling period; their lengths equal distance covered in one hour at average wind speed. Ozone and oxidant concentrations substantially above background levels formed downwind of Wood River and central St. Louis area on most sampling days.

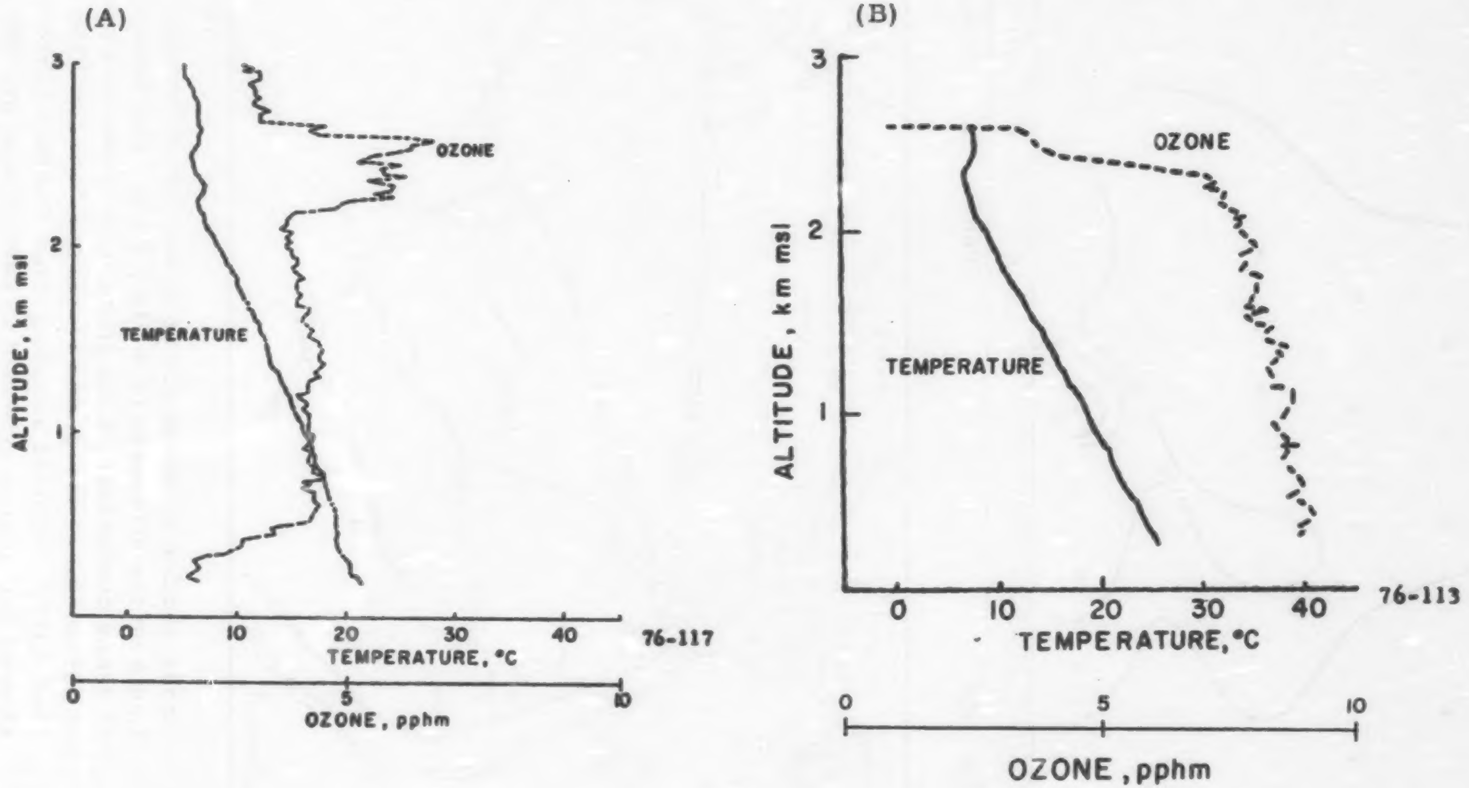

Figure 36. Vertical profiles of ozone concentration and temperature on 30 July 1974. Morning profile (A), recorded during an 0859-0920 CDT spiral ascent near Lambert Field, shows a temperature inversion at about 2400 m msl, together with an elevated layer of ozone which was presumably formed during the previous day. Afternoon profile (B), recorded during a 1604-1616 CDT spiral descent over Oakdale (Ill.), shows temperature inversion remaining at about 2400 m msl, with uniformly high ozone concentrations in mixed layer below. Locations of spirals are shown in Figure 37(B).

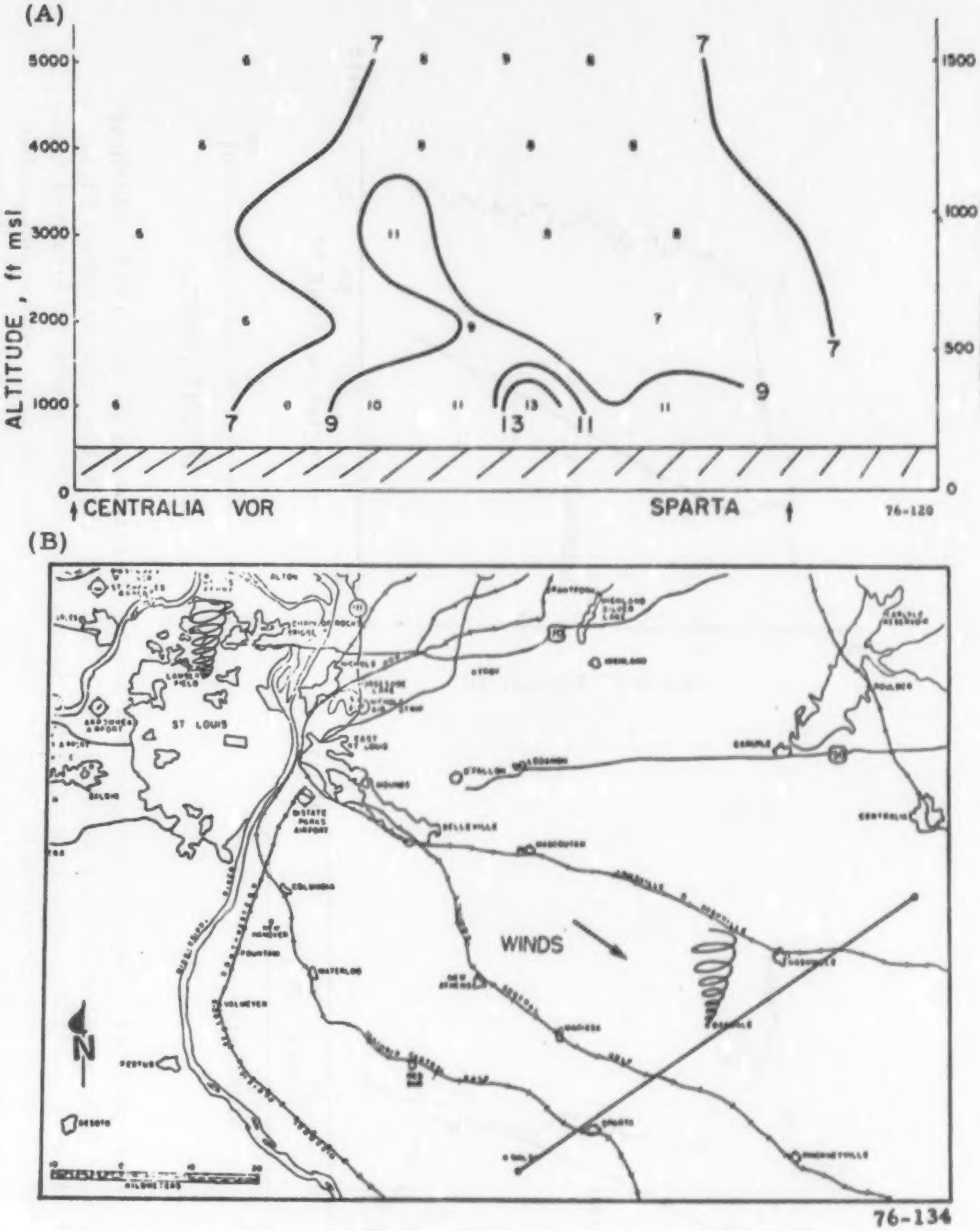

Figure 37. Cross section of ozone plume downwind of Greater St. Louis on the afternoon of 30 July 1974. Isopleths (A) of ozone concentration (in pphm) are drawn from records of horizontal cross-plume traverses between 1356 and 1542 CDT. Vertical sounding over Oakdale (Figure showed that plume extended to 2400 m msl at 1600 CDT. Map (B) shows route of traverses and locations of spiral soundings presented in Figure 36. Arrow shows average wind measured in mixing layer at 1400 and 1500 CDT; its length equals distance covered in one hour at average wind speed.

OXIDANT PROFILES

In terms of total concentration, the most important oxidizing species normally present in polluted urban air are ozone and nitrogen dioxide. Both of these species are of secondary origin. Ozone is formed by the photolysis of nitrogen dioxide, followed by the reaction of oxygen atoms with molecular oxygen:

$$NO_2 + h\nu \rightarrow NO + O \qquad /1/$$

$$O + O_2 + M \rightarrow O_3 + M. \qquad /2/$$

Nitrogen dioxide is a product of the reaction of ozone with nitric oxide:

$$NO + O_3 \rightarrow NO_2 + O_2. \qquad /3/$$

These three reactions form a closed cycle, leaving invariant the total concentration of oxidizing species:

$$\frac{d}{dt}\left\{[O] + [O_3] + [NO_2]\right\} = (r_1 - r_2) + (r_2 - r_3) + (r_3 - r_1) = 0.$$

In the absence of competing reactions, the oxidant* level would thus be constant.

During the daylight hours in polluted urban air, Reactions 1 - 3 proceed faster than do any other known reactions involving the same species (Leighton, 1961). Even relatively slow competing reactions can affect oxidant levels, however. An example is the oxidation of nitric oxide by reaction with a peroxy radical:

$$NO + ROO\cdot \rightarrow NO_2 + RO\cdot \qquad /4/$$

Reactions of this sort destabilize the oxidant concentration, and allow it to rise:

---

*The term "oxidant" is used in different senses by different authors. In this report it is used to refer to any of the oxidizing gases, and the oxidant concentration is taken to be the sum of the concentrations of atomic oxygen, ozone, and nitrogen dioxide.

$$\frac{d}{dt}\left\{[O] + [O_3] + [NO_2]\right\} =$$

$$(r_1 - r_2) + (r_2 - r_3) + (r_3 - r_1 + r_4) = k_4\,[NO]\,[ROO\cdot]\,.$$

During the 1974 MISTT field program, the MRI aircraft monitored O_3, NO, and NO_x concentrations with continuous chemiluminescent analyzers. Figures 35 and 38 - 41 show oxidant profiles recorded on several traverses. (The oxidant concentrations given are derived from the measured concentrations as follows: $[O] + [O_3] + [NO_2] \cong [O_3] + [NO_2] = [O_3] + [NO_x] - [NO]$. This formula is based on the observations that atomic oxygen contributes a negligible fraction of the oxidant concentration and that the low-temperature molybdenum converter in the NO_x analyzer is designed to reduce only NO_2.)

The oxidant profiles of the Labadie and St. Louis/Wood River plumes were distinctly different. The Labadie plume had little effect on ambient oxidant concentrations at the distances sampled, from 1 to 45 km downwind of the plant (Figures 39 and 40). It appears that the competing reactions which lead to the accumulation of oxidant in urban photochemical smog were of minor importance in the somewhat simpler chemical system of the Labadie plume. The St. Louis and Wood River plumes, in contrast, were characterized by oxidant concentrations well above background levels (Figures 35 and 41). Net production of oxidant within these urban-industrial plumes was apparent less than 15 km downwind of hydrocarbon source areas. In such hydrocarbon-rich environments, reactions other than 1 - 3 quickly destroyed the conservation of oxidant.

OZONE IN THE LABADIE PLUME

The oxidant chemistry of power plant plumes has recently come under close scrutiny, following the reported observation by Davis et al (1974) of elevated ozone concentrations downwind of a coal-fired power plant in Maryland. No such ozone "bulge" was observed in the Labadie plume on any of the sampling days.

The sulfur dioxide plume from the coal-fired, steam-generating plant at Labadie was followed for 45 km on 14 August 1974. There was little loss of sulfur dioxide over the sampling distance, so this primary pollutant can be used as a tracer for the effluent of the plant. Ozone concentrations outside the sulfur dioxide plume on 14 August

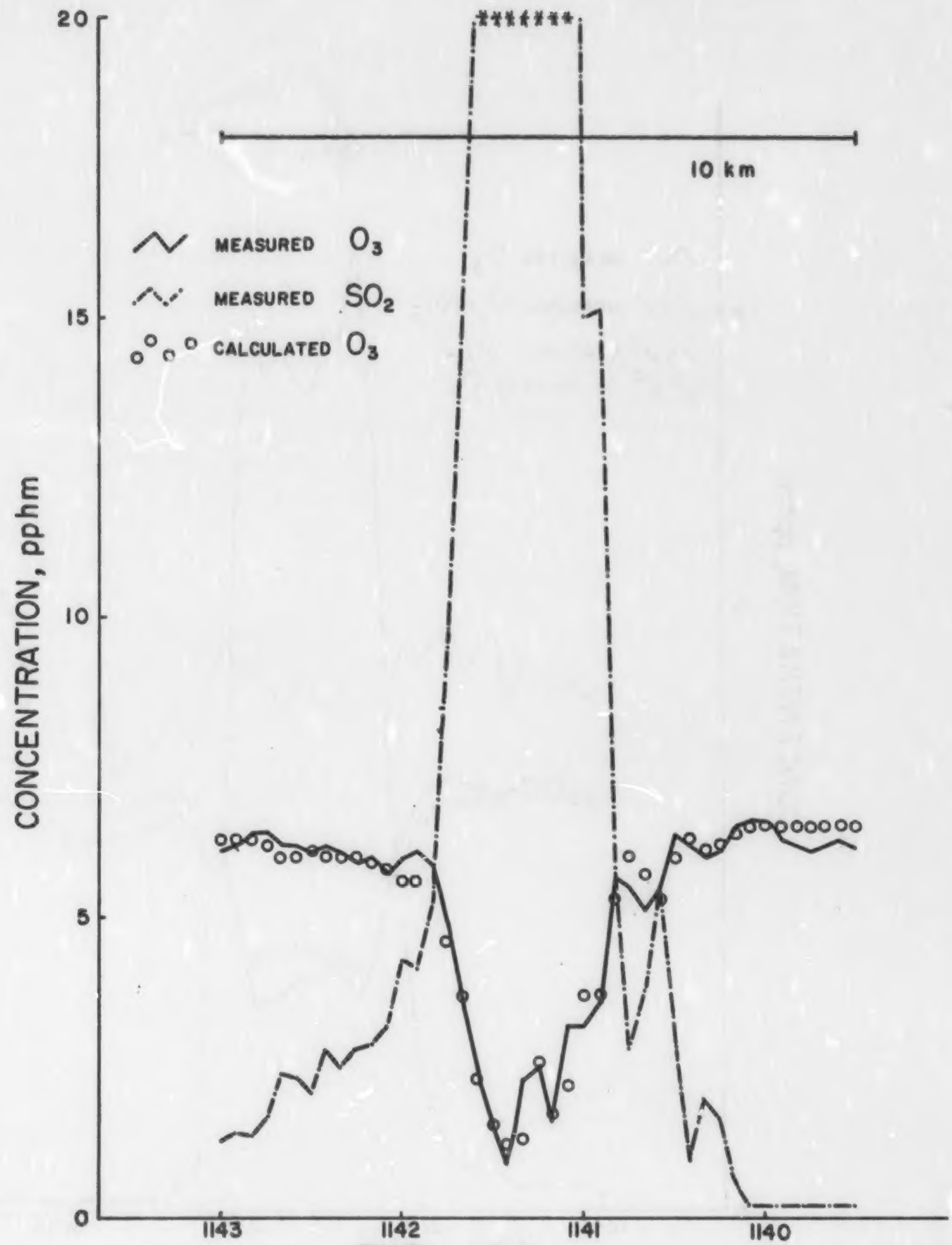

Figure 38. Horizontal plume traverse 10 km downwind of Labadie stacks on 14 August 1974. Ozone concentrations within plume were depressed below background levels on either side. Measured ozone profile agreed well with ozone profile calculated from measured SO_2 profile and oxidant-conserving photochemistry. The altitude of this traverse was 610 m (2000 ft) msl.

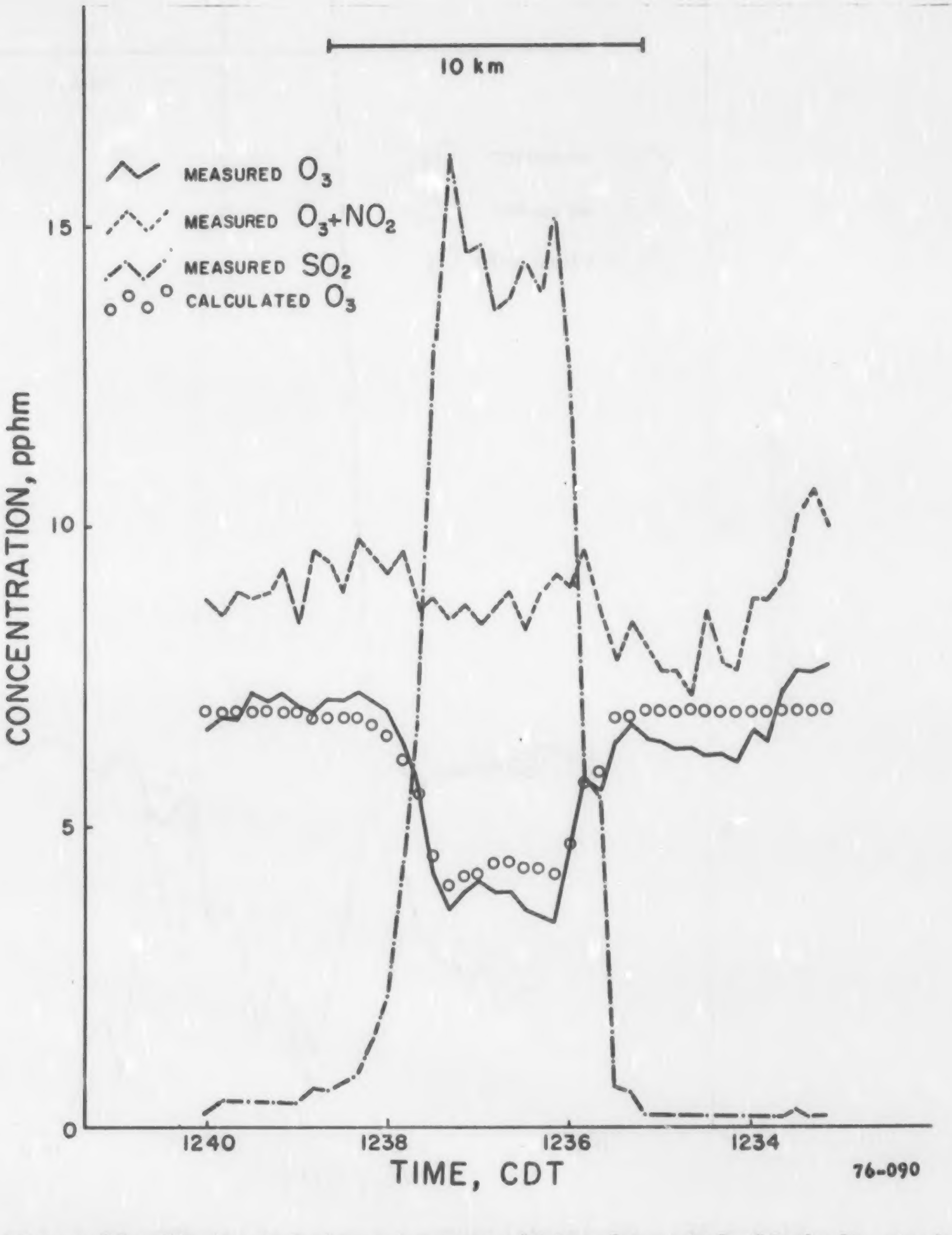

Figure 39. Horizontal plume traverse 21 km downwind of Labadie stacks on 14 August 1974. Ambient ozone concentrations outside plume were slightly higher than for earlier traverse of Figure 38. Oxidant ($O_3 + NO_2$) concentrations within plume were consistent with background levels on either side. This traverse was flown at 455 m (1500 ft) msl.

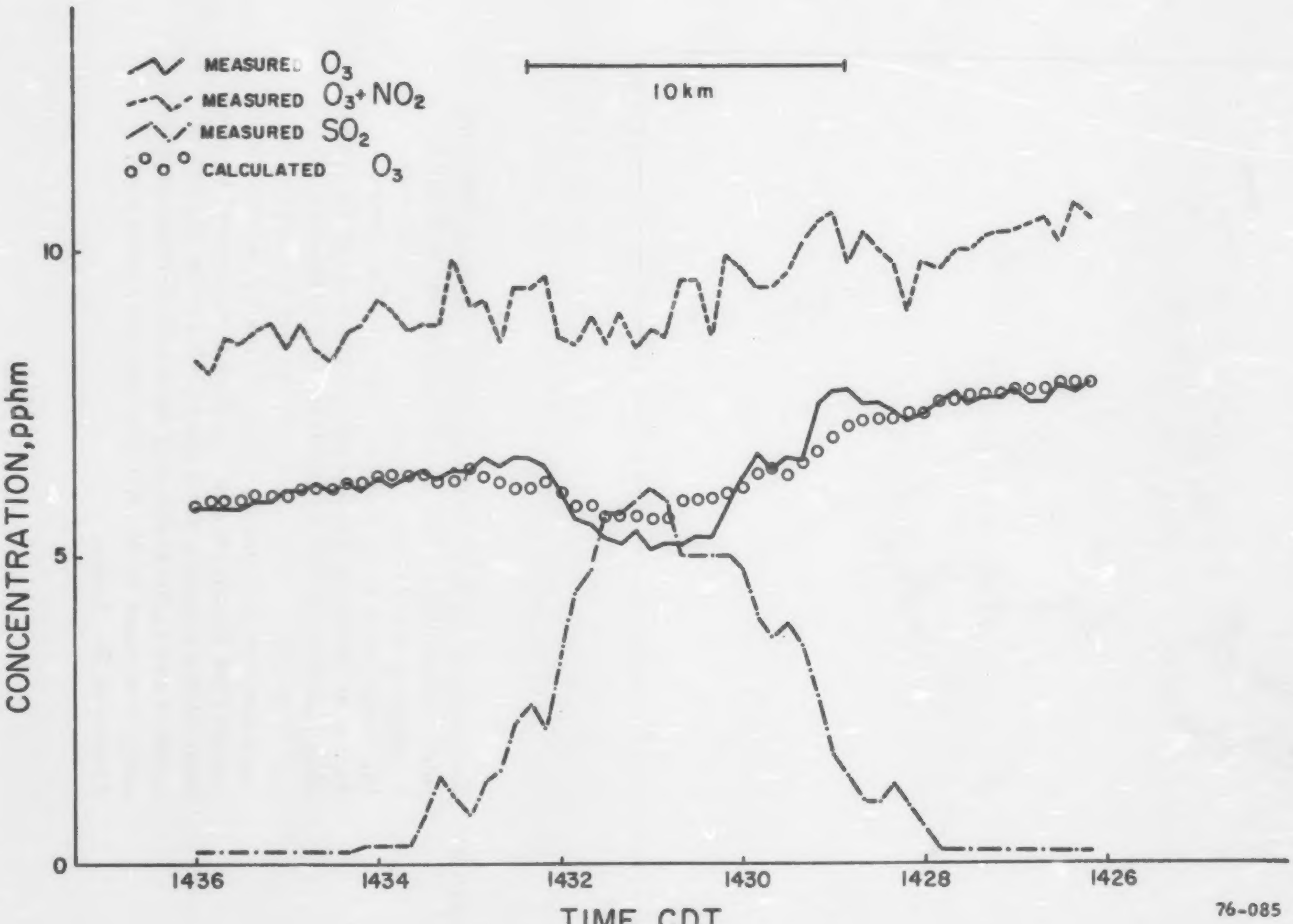

Figure 40. Horizontal plume traverse 45 km downwind of Labadie stacks on 14 August 1974. Ozone concentrations within the plume at this distance were still depressed below background levels on either side, although not as strongly as on traverses nearer the stacks. Measured ozone and oxidant profiles both show large-scale concentration gradient, possible due to urban plume from Greater St. Louis. The altitude of this traverse was 610 m (2000 ft) msl.

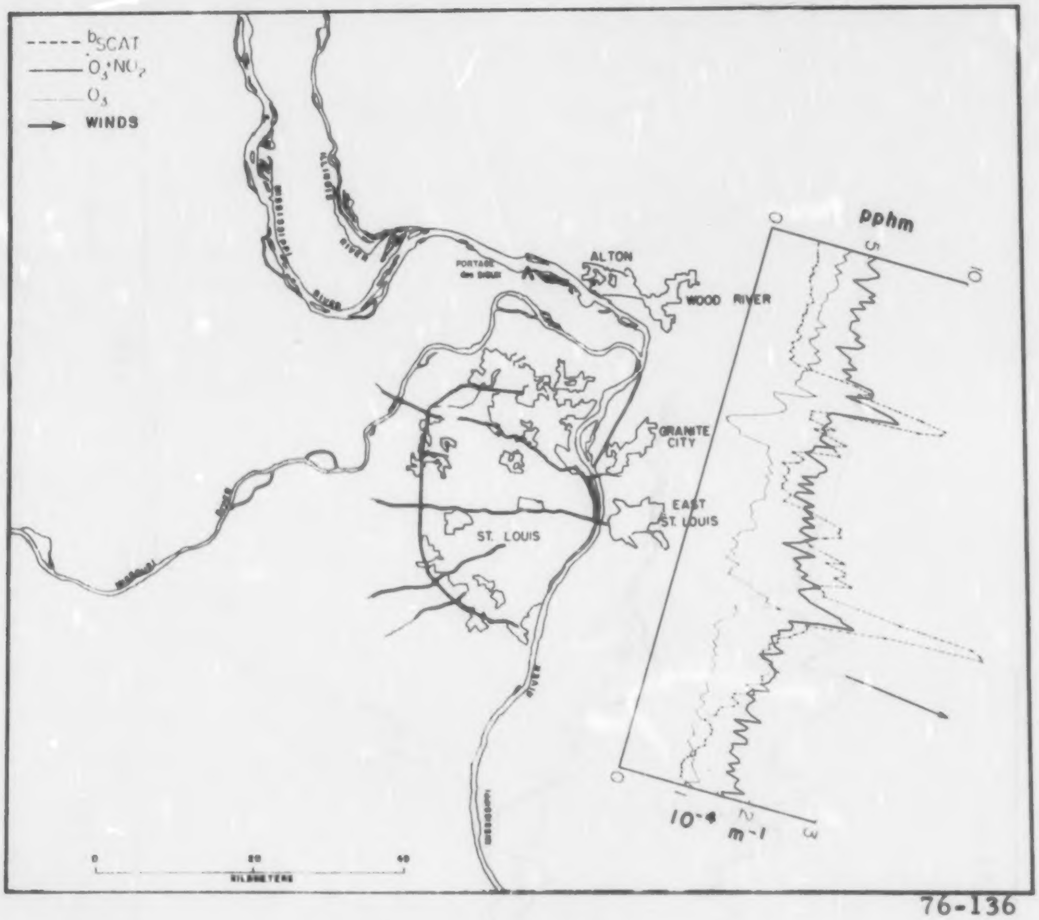

b_{SCAT}
O_3+NO_2
O_3
WINDS
MISSISSIPPI RIVER
ILLINOIS RIVER
PORTAGE des SIOUX
ALTON
WOOD RIVER
GRANITE CITY
EAST ST. LOUIS
ST. LOUIS
MISSOURI RIVER
MISSISSIPPI RIVER
pphm
0
5
10
0
1
2
3
10^{-4} m^{-1}
0
20
40
KILOMETERS

76-136

Figure 41. Early-morning horizontal profiles of ozone concentration, oxidant ($O_3 + NO_2$) concentration, and light-scattering coefficient (b_{scat}) downwind of Greater St. Louis on 3 August 1974. The profiles were recorded during a horizontal traverse of their common baseline at 457 m (1500 ft) msl between 0835 and 0856 CDT. The arrow shows the average wind measured in the mixing layer during the sampling period; its length equals the distance covered in one hour at the average wind speed. Narrow plumes of oxidant and light-scattering aerosols formed immediately downwind of Wood River refinery zone and downtown St. Louis.

1974 were elevated, generally exceeding 6 pphm. Within the plume, ozone concentrations were depressed below these levels (Figures 39 - 40), due to the reduction of ozone by the nitric oxide in the plant effluent.

While ozone concentrations within the plume were depressed relative to those outside at all distances, the absolute ozone concentrations in the center of the plume increased with distance downwind, from 1 pphm at 10 km to 5 pphm at 45 km. In principle, such a rise could be due either to the simple dilution of the plume by background air, or to the net production of oxidant by chemical reactions which would lead eventually to excess ozone levels within the plume. These two effects can be distinguished by quantitatively analyzing the relationship of ozone to plume geometry. Figures 38 - 40 compare measured ozone profiles of the plume with ozone profiles calculated from oxidant-conserving photochemistry and the observed plume geometry, as described in the appendix at the end ofthis section. These calculations use sulfur dioxide as a tracer for the plume and are based on the photolytic cycle governed by Reactions 1 - 3.

The correspondence between calculated and measured concentrations is quite good at 10 km and 21 km from the plant. There is a suggestion in Figure 40 that the agreement was beginning to break down 45 km from the plant, where the observed ozone deficit was narrower and deeper than that calculated from the geometry of the SO_2 plume. The origin of this difference is not known. Possible explanations include the following: (a) ultraviolet radiation was significantly attenuated within the core of the plume due to scattering by aerosols, depressing the rate of nitrogen dioxide photolysis; (b) reactions involving hydrocarbon products were important where the plume mixed into the background air, destabilizing the oxidant concentration; (c) the profile of the background oxidant concentration was somewhat irregular. Overall, the agreement between calculated and measured concentrations indicates that any net production of oxidant was insignificant at the distances sampled, and that the observed downwind decrease in the plume ozone deficit was due to the spreading and dilution of the plume.

OXIDANT AND LIGHT-SCATTERING AEROSOLS IN THE ST. LOUIS AND WOOD RIVER PLUMES

Oxidant concentrations in the urban-industrial plume are established by a complex chemical system involving many reactants which were not monitored by the MRI aircraft. It is nevertheless possible to deduce some of the bulk characteristics of the reaction scheme from the profiles of the species which were measured.

Figures 35, 41, and 42 show oxidant profiles observed immediately downwind of the metropolitan area under three different wind conditions: northwesterly (30 July and 3 August), southerly (12 August), and southeasterly (15 August). All four traverses were flown in the morning, at altitudes from 457 m (1500 ft) to 610 m (2000 ft) msl. The profiles from all four traverses displayed certain regularities; the highest oxidant concentrations were measured downwind of downtown St. Louis and the Wood River refineries, and were associated with high light-scattering coefficients.

The oxidant profiles of 30 July and 15 August, measured on oppostie sides of the city, are almost mirror images. Each shows two distinct oxidant plumes, one downwind of St. Louis/East St. Louis/ Granite City and the other downwind of Alton/Wood River. The apparent superposition of these two plumes, by a southerly wind on 12 August, produced the highest concentrations measured during the 17-day sampling period. The narrow oxidant plumes observed before 0900 CDT on 3 August appear to pinpoint the central business district of St. Louis and the refinery complex of Wood River as the source areas.

The automotive traffic of downtown St. Louis and the refinery operations at Wood River are the most important sources of reactive hydrocarbons in the sampling area, and their emissions evidently played a critical role in the production of oxidant. It is worth noting that the 100 ton/hour estimated net rate of ozone production in the 30 July St. Louis/Wood River plume greatly exceeds the 20 ton/hour estimated annual average rate of hydrocarbon emissions in the St. Louis/Wood River urban-industrial area (U.S. EPA, Illinois EPA). In contrast, the maximum ozone concentrations produced by the irradiation of hydrocarbon mixtures in smog chambers are typically less than the initial concentrations of hydrocarbons (e.g., Wilson, et al, 1972). Possible explanations for the apparent high ozone yield of hydrocarbons in the urban-industrial plume have been discussed by Walker (1976).

In most traverses, the light-scattering coefficient correlated well with oxidant concentrations within a given plume, although the relative concentrations of light-scattering aerosols and oxidant varied from plume to plume. Moreover, the narrow aerosol and oxidant plumes of 3 August and 12 August are remarkably coincident.

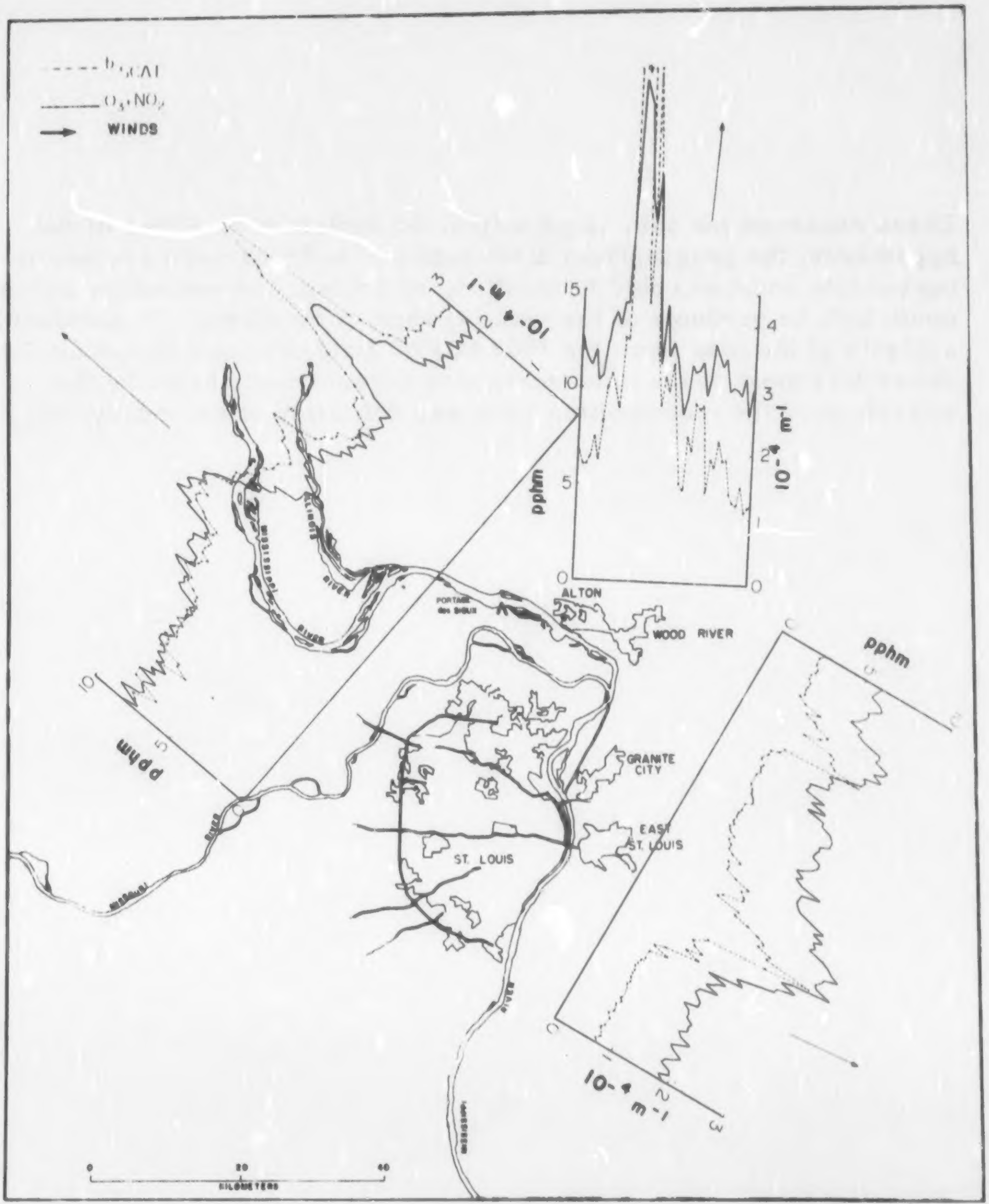
b_SCAT
O3+NO2
WINDS
10^-4 m^-1
pphm
15
10
5
0
4
3
2
1
0
ALTON
WOOD RIVER
PORTAGE des SIOUX
MISSISSIPPI RIVER
ILLINOIS RIVER
MISSOURI RIVER
RIVER
GRANITE CITY
EAST ST. LOUIS
ST. LOUIS
0
20
40
KILOMETERS

76-137

Figure 42. Horizontal profiles of oxidant concentration and light-scattering coefficient (b_{scat}) downwind of Greater St. Louis under three different wind regimes. Traverses and wind arrows are as in Figure 35. High oxidant concentrations were generally associated with high light-scattering coefficients.

These observations can, in principle, be explained by either of two hypotheses; the geographical distribution of hydrocarbons and primary particulate sources could be similar, or oxidant and secondary aerosols could both be products of the same system of reactions. Preliminary analysis of the data from the 1975 MISTT field program (Appendix B) shows that most of the light-scattering aerosol contributed by the emissions of the metropolitan area was definitely of secondary origin.

APPENDIX TO SECTION 5

A MODEL FOR THE OZONE DEFICIT IN POWER PLANT PLUMES

In the following paragraphs, a model is presented which predicts the ozone profile of the plume from the observed sulfur dioxide profile, based on the fundamental photolytic $O_3/NO/NO_2$ cycle:

$$NO_2 + h\nu \xrightarrow{\varphi k_1} NO + O \qquad /1/$$

$$O + O_2 + M \xrightarrow{k_2} O_3 + M \qquad /2/$$

$$O_3 + NO \xrightarrow{k_3} NO_2 + O_2 \qquad /3/$$

In the atmosphere, molecular oxygen and the third body M of Reaction 2 are present at high concentrations which are not disturbed by trace chemistry. The state of the chemical system participating in Reactions 1 - 3 is thus characterized at any point by four variables: the local concentrations of ozone, atomic oxygen, nitric oxide, and nitrogen dioxide. Through a change of coordinates, this state can be expressed in terms of other variables as well. It is particularly convenient to express the state of the system in terms of variables which are invariants of Reactions 1 - 3 and depend only on the environment and geometry of the plume. In these coordinates, the problem reduces to that of the physical dispersion of an inert pollutant.

Since the system under consideration has four degrees of freedom, four chemical invariants must be identified:

- In the atmosphere, atomic oxygen tends to a stationary state in which it is destroyed by Reaction 2 at about the same rate at which it is formed by Reaction 1. In this situation

$$\varphi k_1 [NO_2] = k_2 [O] [O_2] [M],$$

or

$$[O]/[NO_2] = \varphi k_1 / k_2 [O_2] [M] = \varphi k_1 / k_2' . \qquad (3)$$

Based on the value for k_2' given by Leighton (1961), the time required for the atomic oxygen concentration to approach within 10 percent of its stationary value is about 10^{-4} seconds. On macroscopic time scales, the quantity $[O]/[NO_2]$ is thus an invariant of Reactions 1 - 3. Its value, $\varphi k_1 / k_2'$, is determined primarily by the intensity of ultraviolet radiation, and is spatially uniform if the optical thickness of the plume is ignored.

- Like atomic oxygen, ozone in the atmosphere also tends to a stationary state in which it is destroyed and formed at roughly equal rates. In this situation

$$k_1 [NO_2] = k_2 [O] [O_2][M] = k_3 [O_3] [NO],$$

or

$$[O_3] [NO]/[NO_2] = \varphi k_1 / k_3 . \qquad (4)$$

The time required for ozone to approach within 10 percent of its stationary value varies inversely with the nitric oxide concentration; for a relatively low nitric oxide concentration of 0.01 ppm, the approach would take about ten minutes, based on the values for k_3 reported by Schofield (1967). This is much longer than that for atomic oxygen, but is still short compared with the characteristic times for plume dilution at the distances sampled, so that $[O_3] [NO]/[NO_2]$ can be considered an approximate invariant of Reactions 1 - 3. Its value, $\varphi k_1 / k_3$, is determined primarily by the intensity of ultraviolet radiation, and is spatially uniform if the optical thickness of the plume is ignored.

- It was observed in the introduction that the total oxidant concentration is a stoichiometric invariant of Reactions 1 - 3:

$$[O] + [O_3] + [NO_2] = [\text{oxidant}]. \qquad (5)$$

Unlike the relationships in Equations 3 and 4, which could be perturbed only by competing reactions with speeds comparable to those of Reactions 1 - 3, the conservation of oxidant can be perturbed over a period of time even by comparatively slow competing reactions. The background oxidant level in the sampling area is in fact established by the interplay of such competing reactions, but it does not appear to be perturbed by the Labadie plume at the distances sampled. Very little oxidant is emitted by the plant, and the concentration of oxidant within the plume was consistent with the background levels on either side (Figures 39 and 40).

- Like the concentration of oxidant, the concentration of nitrogen oxides is a stoichiometric invariant of Reactions 1 - 3

$$[NO] + [NO_2] = [NO_x]. \qquad (6)$$

Unlike the previous three chemical invariants, which are essentially unaffected by the emissions of the Labadie plant, the concentration of nitrogen oxides is significantly higher within the plume than it is on either side, due to the nitric oxide emitted by the plant. The spatial distribution of nitrogen oxides is easy to model, however, since NO_x can be treated as a chemically inert contaminant. In Figures 43 and 44, SO_2 is used as a tracer for the plume, and the expected NO_x concentration is calculated from the formula

$$[NO_x] = 0.3\,[SO_2] + B,$$

with the background, B, equal to 26 ppb at 21 km and 30 ppb at 45 km. The correspondence between calculated and measured concentration is good. (As with Relation 5,

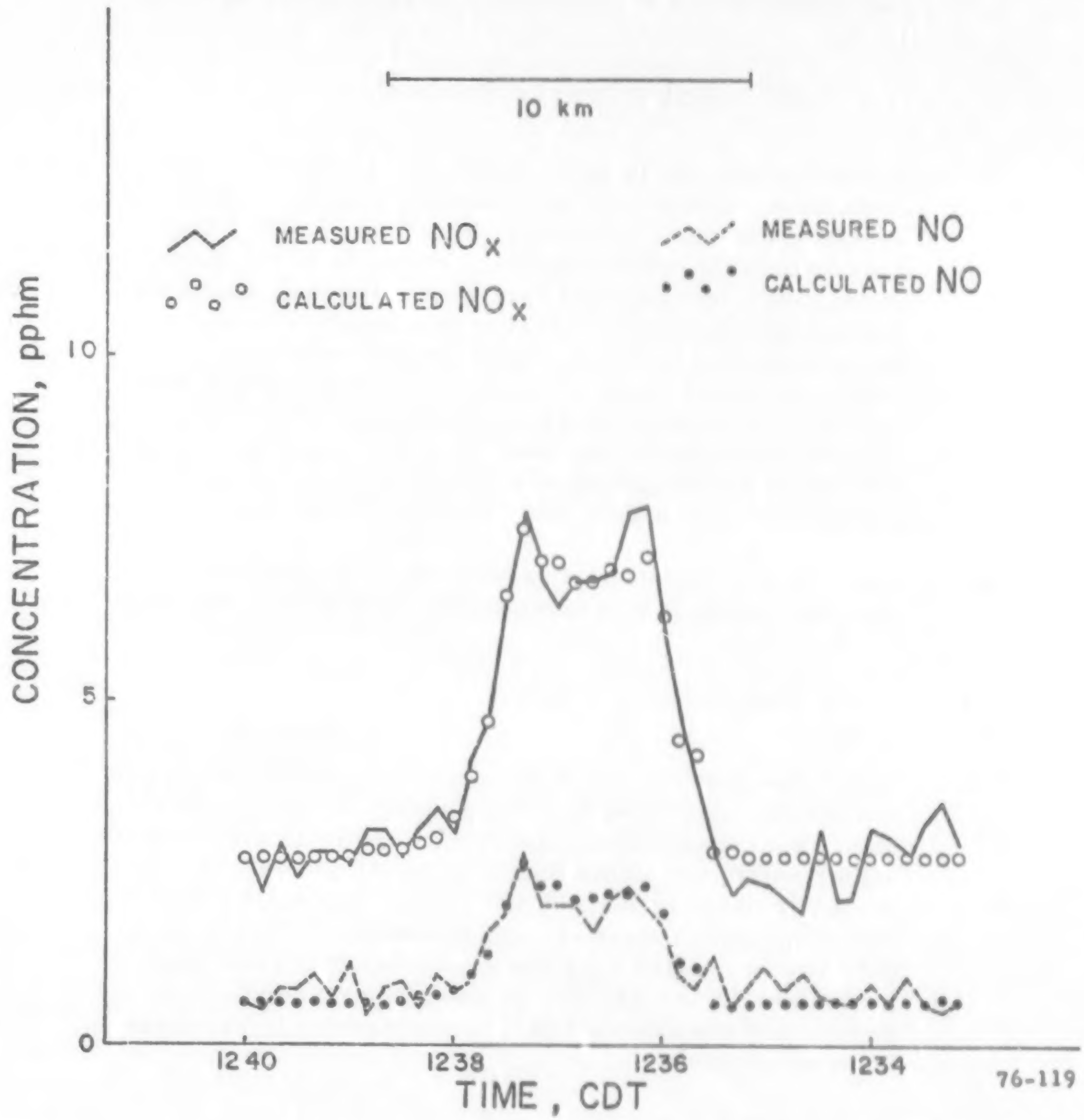

Figure 43. Horizontal plume traverse 21 km downwind of Labadie stacks on 14 August 1974. Most of the NO emitted by the power plant had already been oxidized to NO_2. Measured NO_x profile agreed well with NO_x profile scaled from measured SO_2 concentrations. Measured NO profile agreed well with NO profile calculated from measured SO_2 profile and oxidant-preserving photochemistry. (The same traverse is shown in Figure 39).

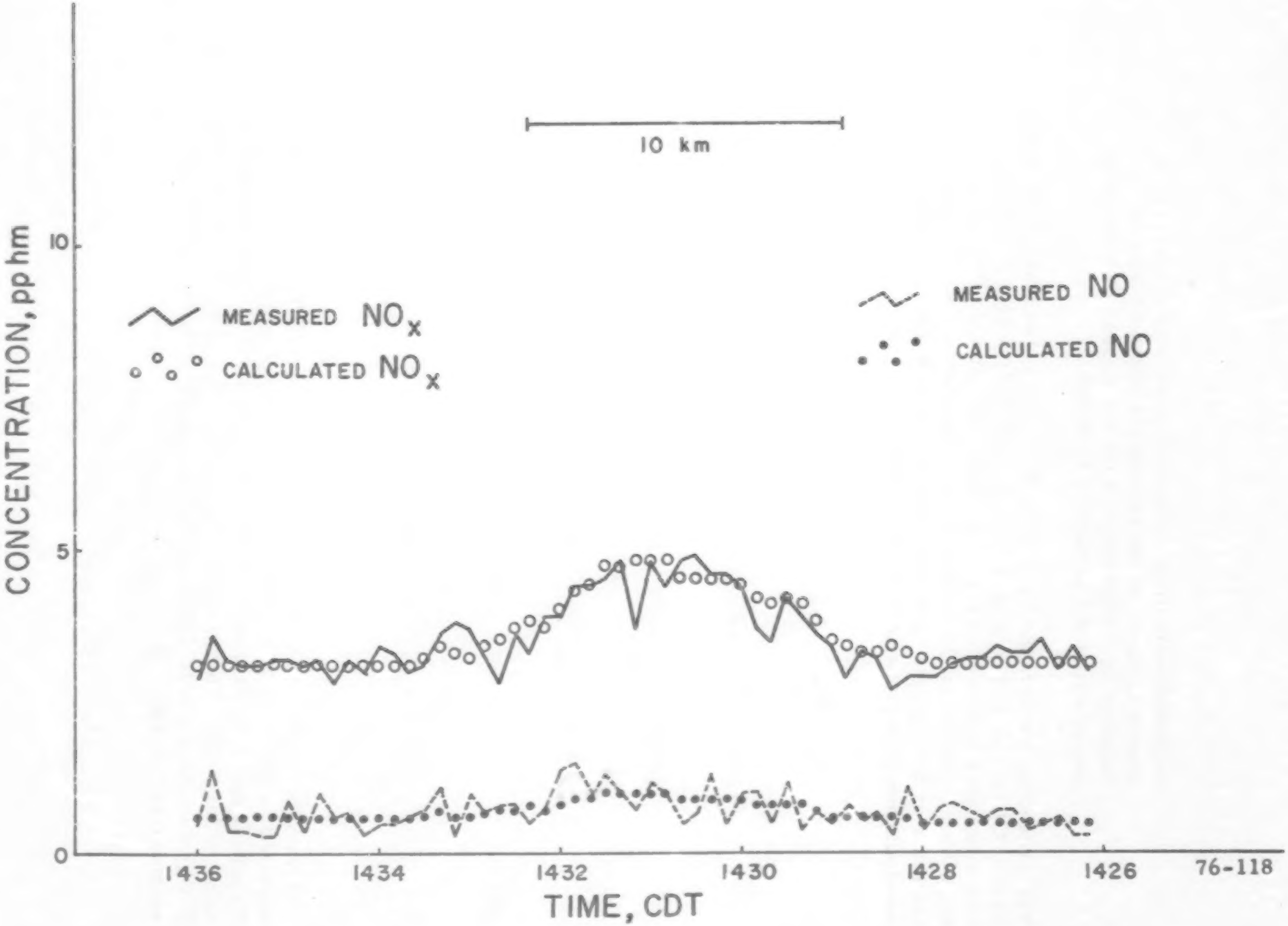

Figure 44. Horizontal plume traverse 45 km downwind of Labadie stacks on 14 August 1974. Nitric oxide concentrations were near the detection limit of the monitor, and very little excess within the plume was observed or predicted. (The same traverse is shown in Figure 40.)

> comparatively slow competing reactions may, over a period of time, erode the conservation of NO_x in Relation 6. This effect does not appear to have been important at the distances sampled.)

The preceding paragraphs have identified four quantities, $[O]/[NO_2]$, $[O_3][NO]/[NO_2]$, $[O] + [O_3] + [NO_2]$, and $[NO] + [NO_2]$, which are invariants of Reactions 1 - 3 under the photostationary conditions which prevail in the atmosphere. Together, they characterize the state of this simple chemical system, and elementary algebraic manipulation of Equations 3 to 6 gives:

$$[O] = \frac{\alpha - 1}{2\alpha} \left(\varphi k_1 / k_3 + [\text{oxidant}] + \alpha [NO_x] - X\right), \tag{7}$$

$$[O_3] = \frac{1}{2} \left(-\varphi k_1 / k_3 + [\text{oxidant}] - [NO_x] + X\right), \tag{8}$$

$$[NO] = \frac{1}{2\alpha} \left(-\varphi k_1 / k_3 - [\text{oxidant}] + \alpha [NO_x] + X\right), \tag{9}$$

$$[NO_2] = \frac{1}{2\alpha} \left(\varphi k_1 / k_3 + [\text{oxidant}] + \alpha [NO_x] - X\right), \tag{10}$$

where $\alpha = 1 + \varphi k_1 / k_2'$ and

$$X = \Big((\varphi k_1 / k_3 + [\text{oxidant}] + \alpha [NO_x])^2 - 4\alpha [\text{oxidant}] [NO_x] \Big)^{1/2} .$$

The variables $\varphi k_1 / k_2'$, $\varphi k_1 / k_3$, [oxidant], and $[NO_x]$ are easily modeled, since they are independent of plume chemistry, and Expressions 7 to 10 then yield analytical models for the concentrations of interest. The profiles of $\varphi k_1 / k_2'$, $\varphi k_1 / k_3$, [oxidant], and $[NO_x]$ used in the calculations for Figures 38 - 40, 43, and 44 are summarized in Table 6 .

Table 6. PARAMETERS USED IN MODEL CALCULATIONS

	(a)	(a)	(b)	(c)	
				$[NO_x] = A\,[SO_2] + B$	
Figure Number	$\varphi k_1/k_2'$ dimensionless	$\varphi k_1/k_3$ pphm	[oxidant] pphm	A dimensionless	B pphm
38(d)	0	1.5	9.0	0.30	3.0
39, 43	0	2.0	9.0	0.30	2.6
40, 44	0	1.5	10.4-8.3	0.30	3.0

The expected profiles for ozone and nitric oxide shown in Figures 38 - 40, 43, and 44 were calculated from formulas 8 and 9, using the above parameter values and the measured profile of sulfur dioxide.

(a) The following sources were consulted for the rate constants: Jackson (1975) for φk_1, with the ultraviolet radiation intensity estimated from the time of day; Leighton (1961) for k_2'; and Schofield (1967) for k_3.

(b) Background oxidant concentrations were determined from ozone and nitrogen dioxide concentrations outside the plume. In the calculations for Figures 40 and 44, the oxidant was taken to decrease linearly with time, dropping from 10.4 pphm at 1426 CDT to 8.3 pphm at 1436 CDT.

(c) The expected NO_x concentration was calculated from the measured sulfur dioxide concentration according to the formula

$$[NO_x] = A\,[SO_2] + B,$$

where B is the average NO_x concentration outside the plume. The same scaling factor A was used at all distances, in accordance with the assumption that NO_x was conserved.

(d) The traverses at 10 km from the plant were flown with the nitrogen oxides monitor on the 0-1 ppm scale, which was not separately calibrated. Nitric oxide, NO_x, and oxidant profiles are therefore not shown for this distance.

SECTION VI

REFERENCES

Adams, D. F., and R. K. Koppe. Instrumenting Light Aircraft for Air Pollution Research. Journal Air Pollution Control Assoc., 19. pp 410-415. 1969.

Ahlquist, N. C., and R. J. Charlson. Measurement of the Vertical and Horizontal Profile of Aerosol Concentration in Urban Air with the Integrating Nephelometer. Environ. Sci. Tech., 2. pp 363-366. 1968.

Anderson, J. A., and D. L. Blumenthal. Aircraft Monitoring Support for an Aerosol Characterization Study in St. Louis. MRI Final Report No. MRI 74 FR-1146. 1974.

Bevington, P. R. Data Reduction and Error Analysis for the Physical Sciences. McGraw-Hill, New York. 1969.

Davis, D. D., G. Smith, G. Klauber. Trace Gas Analysis of Power Plant Plumes via Aircraft Measurement: O_3, NO_x, and SO_2 Chemistry. Science, 186. pp 733-736. 1974.

Gillani, N. V. Data Processing, Management and Analysis Related to Project MISTT, 1975. Report of the Air Pollution Laboratory, Washington University, St. Louis, Missouri. 1975.

Hackney, J. D. Testimony given to the Permanent Subcommittee on Air Quality of the California State Assembly. 26 September 1975.

Husar, R. B. Coagulation of Knudsen Aerosols. Ph.D. Thesis, University of Minnesota, Minneapolis, Minnesota. 1971.

Husar, J. D., R. B. Husar, E. S. Macias, W. E. Wilson, J. L. Durham, W. K. Shepherd, and J. A. Anderson. Particulate Sulfur Analysis: Application to High Time Resolution Aircraft Sampling in Plumes. To be published. 1975.

Jackson, J. O. Ambient Kinetics of the NO_2 Photolysis Rate and Verification of the Atmospheric $NO/NO_2/O_3$ Photostationary State. Ph.D. Thesis, University of Michigan, Ann Arbor, Michigan. 1974.

REFERENCES (continued)

Leighton, P. A. Photochemistry of Air Pollution. Academic Press, New York. 1961.

Link, W. T., D. A. McClatchie, A. B. Watson, and A. Compher. A Fluorescent Source NDIR Carbon Monoxide Analyzer. Joint Conference on Sensing of Environmental Pollutants, Palo Alto, California. 8-10 November 1971.

MacCready, P. B., Jr., R. E. Williamson, S. Berman, and A. Webster. Operational Application of a Universal Turbulence Measuring System. MRI Final Report No. MRI 65 FR-301 to NASA Edw, Contract NASA-784. 1965.

Markowski, G. R. A Useful Method for Transient Response Analysis and Data Correction Applied to Aircraft Plume Sampling. 68th Annual Meeting of the Air Pollution Control Assoc. Paper No. 75-40.3. June 1975.

Mirabel, P. and J. L. Katy. Binary Homogeneous Nucleation as a Mechanism of the Formation of Aerosols. J. Chem. Phys., 60. pp 1138-1144. 1974.

Owens, M. J. and A. W. Powell. Deposition Velocity of Sulfur Dioxide on Land and Water Surfaces Using a ^{35}S Tracer Method. Atmos. Environ., 8. pp 63-67. 1974.

Rich, T. A. Particles in Air Pollution. Colloquium on the Physics and Chemistry of Aerosols, Fontenay-Aux-Roses, France. September 1970.

Roberts, P. T. Gas-to-Particle Conversion: Sulfur Dioxide in a Photochemically Reactive System. Ph.D. Thesis, California Institute of Technology, Pasadena, California. 1975.

Schofield, K. An Evaluation of Kinetic Rate Data for Reactions of Neutrals of Atmospheric Interest. Planetary and Space Sciences, 15. pp 643-670. 1967.

Shepherd, J. G. Measurements of the Direct Deposition of Sulfur Dioxide onto Grass and Water by the Profile Method. Atmos. Environ., 8. pp 69-74. 1974.

REFERENCES (continued)

Walker, H. M. Some Considerations Regarding Rural Ozone. Air Pollution Control Assoc. Conference on Ozone/Oxidants, Dallas, Texas. March 11-12, 1976.

Whitby, K. T., B. K. Cantrell, R. B. Husar, N. V. Gillani, J. A. Anderson, D. L. Blumenthal, W. E. Wilson, Jr. Aerosol Formation in a Coal Fired Power Plant Plume. For presentation before the Division of Environmental Chemistry, Americal Chemical Society, New York. April 4-9, 1976.

White, W. H., P. T. Roberts, and S. K. Friedlander. On the Nature and Origins of Visibility-Reducing Aerosols in the Los Angeles Air Basin. In the Characteristics and Origins of Smog Aerosol, G. M. Hidy and P. K. Mueller, Editors. To Appear. 1975.

Wilson, W. E. Jr., A. Levy, and D. B. Wimmer. A Study of Sulfur Dioxide in Photochemical Smog II. Effect of Sulfur Dioxide on Oxidant Formation in Photochemical Smog. J. Air Poll. Control Assoc., 22. pp 27-32. 1972.

APPENDIX A

SAMPLING PATTERNS

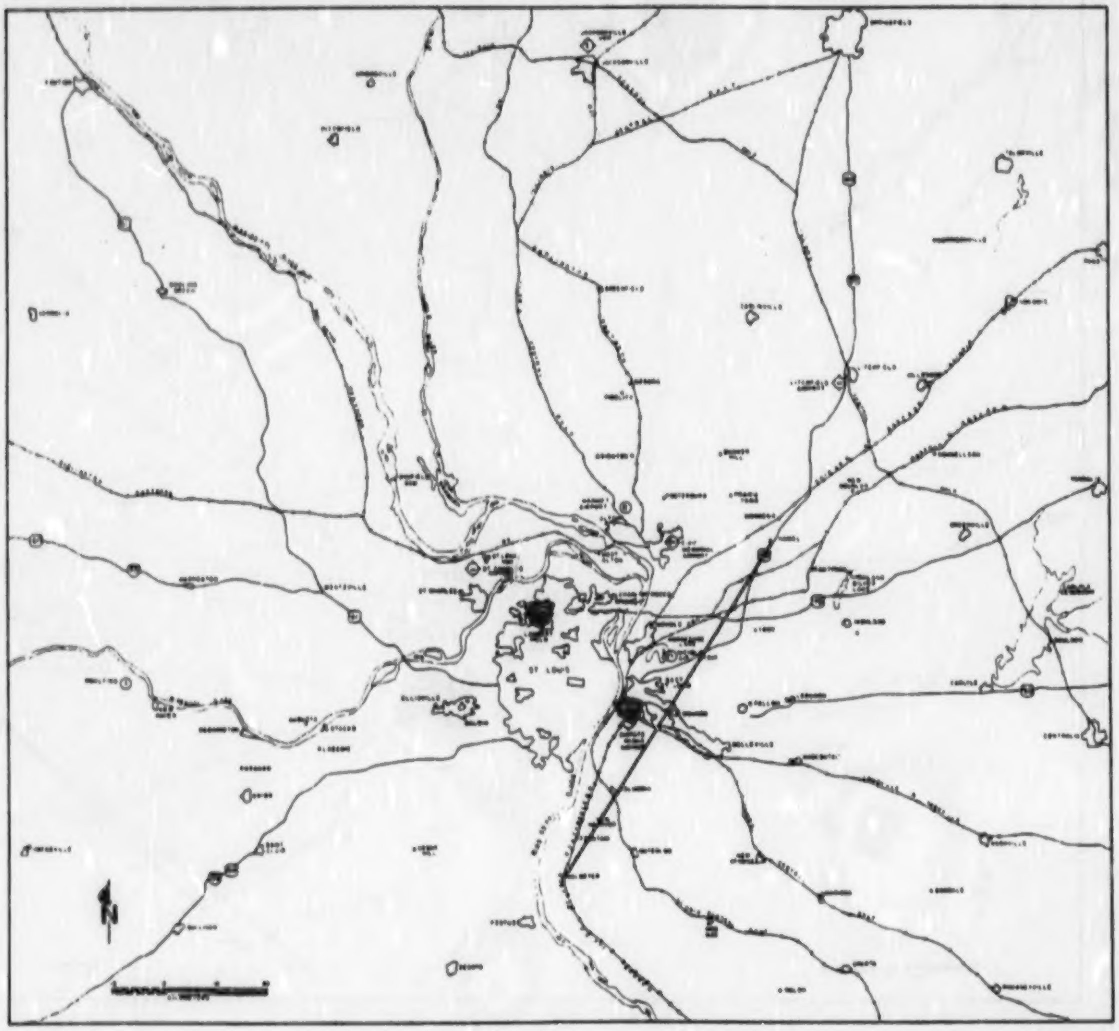

Fig. 45. LOCATION OF AIRCRAFT SAMPLING ROUTES, MORNING, JULY 30, 1974

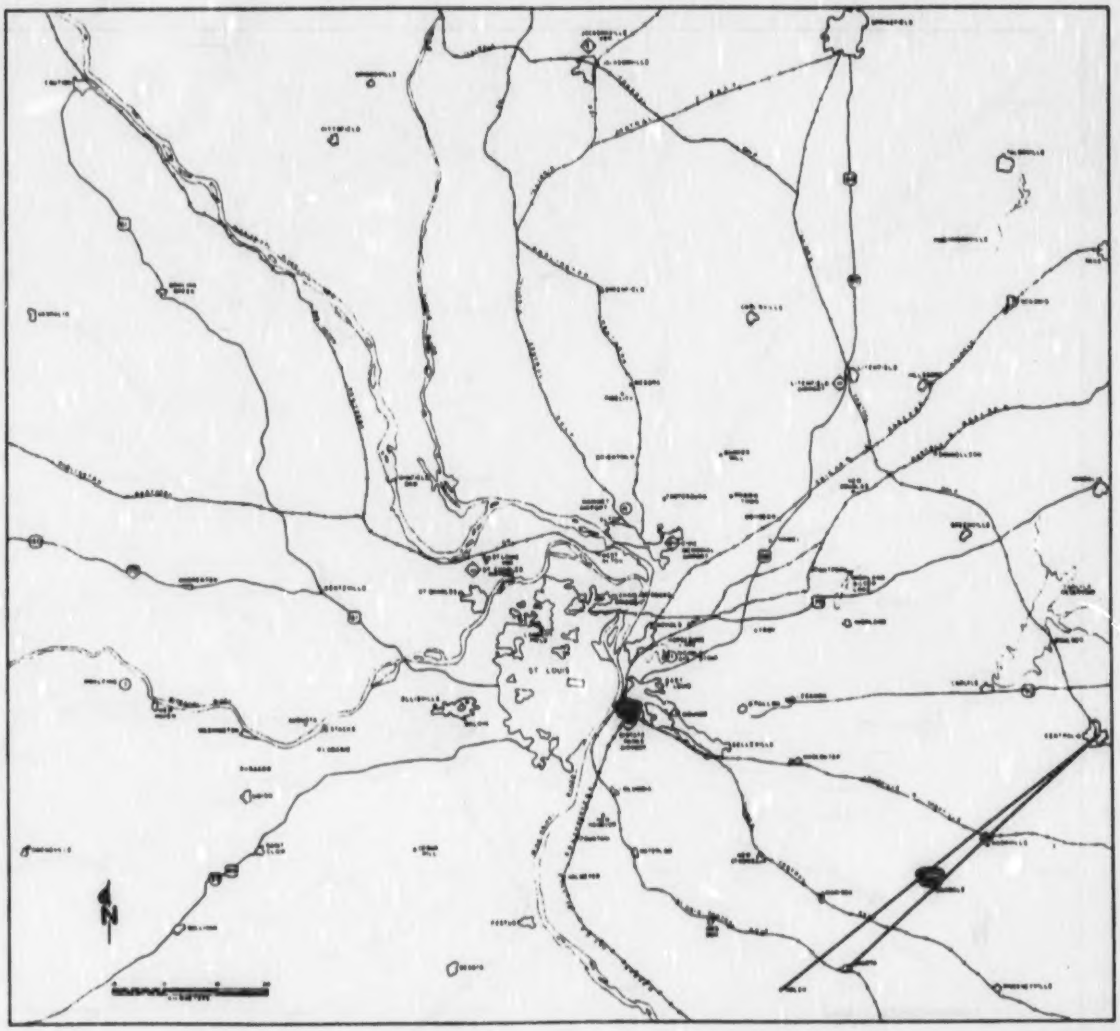

Fig. 46. LOCATION OF AIRCRAFT SAMPLING ROUTES, AFTERNOON, JULY 30, 1974

TABLE 7.

Flight Outline

Date: July 30, 1974 (Morning)
Cartridge No. 036

Pass No.	Route	Start Time (CDT)	Stop Time (CDT)	Altitude (m msl)	Sulfate Filter
Spiral	East of Lambert	0859	0920	180-2896	
2	New Hanover-Hamel	0933	0952	457	1
3	Hamel-Valmeyer	0958	1021	610	1
4	Valmeyer-Hamel	1025	1047	914	1
5	Hamel-New Hanover	1052	1111	1219	1
6	New Hanover-Hamel	1115	1134	1524	1
7	Hamel-Bi-State	1142	1152	2134	1
Spiral	Bi-State Airport	1153	1204	2134-126	

TABLE 8.

Flight Outline

Date: July 30, 1974 (Afternoon)
Cartridge No. 027

Pass No.	Route	Start Time (CDT)	Stop Time (CDT)	Altitude (m msl)	Sulfate Filter
Spiral	Bi-State Airport	1323	1341	126-2591	
2	Sparta-Centralia	1356	1411	305	2
3	Centralia-Walsh	1415	1437	610	2
4	Walsh-Centralia	1440	1500	914	2
5	Centralia-Sparta	1504	1522	1211	2
6	Sparta-Centralia	1525	1542	1524	2
Spiral	Oakdale	1604	1616	2591-183	

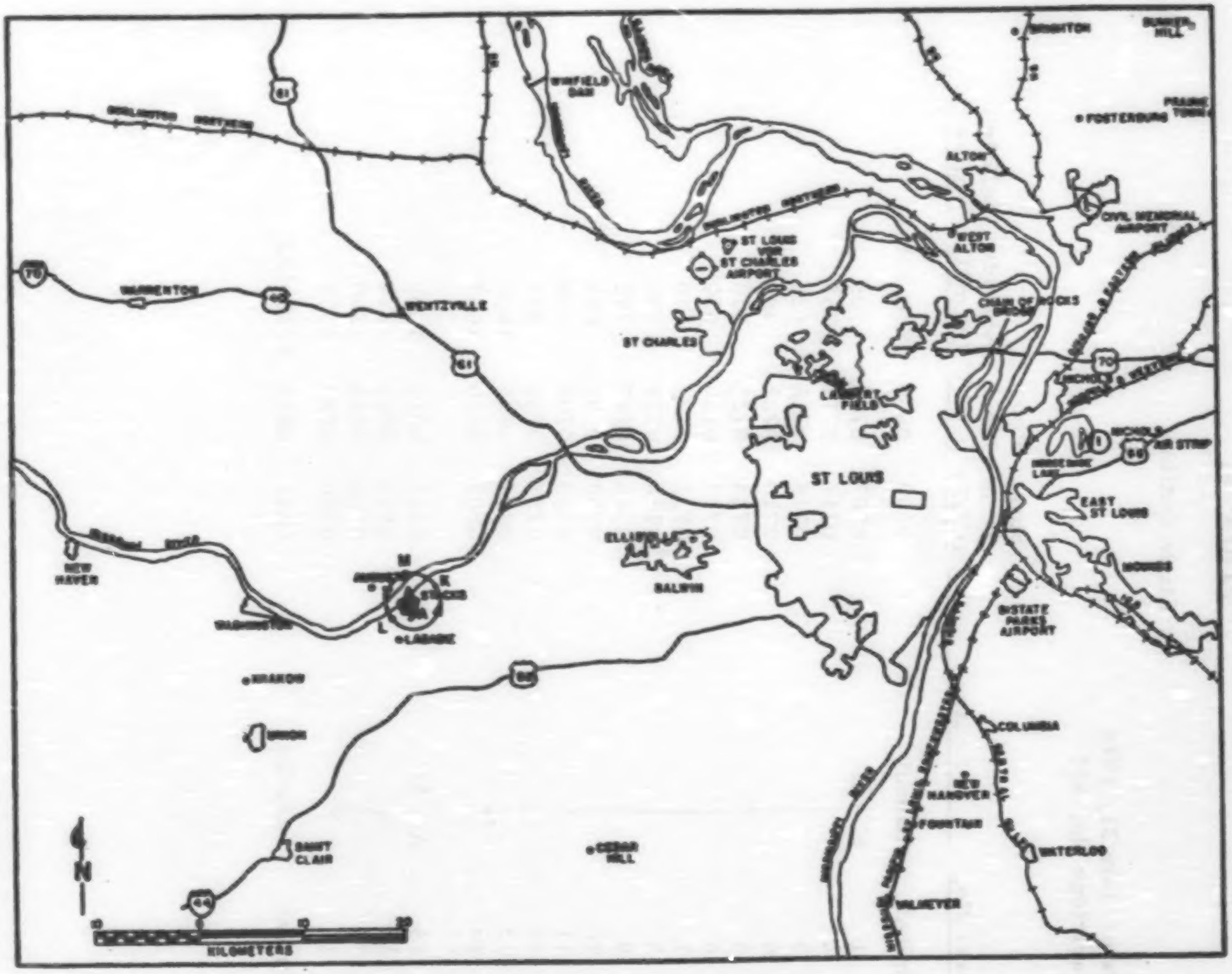

BRIGHTON
BUNKER HILL
FOSTERBURG
PRAIRIE TOWN
WINFIELD DAM
BURLINGTON NORTHERN
ALTON
WEST ALTON
CIVIL MEMORIAL AIRPORT
ST LOUIS VOR
ST CHARLES AIRPORT
WARRENTON
WENTZVILLE
ST CHARLES
CHAIN OF ROCKS BRIDGE
LAMBERT FIELD
NICHOLS AIR STRIP
HORSESHOE LAKE
ST LOUIS
EAST ST LOUIS
ELLISVILLE
BALWIN
MONKS
BISTATE PARKS AIRPORT
NEW HAVEN
WASHINGTON
M
K
STACKS
L
LABADIE
KRAKOW
UNION
COLUMBIA
NEW HANOVER
FOUNTAIN
WATERLOO
VALMEYER
SAINT CLAIR
CEDAR HILL
MISSOURI RIVER
MISSISSIPPI RIVER
70
40
61
66
44
55
67
N
10
0
10
20
KILOMETERS

Fig. 47. LOCATION OF AIRCRAFT SAMPLING ROUTES, JULY 31, 1974

TABLE 9.

Flight Outline

Date: July 31, 1974
Cartridge No. 033

Pass No.	Route	Start Time (CDT)	Stop Time (CDT)	Altitude (m msl)	Sulfate Filter
Spiral	Labadie	0650	0659	1370-305	
1	K - L	0707	0708	305	
2	↓	0711	0712	365	
3		0715	0716	425	
4		0719	0722	487	
5		0723	0725	548	
6		0728	0730	610	
7		0733	0734	670	
8		0738	0739	730	
9		0745	0747	792	
10		0750	0751	853	
11		0753	0755	914	
12		0757	0759	975	
13		0804	0806	1036	
14		0808	0810	1097	
15	A - M	0811	0814	1158	
16	↓	0816	0819	1219	
17		0821	0823	1280	
18		0826	0828	1158	
Spiral	Labadie	0842	0854	1829-152	

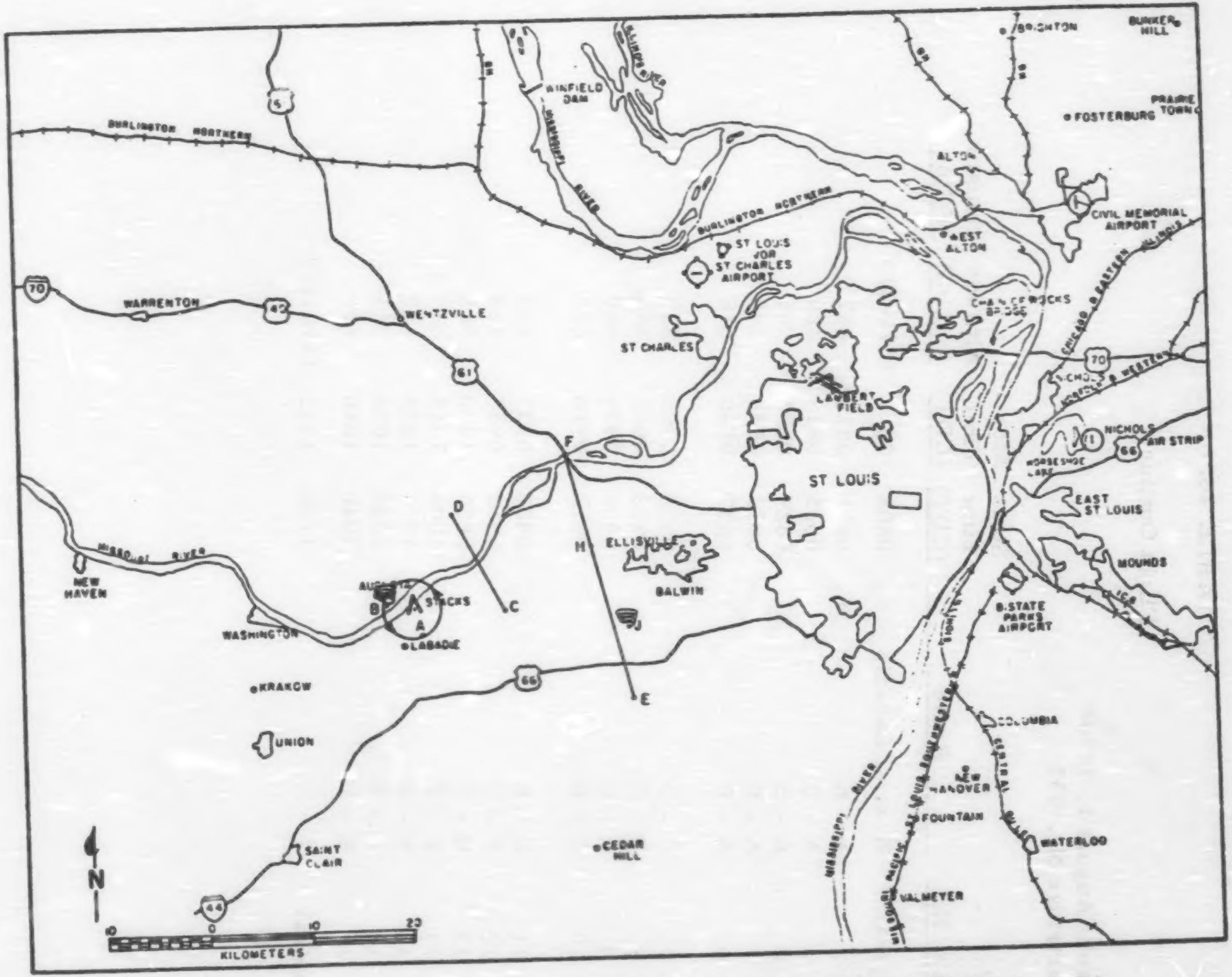
BRIGHTON
BUNKER HILL
FOSTERBURG
PRAIRIE TOWN
WINFIELD DAM
ILLINOIS RIVER
MISSISSIPPI RIVER
BURLINGTON NORTHERN
ALTON
EAST ALTON
CIVIL MEMORIAL AIRPORT
ST LOUIS JOR ST CHARLES AIRPORT
70
WARRENTON
42
WENTZVILLE
61
5
CHAIN OF ROCKS BRIDGE
CHICAGO & EASTERN ILLINOIS
NORFOLK & WESTERN
ST CHARLES
LAMBERT FIELD
NICHOLS
AIR STRIP
66
HORSESHOE LAKE
ST LOUIS
EAST ST LOUIS
MOUNDS
F
D
H
ELLISVILLE
BALWIN
MISSOURI RIVER
NEW HAVEN
AUGUSTA
B
A
STACKS
C
J
WASHINGTON
LABADIE
B-STATE PARKS AIRPORT
E
KRAKOW
UNION
COLUMBIA
NEW HANOVER
FOUNTAIN
CENTRAL
WATERLOO
CEDAR HILL
SAINT CLAIR
44
VALMEYER
MISSOURI PACIFIC
ST LOUIS SOUTHWESTERN
N
10
0
10
20
KILOMETERS

Fig. 48. LOCATION OF AIRCRAFT SAMPLING ROUTES, AUGUST 1, 1974

TABLE 10.

Flight Outline

Date: August 1, 1974
Cartridge No. 037

Pass No.	Route	Start Time (CDT)	Stop Time (CDT)	Altitude (m msl)	Sulfate Filter
Spiral	West of Labadie	0808	08	1371-213	
2	A - B	0821	0824	457	
3	A - B	0825	0828	426	
4	A - B	0829	0832	488	
5	A - B	0833	0836	549	
6	A - B	0837	0840	518	
7	C - D	0850	0855	427	
8	D - C	0858	0902	488	
9	C - D	0905	0909	549	
10	C - D	0912	0918	610	
11	E - F	0927	0937	427	
12	F - E	0938	0948	488	
13	E - F	0950	1000	365	
14	F - E	1004	1014	549	
15	E - H	1020	1028	488	
16	H - E	1030	1036	365	
17	E - H	1040	1048	610	
Spiral	J	1100	1112	1676-183	

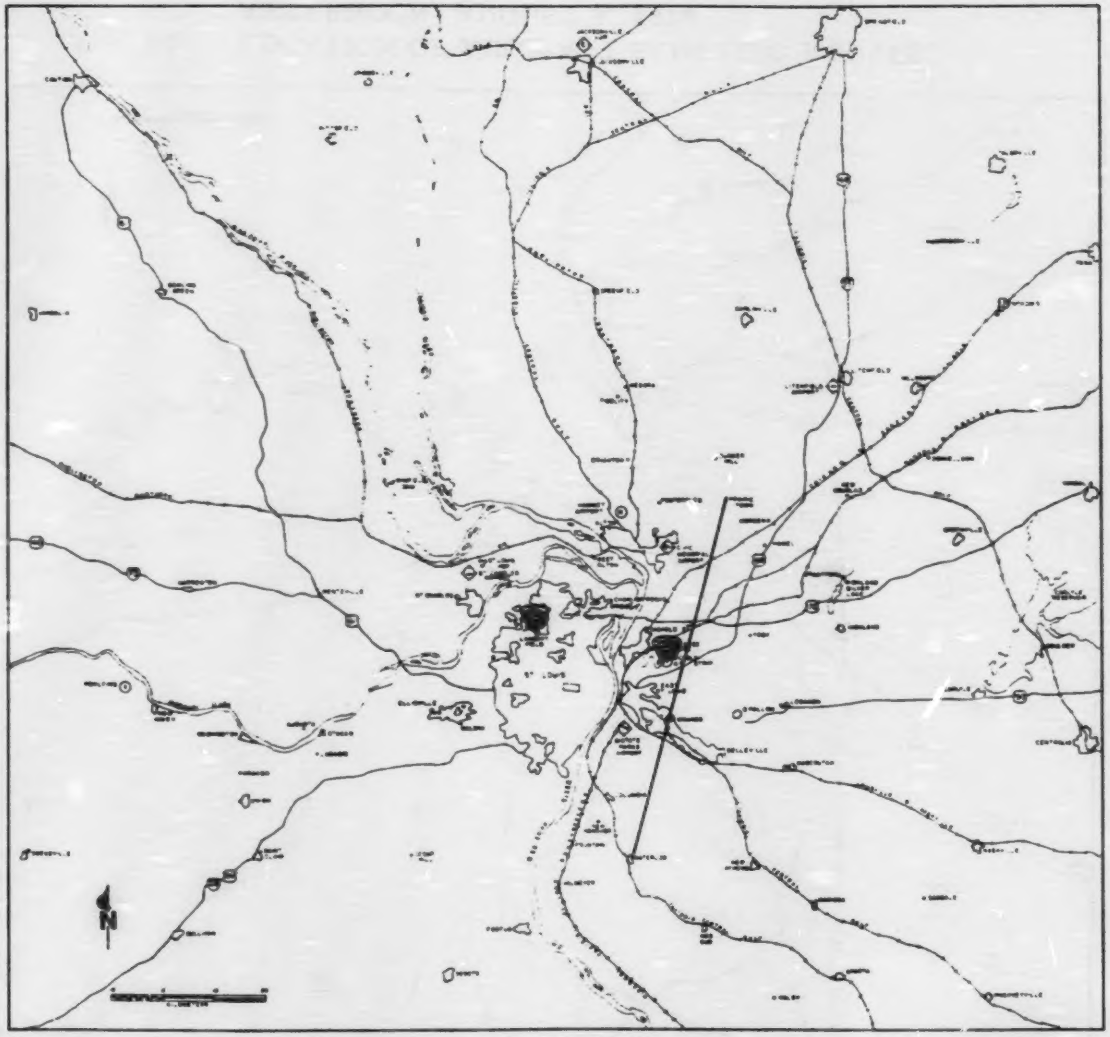

Fig. 49. LOCATION OF AIRCRAFT SAMPLING ROUTES, MORNING, AUGUST 3, 1974

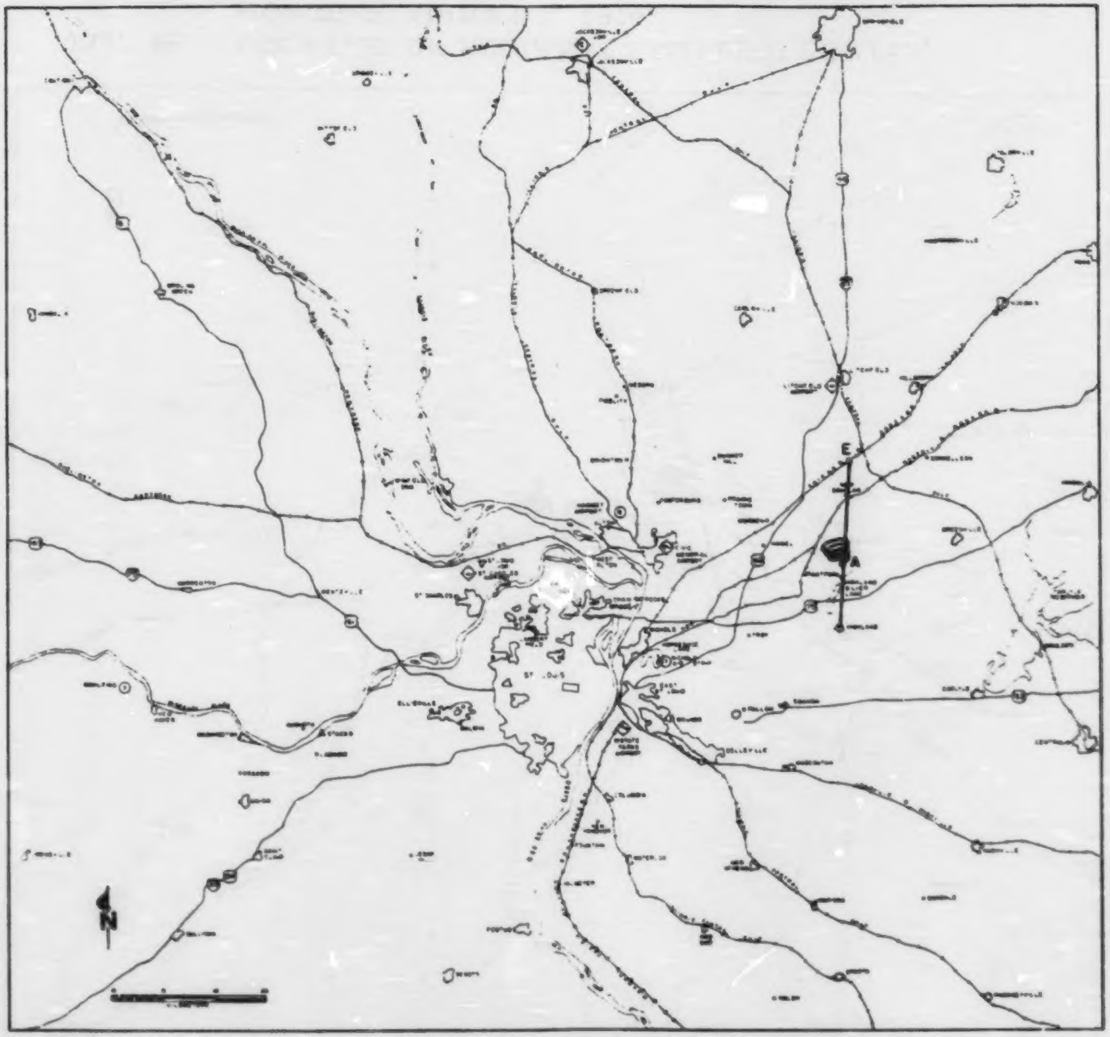

Fig. 50. LOCATION OF AIRCRAFT SAMPLING ROUTES, AFTERNOON, AUGUST 3, 1974

TABLE 11.

Flight Outline

Date: August 3, 1974 (Morning)
Cartridge No. 034

Pass No.	Route	Start Time (CDT)	Stop Time (CDT)	Altitude (m msl)	Sulfate Filter
Spiral	Lambert	0810	0821	180-1524	
2	Prairietown-Waterloo	0835	0856	457	1
3	Waterloo-Prairietown	0859	0920	762	1
4	Prairietown-Waterloo	0923	0943	914	1
5	Waterloo-Prairietown	0945	1007	610	1
6	Prairietown-Waterloo	1013	1035	1067	
7	Waterloo-Prairietown	1040	1100	1372	
Spiral	Nichols Airstrip	1128	1146	2897-128	

TABLE 12.

Flight Outline

Date: August 3, 1974 (Afternoon)
Cartridge No. 747

Pass No.	Route	Start Time (CDT)	Stop Time (CDT)	Altitude (m msl)	Sulfate Filter
Spiral	A	1327	1336	1981-152	
2	New Douglas-Highland	1341	1350	305	2
3	Highland-New Douglas	1352	1400	457	2
4	New Douglas-Highland	1402	1410	610	2
5	Highland-E	1413	1422	762	2
6	E-Highland	1427	1436	914	2
7	Highland-E	1439	1448	1067	2
8	E-Highland	1452	1501	1219	2
9	Highland-E	1504	1513	1372	2
10	E-Highland	1517	1527	1524	2
11	Highland-E	1529	1537	1676	2
12	E-Highland	1540	1550	1829	2
Spiral	A	1556	1610	2438-183	

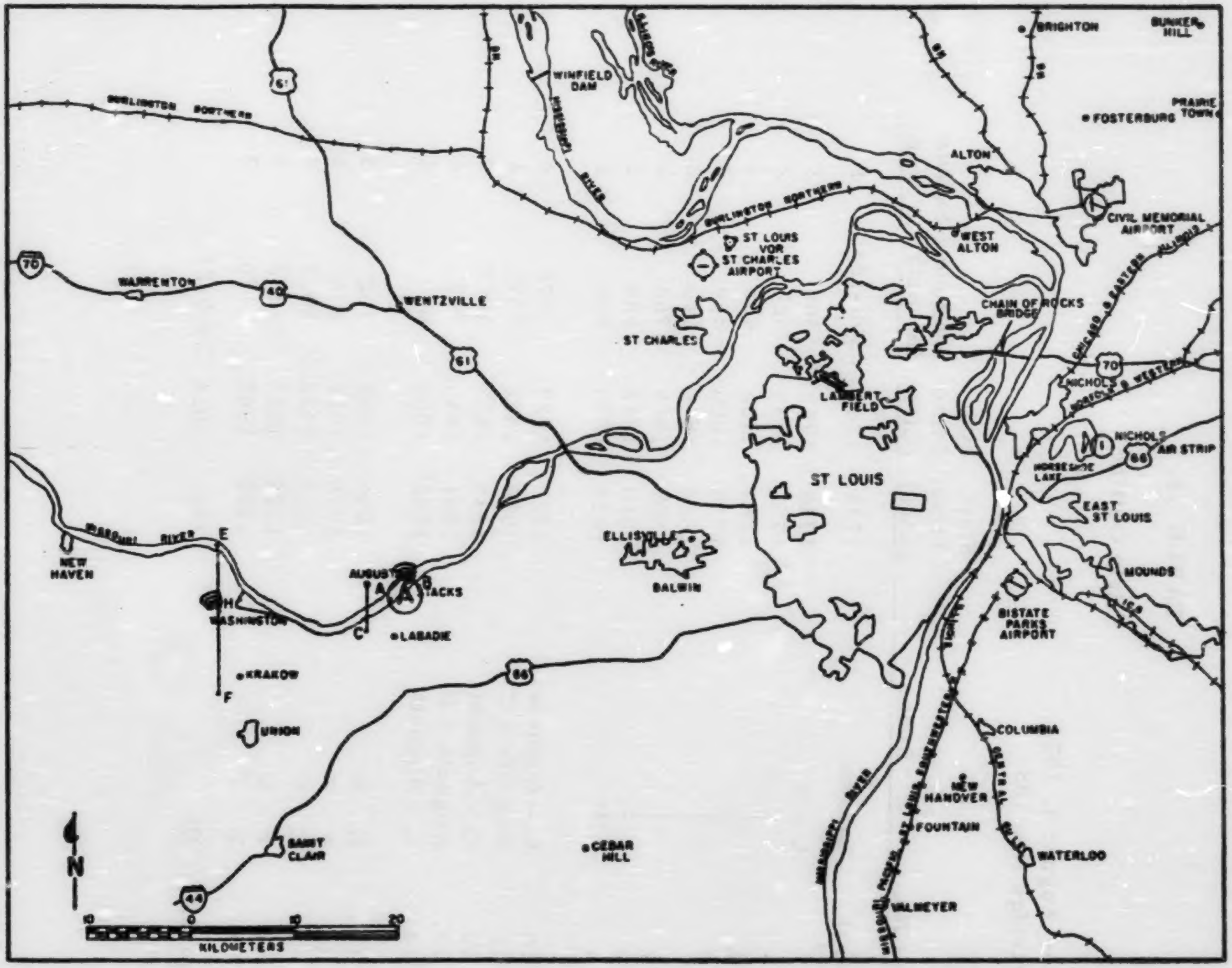
BRIGHTON
BUNKER HILL
PRAIRIE TOWN
FOSTERBURG
ALTON
CIVIL MEMORIAL AIRPORT
WEST ALTON
WINFIELD DAM
ILLINOIS RIVER
MISSISSIPPI RIVER
BURLINGTON NORTHERN
BURLINGTON NORTHERN
BN
BN
BN
61
61
70
70
40
66
66
44
WARRENTON
WENTZVILLE
ST LOUIS VOR
ST CHARLES AIRPORT
ST CHARLES
CHAIN OF ROCKS BRIDGE
CHICAGO & EASTERN ILLINOIS
NORFOLK & WESTERN
NICHOLS
NICHOLS AIR STRIP
HORSESHOE LAKE
LAMBERT FIELD
ST LOUIS
EAST ST LOUIS
MOUNDS
ICG
BISTATE PARKS AIRPORT
MISSOURI RIVER
NEW HAVEN
E
F
H
WASHINGTON
AUGUSTA
A
B
C
STACKS
LABADIE
KRAKOW
UNION
ELLISVILLE
BALWIN
SAINT CLAIR
CEDAR HILL
COLUMBIA
NEW HANDOVER
FOUNTAIN
WATERLOO
VALMEYER
MISSOURI PACIFIC
ST LOUIS SOUTHWESTERN
CENTRAL ILLINOIS
MISSISSIPPI RIVER
N
10
0
10
20
KILOMETERS

Fig. 51. LOCATION OF AIRCRAFT SAMPLING ROUTES, AFTERNOON, AUGUST 5, 1974

TABLE 13.

Flight Outline

Date: August 5, 1974
Cartridge No. 788

Pass No.	Route	Start Time (CDT)	Stop Time (CDT)	Altitude (m msl)	Sulfate Filter
Spiral	Labadie	1724	1744	2590-183	1
2	A - B	1748	1749	365	2
3	↓	1751	1753	427	2
4		1754	1756	488	2
5		1759	1800	549	2
6		1804	1806	610	2
7		1807	1809	762	2
8		1810	1812	884	2
9		1814	1815	686	2
10	C - Augusta	1825	1827	1676	4
11	Augusta - C	1830	1832	1372	4
12	C - Augusta	1835	1837	1067	4
13	Augusta - C	1841	1843	762	4
14	C - Augusta	1848	1850	457	4
15	E - F	1856	1902	762	3
16	F - E	1905	1911	396	3
17	E - F	1918	1924	1067	3
18	F - E	1928	1935	1372	3
19	E - F	1940	1947	1676	3
Spiral	H	1954	2014	2590-213	

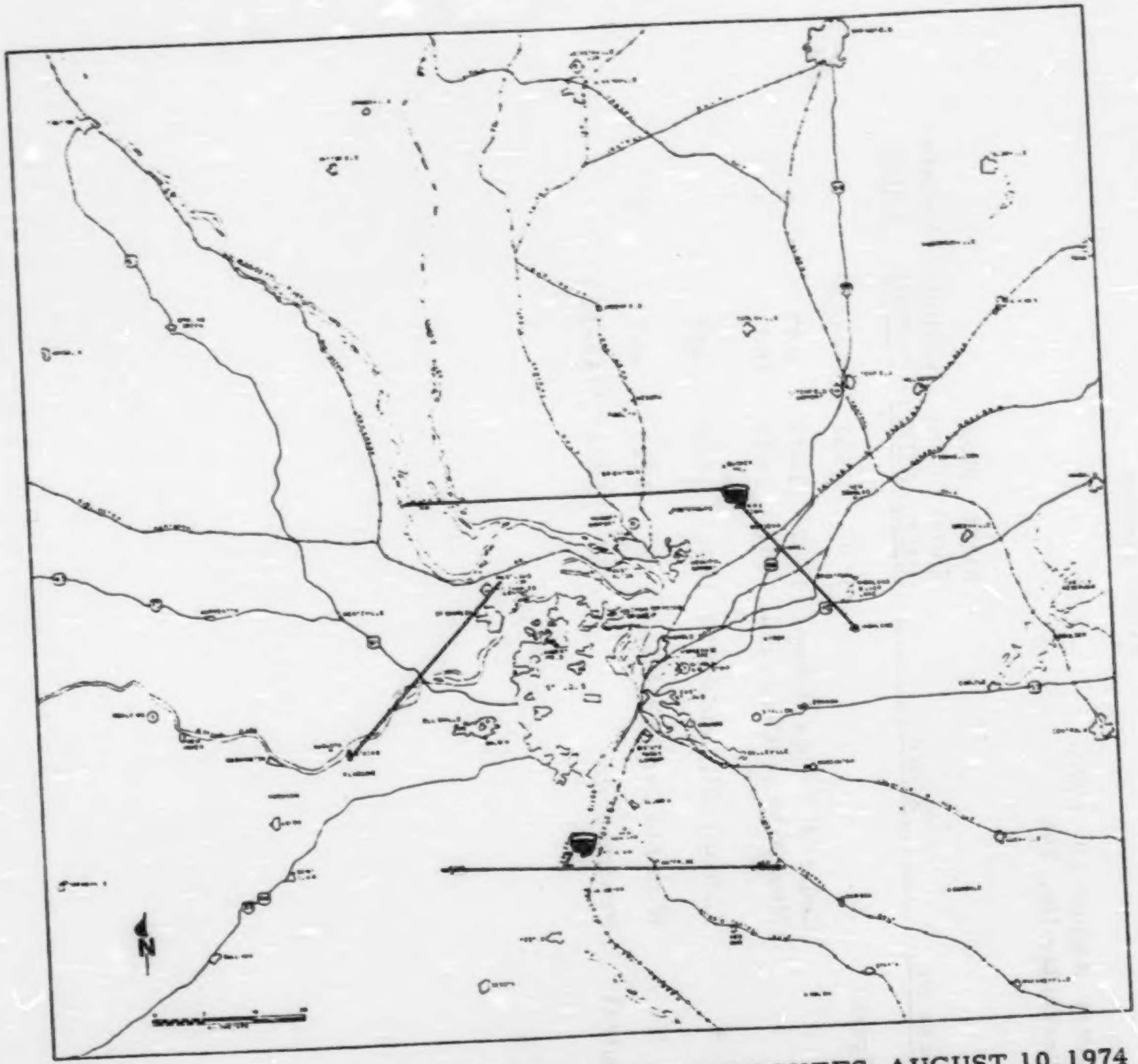

Fig. 52. LOCATION OF AIRCRAFT SAMPLING ROUTES, AUGUST 10, 1974

TABLE 14.

Flight Outline

Date: August 10, 1974
Cartridge No. 795

Pass No.	Route	Start Time (CDT)	Stop Time (CDT)	Altitude (m msl)	Sulfate Filter
Spiral	Z	1505	1532	2743-153	
2	Cedar Hill-New Athens	1547	1603	457	3
3	New Athens-Cedar Hill	1607	1629	1067	4
4	Labadie-St. Louis VOR	1637	1652	457	
5	Winfield Dam-Highland	1700	1729	457	2
Spiral	Prairietown	1751	1820	2743-153	

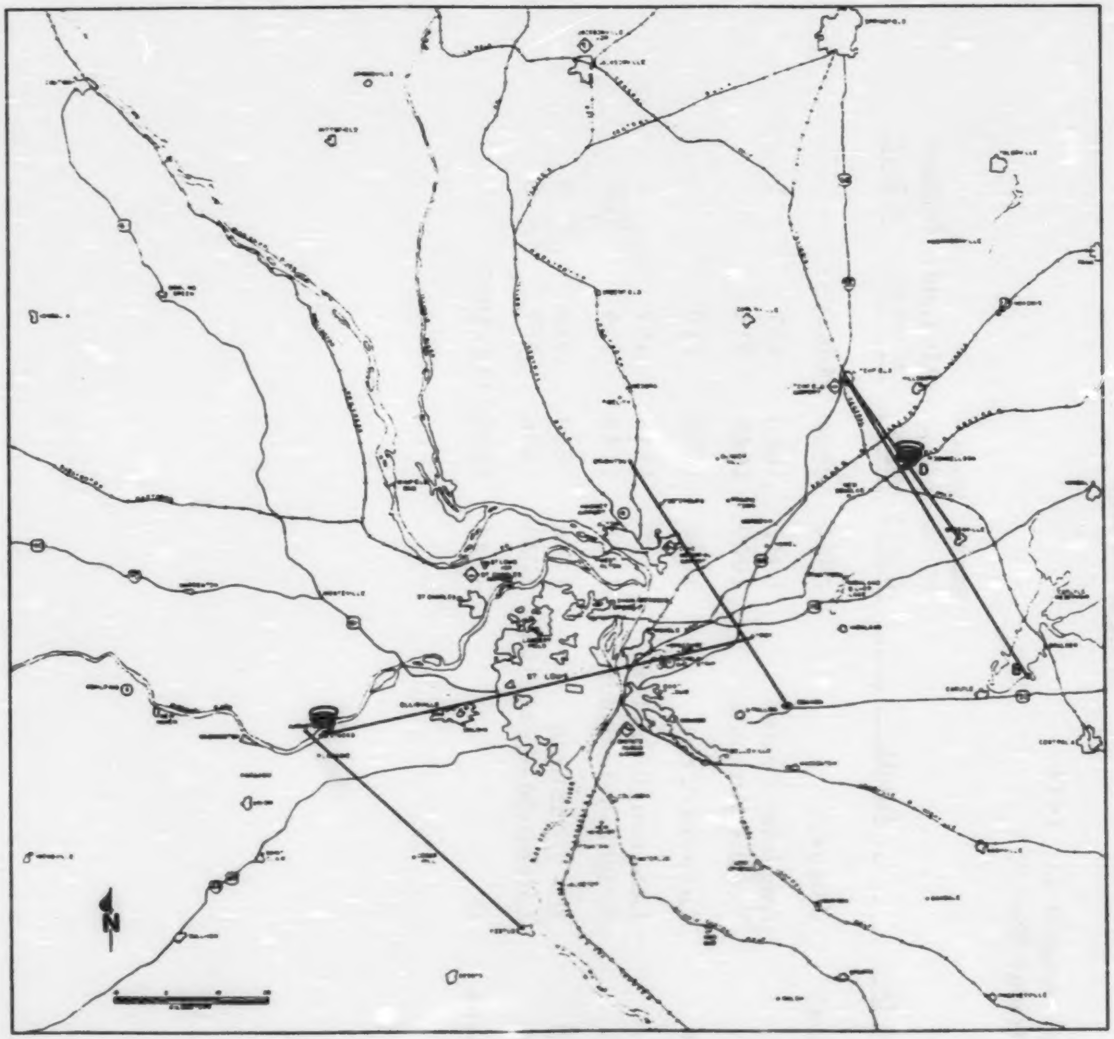

Fig. 53. LOCATION OF AIRCRAFT SAMPLING ROUTES, AUGUST 11, 1974

TABLE 15.

Flight Outline

Date: August 11, 1974
Cartridge No. 755

Pass No.	Route	Start Time (CDT)	Stop Time (CDT)	Altitude (m msl)	Sulfate Filter
Spiral	Augusta	0904	0934	2896-153	
2	Augusta-Festus	0942	1000	457	1
3	Festus-Augusta	1009	1028	914	1
4	Labadie-Troy	1030	1054	610	
5	Lebanon-Brighton	1100	1118	457	2
6	Brighton-Lebanon	1123	1140	914	2
7	B - Litchfield	1158	1219	914	3
8	Litchfield-Greenville	1224	1236	457	3
Spiral	D	1244	1253	152-1067	

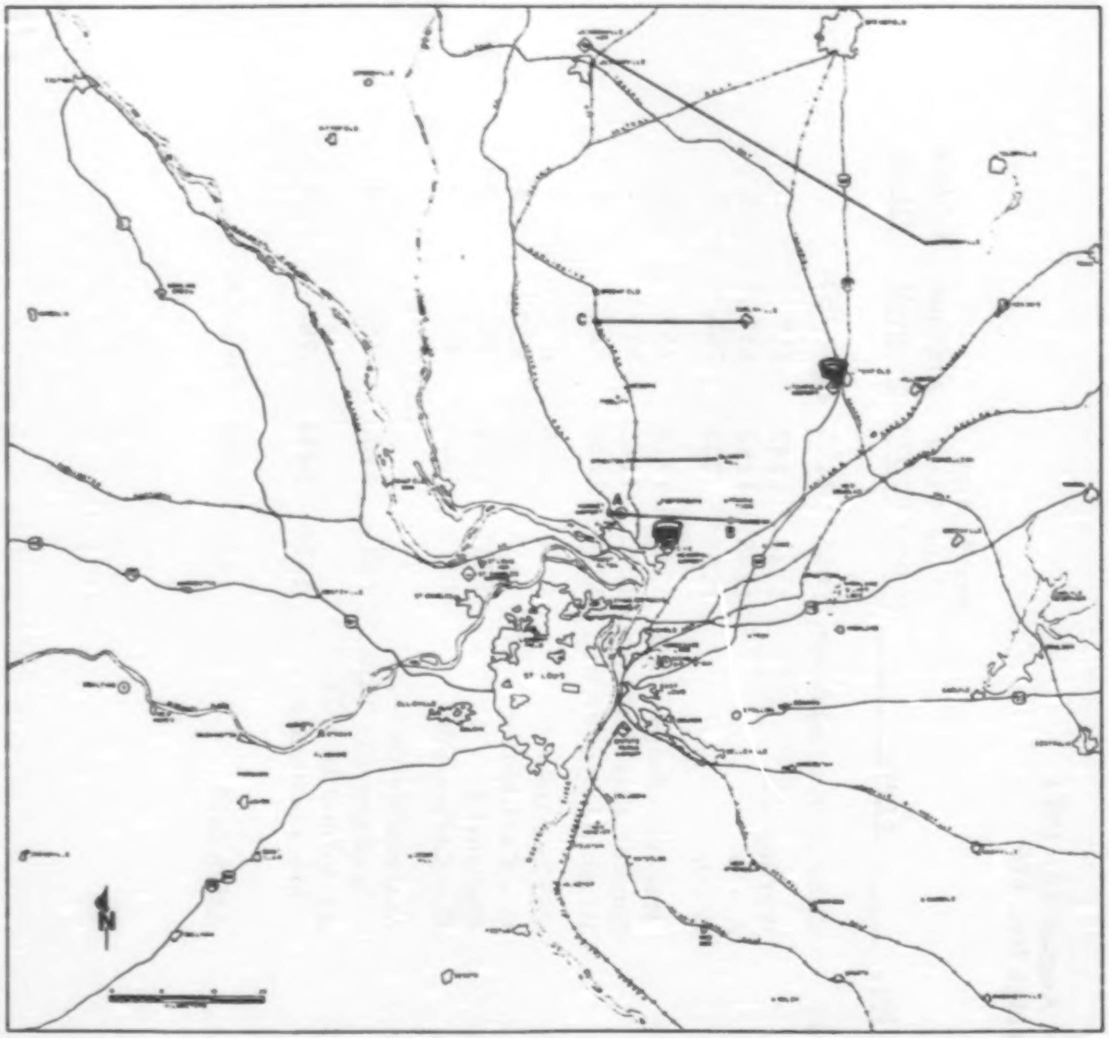
A
B
C
ST LOUIS
N

Fig. 54. LOCATION OF AIRCRAFT SAMPLING ROUTES, AUGUST 12, 1974

TABLE 16.

Flight Outline

Date: August 12, 1974
Cartridge No. 809

Pass No.	Route	Start Time (CDT)	Stop Time (CDT)	Altitude (m msl)	Sulfate Filter
Spiral	Civic Memorial Airpt.	1055	1125	2743-153	
2	Wordon - A	1134	1143	457	1
3	A - B	1145	1152	610	1
4	B - A	1158	1205	762	1
5	Brighton-Bunker Hill	1213	1218	457	2
6	Bunker Hill-Brighton	1220	1225	610	2
7	Brighton-Bunker Hill	1229	1234	762	2
8	Carlinville - C	1242	1250	457	3
9	C - Carlinville	1253	1302	610	3
10	Carlinville - C	1304	1312	762	3
11	C - Carlinville	1315	1323	457	3
12	Morrisonville - Jacksonville VOR	1345	1408	457	4
13	Jacksonville VOR - Morrisonville	1412	1434	762	4
Spiral	Litchfield	1443	1503	1981-GR	

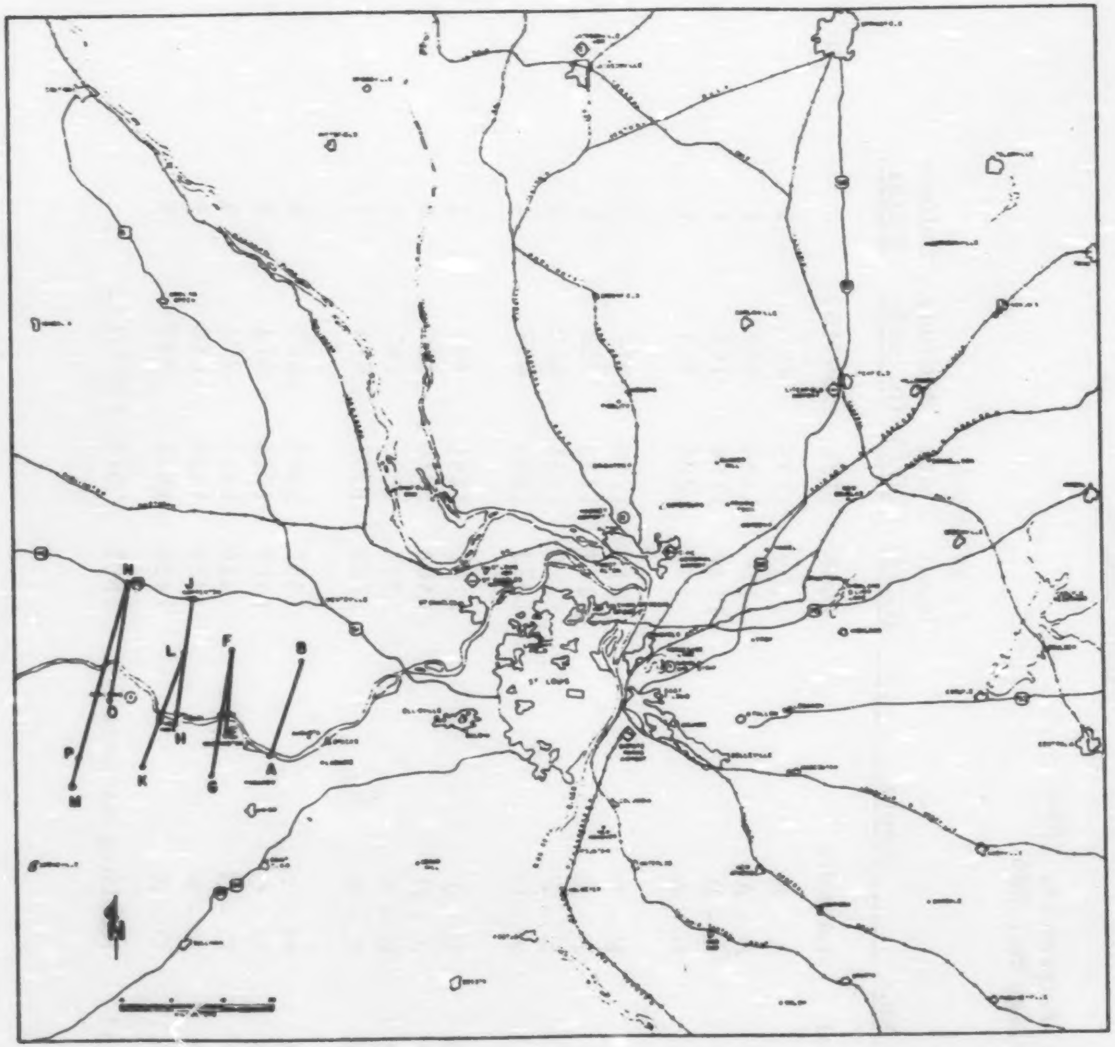
B
F
J
N
L
O
P
H
A
G
K
M
ST LOUIS
N

Fig. 55. LOCATION OF AIRCRAFT SAMPLING ROUTES, AUGUST 14, 1974

TABLE 17.

Flight Outline

Date: August 14, 1974
Cartridge No. 885

Pass No.	Route	Start Time (CDT)	Stop Time (CDT)	Altitude (m msl)	Sulfate Filter
Spiral	Labadie	1045	1121	3505-153	
2	A - B	1129	1135	457	1
3	B - A	1137	1144	610	1
4	A - B	1147	1154	762	1
5	B - A	1157	1204	914	1
6	E - F	1210	1215	914	2
7	F - E	1218	1223	762	2
8	E - F	1225	1231	610	2
9	F - G	1233	1243	457	2
10	H - J	1251	1259	457	3
11	J - H	1302	1310	610	3
12	K - L	1316	1323	762	3
13	L - K	1326	1332	914	3
14	M - N	1351	1405	1220	4
15	N - O	1407	1414	914	4
16	O - N	1416	1423	762	4
17	N - P	1425	1436	610	4
18	P - N	1438	1451	457	4
Spiral	Rohlfing Airport	1501	1518	1829-153	

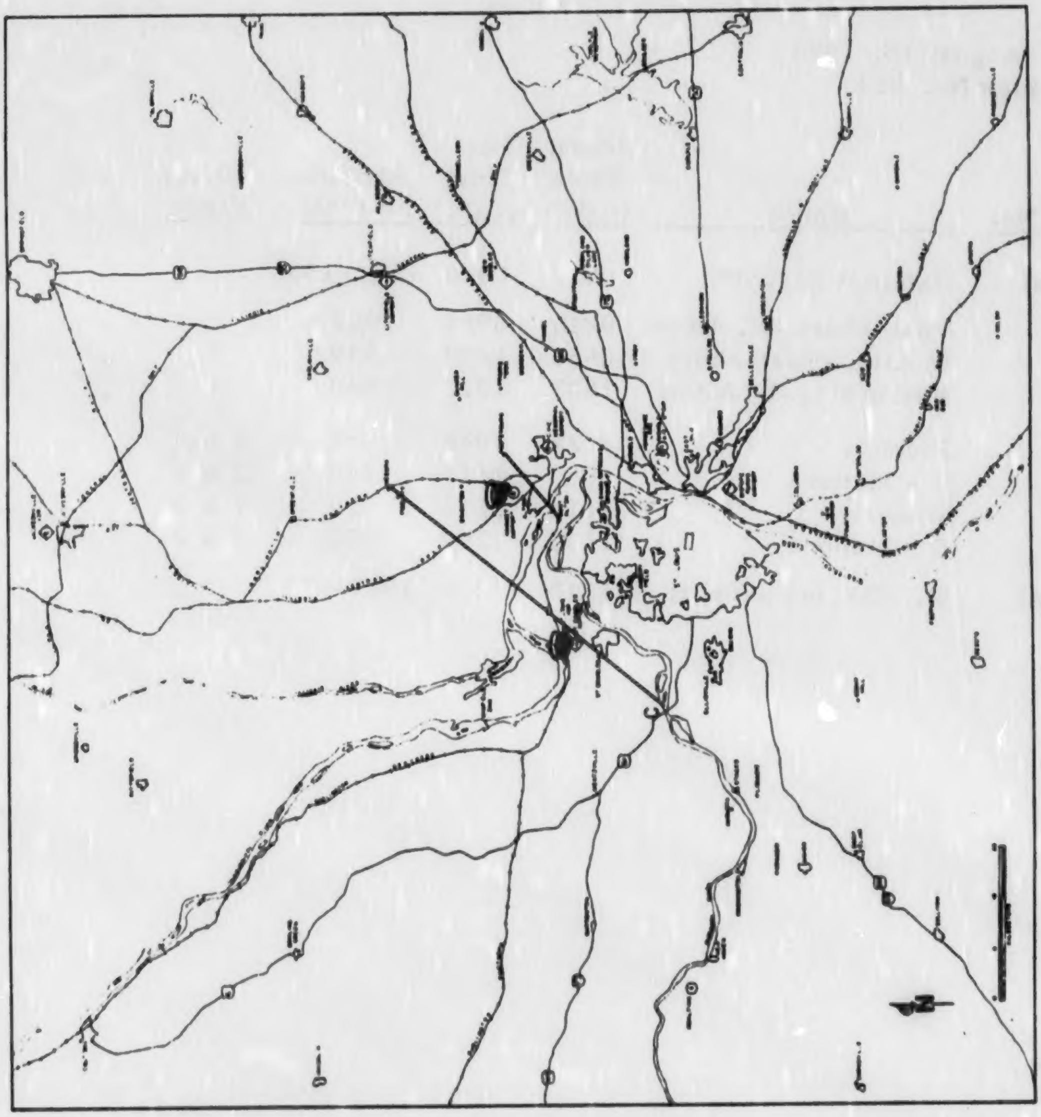

Fig. 56. LOCATION OF AIRCRAFT SAMPLING ROUTES, AUGUST 15, 1974

TABLE 18.

Flight Outline

Date: August 15, 1974
Cartridge No. 824

Pass No.	Route	Start Time (CDT)	Stop Time (CDT)	Altitude (m msl)	Sulfate Filter
Spiral	Hammet Airport	0912	0940	2896-153	
2	Fosterburg-W. Alton	0946	0951	457	1
3	W. Alton-Fosterburg	0953	1000	549	1
4	Fosterburg-W. Alton	1007	1012	640	1
5	Fidelity - C	1027	1048	457	2 & 3
6	C - Medora	1050	1111	549	2 & 3
7	Medora - C	1114	1136	670	2 & 3
8	C - Medora	1139	1200	793	2 & 3
Spiral	St. Charles Airport	1215	1236	1981-137	

APPENDIX B

FORMATION AND TRANSPORT OF SECONDARY AIR POLLUTANTS: OZONE AND AEROSOLS IN THE ST. LOUIS URBAN PLUME

MRI 76 Pa-1392 (revised), accepted for publication in SCIENCE.

ABSTRACT

Emissions from metropolitan St. Louis caused reduced visibilities and violations of the Federal Ambient Standard for ozone 160 km or more downwind of the city on July 18, 1975. Atmospheric production of ozone and visibility-reducing aerosols continues long after their primary precursors have been diluted to low concentrations.

Metropolitan St. Louis is a major urban-industrial center, encompassing coal-fired power plants with a combined capacity of 4600 MW, oil refineries with a combined capacity of 4.4×10^5 bbl/day, various other industry, and a population of about two million. It is surrounded by flat, predominantly agricultural terrain, the nearest neighboring city of 50,000 or more people being 135 km distant. Due to its isolation, the impact of St. Louis on ambient air quality is relatively easy to identify; air which has been modified by the aggregate emissions of the metropolitan area forms an "urban plume" downwind. The Fate of Atmospheric Pollutants Study[1-4] (FAPS) has shown that this plume is often identifiable 80 or 120 km from the city.

As part of Project MISTT[5,6] (Midwest Interstate Sulfur Transformation and Transport), pilot balloons and instrumented aircraft were used during the summer of 1975 to quantify the three-dimensional flow of aerosols and trace gases in the St. Louis urban plume. The plume was successfully tracked out to 240 km, and was mapped in detail out to 160 km (distances are measured from the Gateway Arch). At these distances the plume was still well defined, and on the order of 50 km wide. Our observations indicate that much of the pollutant background in the eastern United States may be due to the combined emissions of metropolitan areas far upwind.

Ozone was a conspicuous indicator of the St. Louis urban plume during the summer sampling period. Daytime ozone concentrations within the plume generally exceeded the 0.08 ppm Federal Ambient Standard, even on the most distant sampling runs. Peak concentrations in the plume were typically twice those in the unmodified background air, and surpassed 0.15 ppm on most sampling days. It is estimated that one to two parts ozone were produced for each part (C) non-methane hydrocarbons emitted by the city.

Reduced visibilities were a second characteristic feature of the St. Louis urban plume. Most of the light-scattering aerosol responsible for this reduction was of secondary origin, and its production was observed farther downwind and later in the day than that of ozone. At 100 km or more downwind, the average light-scattering coefficient[7] (b_{scat}) within the plume was typically 50 percent above the background levels on either side, with sulfate compounds accounting for most of the excess.

The results reported here generally corroborate those of FAPS on the identifiability and geometry of the St. Louis urban plume. The primary contribution of Project MISTT was to quantify the flow of material at increasing downwind distances. This made possible the study of transformations undergone by pollutants in the atmosphere, at dilutions and time scales which are difficult to simulate in the laboratory.

Figure 1 shows ozone and b_{scat} profiles recorded by the sampling aircraft[8] during selected cross-wind traverses downwind of St. Louis on July 18, 1975. Each traverse path was flown at three different altitudes, as indicated in Figure 2a, starting just downwind of St. Louis at 0900 CDT and finishing near Decatur, Illinois, at 1900 CDT. These horizontal traverses, together with vertical soundings from 1500 m msl to near ground level, documented a broad, shallow pollutant plume extending from St. Louis out past Decatur, 170 km to the northeast. The polluted airmass was about 50 km wide and deepened during the day, the mixing depth exceeding 1 km in the afternoon.

Ozone and light-scattering aerosols were the most prominant indicators of the aged plume 50 km or more downwind of St. Louis. Outside the plume, background concentrations of these contaminants were fairly uniform on July 18, although some large-scale gradients were noted (cf. ref. 2); ozone concentrations were generally below the 0.08 ppm Federal Ambient Standard, scattering coefficients were below 2.8×10^{-4} m^{-1}, and particulate sulfur concentrations were below 3.6 $\mu g/m^3$ in the few passes made completely outside the plume. Within the plume, the measured ozone concentration peaked at 0.17 ppm 66 km out, the measured scattering coefficient reached 4.9×10^{-4} m^{-1} at 125 km, and the particulate sulfur concentration, averaged over an entire traverse, measured as high as 7.5 $\mu g/m^3$ at 125 km, corresponding to an estimated average in-plume concentration of about 15 $\mu g/m^3$. In contrast, SO_2 and NO_x concentrations fell rapidly to within 0.03 ppm of background, away from major point sources.

The July 18 plume was mapped under hazy skies, with some scattered thundershowers appearing toward evening. The continued presence of a low pressure trough over the western plains produced decreasing stability and strong southwesterly flow over the Missouri and upper Mississippi valleys, which was documented in the sampling area by a total of 36 pilot balloon observations carried out as part of Project MISTT. The mean transport vector (cf. ref. 1) lay between 230° and 243° during the middle of the day, at speeds of 20-36 km/hr. At these speeds, among the highest encountered during the program, emissions from the city would have aged roughly 5-7 hours by the time they were sampled in the farthest passes.

The general direction of the airflow was corroborated by the alignment of power plant plumes in successive traverses. All of the major (greater than 1,000 MW capacity) power plants lying in and immediately upwind of the sampling area are noted in Figure 1. The plumes from some of these plants can be identified in Figure 1 by their ozone "deficits", which result from the scavenging of ambient ozone by plume NO. The Coffeen plant, 85 km WNW of St. Louis, is the only major downwind source known to the authors which lay within the July 18 urban plume.

The MISTT plume mapping program was designed to characterize pollutant concentrations and winds over cross sections of the plume at discrete distances downwind from the sources. From these measurements, the horizontal mass flow rates of pollutants at each distance can be calculated directly[5]:

$$\text{FLOW RATE} = \int u_x(x, z) \int \left(C(x, y, z) - C_o(x, z) \right) dy\, dz \quad ,$$

where x is distance downwind, y, z are cross-wind and vertical coordinates, u_x is wind speed (from pilot balloon observations), C is pollutant concentration (from aircraft measurements), and C_o is average pollutant concentration outside the plume (from aircraft measurements). Figure 2b shows the flow rates of ozone, b_{scat}, and particulate sulfur on July 18. These flow rates represent the contribution of metropolitan St. Louis (augmented slightly by the Coffeen power plant) to atmospheric loadings, and are unaffected by cross-plume and vertical dispersion.

The flow rates of ozone, b_{scat}, and particulate sulfur all increased with distance downwind of St. Louis on July 18, reflecting the secondary origin of all of the ozone and most of the light-scattering aerosol. The ozone flow rate leveled off at about 125 T/hr, which can be interpreted as the rate at which ozone was produced within the urban plume. The estimated annual average emissions of non-methane hydrocarbons in metropolitan St. Louis are about 1.6×10^5 T/yr (ref. 9); this corresponds to 18-36 T/hr, depending on whether emissions are spread out through the day or concentrated in the daylight hours. Comparison of these two figures shows that a net one to two parts ozone was produced in the urban plume for each part (C) hydrocarbons emitted in the metropolitan area[10]. This is much more efficient production than is found in most laboratory studies[11], which are conducted at higher reactant concentrations.

Most of the increase in the b_{scat} flow rate was observed downwind of the major increase in the ozone flow rate, which is consistent with the finding in laboratory studies[11] that aerosol production lags ozone production. The calculated particulate sulfur flow rates are less accurate than those for ozone and b_{scat}, particularly at the last two sampling distances, due to the more limited data available on background concentrations. The ratio of the b_{scat}

and particulate sulfur flow rates indicates[12] that sulfate compounds accounted for most of the new aerosol.

The St. Louis urban plume was mapped on a total of eight days during the July 15-August 15, 1975 MISTT experiment. The object of Project MISTT was not to develop a climatology of the urban plume, but to measure it in detail under conditions favorable for doing so, and sampling days were chosen according to this criterion. A plume of polluted air was always found downwind of the city, regardless of wind direction , confirming our attribution here of the excess concentrations to emissions from metroplitan St. Louis rather than some upwind source. On August 11, 1975, the plume again stretched out toward the northeast, and was mapped in detail out to 145 km and tracked out to 240 km. Winds on this date were lighter than on July 18, but the plume was as well defined, and concentrations and flow rates were similar.

W. H. White, J. A. Anderson and D. L. Blumenthal
Meteorology Research, Inc.
Altadena, California 91001

R. B. Husar, N. V. Gillani and J. D. Husar
Washington University
St. Louis, Missouri 63130

W. E. Wilson, Jr.
U. S. Environmental Protection Agency
Research Triangle Park, North Carolina 27711

FOOTNOTES AND REFERENCES

1. P. L. Haagenson and A. L. Morris, J. of Applied Meteorology 13, 901 (1974).
2. J. F. Stampfer, Jr. and J. A. Anderson, Atmospheric Environment 9, 301 (1975).
3. R. J. Breeding, P. L. Haagenson, J. A. Anderson, J. P. Lodge, Jr., and J. F. Stampfer, Jr., J. of Applied Meteorology 14, 204 (1975).
4. R. J. Breeding, H. B. Klonis, J. P. Lodge, Jr., J. B. Pate, D. C. Sheesley, T. R. Englert and D. R. Sears, Atmospheric Environment 10, 181 (1976).
5. R. B. Husar, J. D. Husar, N. V. Gillani, S. B. Fuller, W. H. White, W. M. Vaughan and W. E. Wilson, Jr., Proc. of the Div. Environmental Chemistry, 171st National ACS Meeting, New York, April 1976.
6. K. T. Whitby, B. K. Cantrell, R. B. Husar, N. V. Gillani, J. A. Anderson, D. L. Blumenthal and W. E. Wilson, Jr., ibid; W. E. Wilson, Jr., R. J. Charlson, R. B. Husar, K. T. Whitby, D. L. Blumenthal, Proc. 69th Annual Meeting Air Pollution Control Assoc., paper #76-30-06, June 1976.
7. The light-scattering coefficient gives the rate (fraction per distance) at which a beam of light is scattered in all directions, and is the main determinant of visual range in the atmosphere. In polluted urban air, the light-scattering coefficient is roughly proportional to the mass concentration of aerosol particles in the 0.2-2.0 μm diameter range, those inhaled most deeply into the lungs. See R. J. Charlson, N. C. Ahlquist, H. Selvidge, and P. B. MacCready, Jr., J. Air Pollution Control Assoc. 19, 937 (1969).
8. The sampling aircraft was instrumented for O_3, NO, NO_2 and SO_2 concentrations, aerosol size distribution, light scattering coefficient, electrical charge acceptance and condensation nuclei count, temperature, relative humidity, dew point and turbulent dissipation, as described by W. H. White, J. A. Anderson, W. R. Knuth, D. L. Blumenthal, J. C. Hsiung and R. B. Husar, Final Report No. MRI76-FR-1414 by Meteorology

Research, Inc., Altadena, CA. Submicron aerosol samples were collected for sulfate analysis as described by J. D. Husar, R. B. Husar, and P. K. Stubits, Analytical Chemistry 47, 2062 (1975).

9. U.S.E.P.A., Illinois E.P.A.

10. This point was brought to the authors' attention by H. M. Walker, Proc. of the Conf. on Ozone/Oxidants, Air Pollution Control Assoc., Dallas, March 1976.

11. W. E. Wilson, Jr., D. F. Miller, A. Levy and R. K. Stone, J. Air Pollution Control Assoc. 23, 949 (1973).

12. A. P. Waggoner, A. J. Vanderpol, R. J. Charlson, S. Larsen, L. Granat and C. Trägårdh, Nature 261, 120 (1976); W. H. White, P. T. Roberts and S. K. Friedlander, in the Character and Origins of Smog Aerosol, G. M. Hidy and P. K. Mueller, Eds. to appear.

This research was supported by the U. S. Environmental Protection Agency, Environmental Sciences Research Laboratory, Aerosol Research Branch. This paper is MISTT Report Number 4.

LEGENDS

Figure 1. Ozone concentration and light-scattering coefficient, b_{scat}, downwind of St. Louis on July 18, 1975. Data are taken from horizontal traverses by instrumented aircraft, at altitudes indicated in Figure 2a. Graph baselines show sampling paths; note that baseline concentrations are not zero.

Figure 2. Traverse altitudes and pollutant flow rates in St. Louis urban plume on July 18, 1975. Data are plotted against distance downwind of the St. Louis Gateway Arch. (a) Location of horizontal traverses; solid dots correspond to traverses shown in Figure 1. Mixing heights were determined from aircraft soundings. Approximate time (CDT) of sampling is shown at bottom. (b) Flow rates (in excess of background) of ozone (O_3), light-scattering coefficient (b_{scat}), and particulate sulfur (S_p).

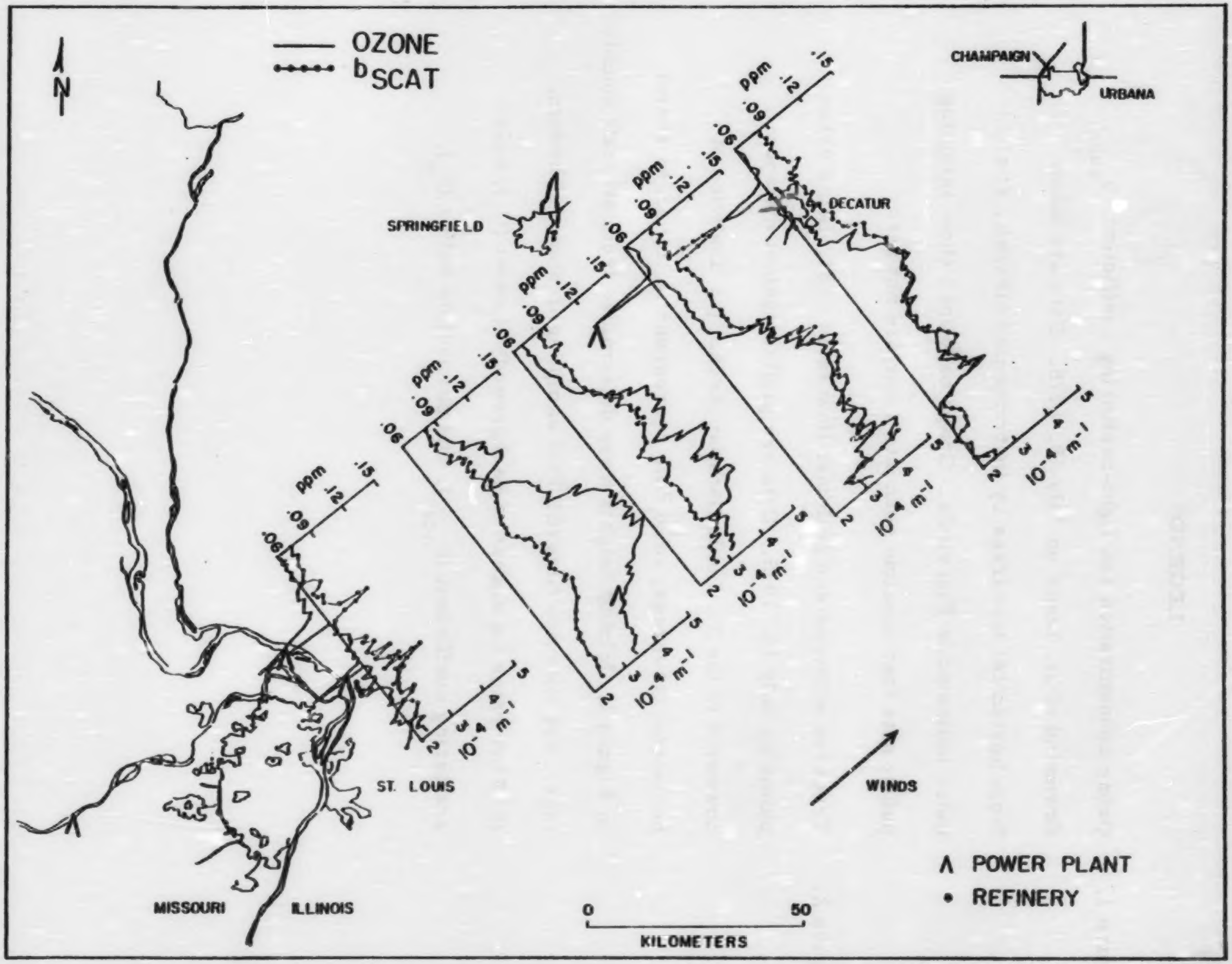
N
OZONE
bSCAT
CHAMPAIGN
URBANA
SPRINGFIELD
DECATUR
ST. LOUIS
MISSOURI
ILLINOIS
ppm
.06
.09
.12
.15
2
3
4
5
10⁻⁴ m⁻¹
WINDS
Λ POWER PLANT
• REFINERY
0
50
KILOMETERS

Figure 1

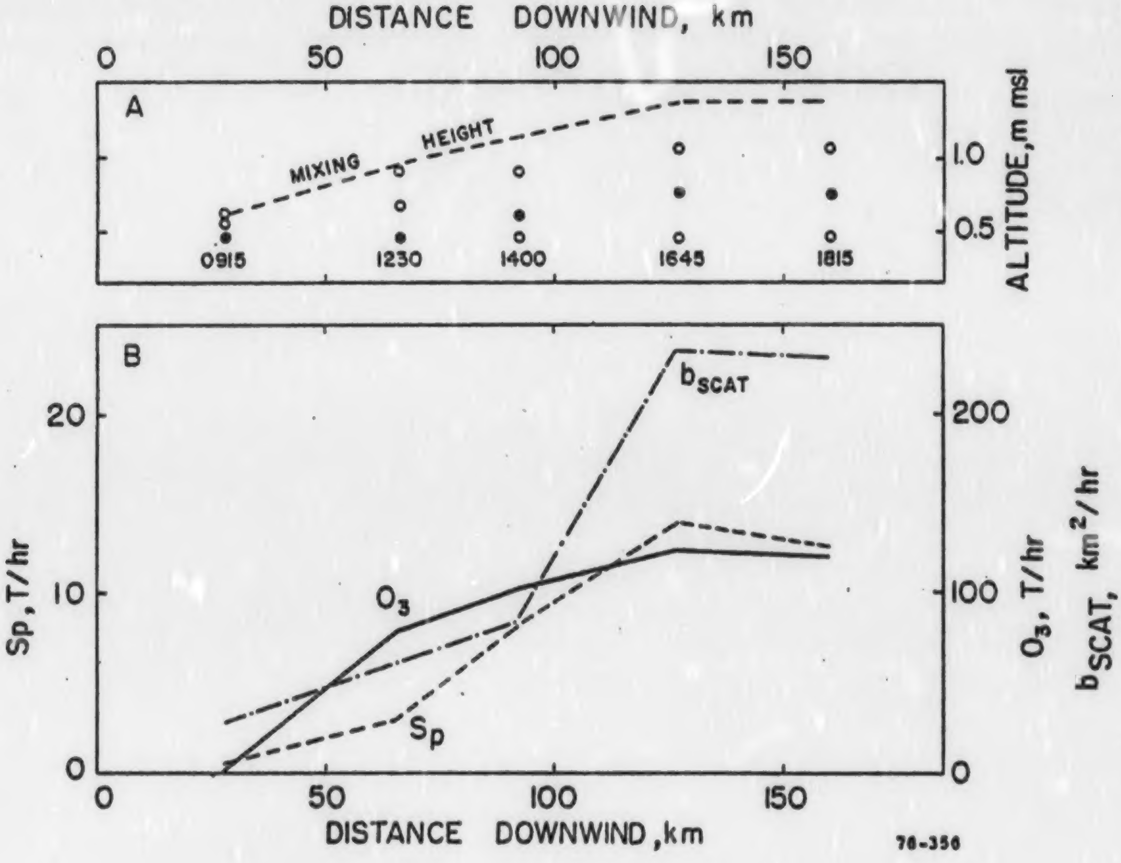
DISTANCE DOWNWIND, km
0
50
100
150
A
MIXING HEIGHT
1.0
0.5
ALTITUDE, m msl
0915
1230
1400
1645
1815
B
bSCAT
20
10
0
200
100
0
O3
Sp
Sp, T/hr
O3, T/hr
bSCAT, km2/hr
0
50
100
150
DISTANCE DOWNWIND, km
78-356

Figure 2